REPORT

November 4, 2003
EWI Project No. 45891GTH

Final Report
Evaluation of Methods for Detecting and Monitoring of Corrosion and Fatigue Damage in Risers

Submitted to:

U.S. Department of the Interior, Minerals Management Service
Herndon, VA

EWI

MATERIALS JOINING TECHNOLOGY

Final Report

Project No. 45891GTH

on

Evaluation of Methods for Detecting and Monitoring of Corrosion and Fatigue Damage in Risers

to

U.S. Department of the Interior, Minerals Management Service
Herndon, VA

November 4, 2003

Mark Lozev, Ben Grimmett, Eric Shell, and Roger Spencer
EDISON WELDING INSTITUTE
1250 Arthur E. Adams Drive
Columbus, OH 43221

This study was funded by the Minerals Management Service, U.S. Department of the Interior, Washington, D.C., under Contract Number 1435-01-02-CT-85094

Contents

Contents (Continued)

Page

Tables

Figures

Contents (Continued)

Contents (Continued)

Disclaimer

This report has been reviewed by the Minerals Management Service and approved for publication. Approval does not signify that the contents necessarily reflect the views and policies of the Service, nor does mention of trade names or commercial products constitute endorsement or recommendation for use.

Executive Summary

Offshore pipeline failure statistics have been collected for more than 30 years now and illustrate that the riser predominantly fails as a result of corrosion. The consistent wetting and drying in the splash zone combined with defects in the coatings are the usual contributors to the problem. Risers are inspected at some determined frequency and can be done by internal and external methods. Inspecting by either means brings into account caveats and limitations from the technology used as well as human factors. For example, external inspections can be inefficient and inaccurate with some tools missing defects in areas of coating disbondment. In addition, internal inspections sometimes create false positives and can miss defects. These inaccuracies in the technologies or the techniques used may miss defects that eventually lead to failure. On the other hand, using corrosion mapping and fitness-for-service (FFS) assessment from the data collected, along with the inherent conservatism of this data from limited measurement accuracy, may result in the premature replacement of risers.

A literature search is being conducted to review existing riser inspection methods and identify candidate nondestructive methods for riser inspection. These methods should be capable of detecting and monitoring general corrosion, localized corrosion pitting, and stress-corrosion cracking (sulfide or hydrogen induced) as external or internal corrosion damage. Thus far, this search has found that assessing the remaining service life of aging risers is largely dependent on the accuracy of analyzing corrosion damage to the riser surface in the atmospheric, splash (tidal), submerged, and buried environmental zones.

The accuracy of each technology was analyzed. The capabilities and limitations of each method/technique used for riser inspection are summarized.

The investigation is focused on long- and short-range ultrasonic techniques used for initial screening and corrosion mapping. These techniques can be deployed to detect a significant reduction in wall thickness using guided waves or to map accurately a corrosion damage using single/multiple transducers and phased-array (PA) probes in manual or automated mode. A pulsed eddy-current technique that uses a stepped or pulsed input signal for the detection of corrosion areas under insulation (CUI) is also being evaluated. This allows the detection of wall-thinning areas in the riser without removing the outside coatings. In addition, it is found that filmless, real-time and digital radiography can be used to find internal and external corrosion defects in an insulated splash zone while the riser remains in service. Current piping pigs adapted for riser inspection were also evaluated.

A survey of nondestructive evaluation (NDE) manufacturing companies, NDE inspection companies, and operating companies was completed to collect information about current instrumentation and inspection/operator's experience for riser inspection. Examples of advanced riser inspection instrumentation and testing results are included. The ability of the candidate technologies to be adapted to riser variations and the stage of standardization, are also discussed.

1.0 Introduction

The continuing trend to produce oil and gas in deeper water is forcing the evolution of the current methods of detecting and monitoring of corrosion and fatigue damages in risers. Marine riser systems form the link between the seabed pipeline and the topsides processing equipment. Various production and export risers used currently in the field have both structural (including rigid risers, catenaries, and hybrids) and material (including steel, titanium, and composites) considerations that influence the design. The chosen design usually dictates or limits how the riser can be inspected. Riser inspectability can be classified by several distinct characteristics: material of construction (e.g., carbon steel, stainless steel, titanium, composite, etc.), bare pipe without coating, coated pipe (but not insulated) with paint or sprayed aluminum coating, and insulated pipe (i.e., coated with long-lasting protection elastomer "Splashtron" or Bio-Shield). Very often external riser surface is covered with thick biomass.

The consistent wetting and drying in the splash zone combined with defects in the coatings are the usual contributors to the corrosion problem. Anticipated major mechanisms of corrosion and non-corrosion damage in risers are the following:

- General corrosion
- Localized corrosion pitting
- Erosion corrosion
- Crevice corrosion
- Mesa corrosion
- Stress-corrosion cracking (sulfide or hydrogen or chloride, etc. induced)
- Fatigue cracking (as small as 2-mm deep and 10-mm long for deep-water risers).

The appearance and location of potential riser corrosion and non-corrosion phenomena is shown in Figure 1. High (1 mm/yr) corrosion rate in a riser splash zone without coating protection has been reported in the Gulf of Mexico (GOM).[1] Below the splash zone moderate (0.1 mm/yr) corrosion rate has been predicted. High (1 mm/yr) corrosion rate for local corrosion or pitting could be observed for local riser connections and other elements below the splash zone.

Offshore pipeline failure statistics have been collected for more than 30 yr now and illustrate that 2,168 (55%) of all 3,971 GOM incidents reported to the U.S. Department of the Interior, Minerals Management Service (MMS), have been caused by corrosion damage.[2,3] MMS general pipeline failure statistics for GOM are shown in Figure 2. External corrosion contributed

to 70% of reported cases and internal corrosion to 30% (see Figure 3). The largest cause of failure of risers is corrosion. The recent MMS analysis revealed that the riser also predominantly fails due to external corrosion (see Figure 4). From this analysis, 92% of riser corrosion failures were due to external corrosion with 8% due to internal corrosion damage (see Figure 5). Currently, no failure due to fatigue cracking in deep-water applications is reported.

From these corrosion statistics, one could raise several questions about the causes of these elevated riser failure rates. Some of these possible causes are listed below:

- Lack of required inspection because of ineffective regulations
- Lack of inspection because of ineffective operator policy/procedures
- Lack of corrosion protection because of ineffective design
- Ineffective coatings in the splash zone
- Ineffective cathodic protection
- Corrosive operating environment
- Wave and working boat induced damage
- Human factors
- Internal/external inspection tool inefficiencies.

Risers are inspected at some determined frequency and can be done by internal and external methods. Inspecting by either means brings into account caveats and limitations from the technology used as well as human factors. For example, external inspection can be inefficient and inaccurate with some tools missing defects in areas of coating disbonding. In addition, internal inspections (seldom used) sometimes create false positives and can miss defects. These inaccuracies in the technologies or the techniques used may miss defects that eventually lead to failure. On the other hand, using corrosion mapping and fitness-for-service (FFS) assessment from the data collected, along with the inherent conservatism of this data from limited measurement accuracy, may result in the premature replacement of risers. Current methods of assessing the effect of corrosion defects on the maximum allowable operating pressure, including ASME B31G, NG-18, RSTRENG and Shell '92, along with recent probabilistic methods require detailed information for treating spiral and circumferentially aligned defects in addition to the more common axially aligned defects.

Corrosion damage can be inspected either from the outside or inside of the riser. Internal inspection using techniques other than magnetic flux leakage (MFL) technique requires bleeding down the riser and filling it with fluid resulting in significant lost production costs. A compact riser inspection tool (pig) was developed in the early 1990s to inspect risers from the

inside.[4] The system uses straight beam conventional ultrasonic multiple transducers for corrosion mapping and time-of-flight diffraction (TOFD) technique for circumferential weld inspection. Internal inspection is performed on a routine basis using pigs in those lines that are "piggable".[5] Significant uncertainties for wall piping thickness measurements based on the pig's recordings were reported.[1] Current piping pigs adapted for riser inspection can miss significant defects (false positives) and indicate the presence of defects that are not present (false negatives).

Pigging of flexible risers has been reported for geometric verification. Flexible risers are difficult to inspect from the outside due to their complex structure and the lack of developed nondestructive techniques.[6]

External inspection of risers with surface coatings and without casings typically involves marking the riser surface into a grid pattern, followed by point-by-point ultrasonic thickness measurements of individual grid sections using manually manipulated measuring instruments or multiple scans with single or multiple conventional ultrasonic transducers. This tedious task often results in limited measurement accuracy. The costs and difficulties of this process are compounded by the need for inspection personnel or divers to work in the hazards of the splash zone.

For the purposes of this report and research project, a review of riser nondestructive evaluation (NDE) methods and techniques will be presented in order to help identify how these issues could be contributing to the problem and to the solution of the high riser failure rate.

2.0 Objectives

The objectives of this program are to evaluate current and candidate inspection methods for detecting and monitoring corrosion and fatigue damage in risers.

3.0 Review and Evaluation of NDE Methods and Techniques

The research focus of this project was not limited to one specific type of riser. Rather, the program goal was to evaluate current and candidate methods for detecting and monitoring corrosion damage in all riser types and potentially develop ranking criteria or guidance for riser inspection based on the viability of these methods. A literature search is being conducted to review existing riser inspection methods and identify candidate NDE methods for riser inspection. Publications related to riser inspection are very limited. The majority of reviewed

papers described NDE methods and techniques developed and used for detection, sizing, and monitoring of corrosion damage in plant pipes, cross-country pipelines, and steel tubulars on offshore structures.[7-24] It was found that some of these techniques are already in use for riser inspection and others are in a process of adaptation for riser applications. .[3-6,25-28] A summary of the technologies that could be capable of detecting, locating, and monitoring of corrosion damage in risers is shown in Table 1. Advantages, disadvantages, and primary corrosion damage detected by each technique are described shortly in the table. In addition, a brief summary of the limitations of the technologies is shown in Table 2.

It is well known that no single means of corrosion detection is either ideal or suitable for all corrosion mechanisms. Traditionally, riser inspection relies on visual inspection and manual ultrasonic testing (UT) for corrosion damage assessment.[7-8] Mainly for the splash zone of offshore tubulars including risers and in the last 5-10 yr, new NDE techniques have been applied to detect and monitor general corrosion, localized corrosion pitting, and stress-corrosion cracking (sulfide or hydrogen induced) as external or internal corrosion damage.[3-5, 25-27] The principals, resolution, accuracy, and limitations for some of the commonly used or the most promising innovative inspection techniques are discussed in more details below. Examples of advanced riser inspection instrumentation and testing results are included.

3.1 Ultrasonics

3.1.1 Short-Range Ultrasonics

Corrosion damage can be inspected from either the outside or inside of the riser using short-range conventional or advanced UT techniques. Ultrasonic waves for the traditional short-range ultrasonic riser applications can be generated in two modes: longitudinal (L) (compression) and transverse [shear – shear vertical (SV) or shear horizontal (SH)].[29] A schematic of the particle motions and propagation through a crystalline medium is shown in Figure 6.

3.1.1.1 Ultrasonic Thickness Measurements and Corrosion Mapping of Risers

Longitudinal waves are commonly used for ultrasonic thickness measurements at specific point and angle beam shear wave for detection and assessment of surface open or internal corrosion damage in a localized area. Risers without coatings (bare pipe), with a smooth external surface after cleaning that surface from the biomass, can be inspected for internal corrosion or erosion wall losses after applying the traditional single backwall echo approach (Figure 7).[30] Through-coating measurements allow coated risers to be inspected without removal of the coating after applying echo-to-echo technique and A-scan imaging if the coating is well bonded to the metal

surface and the thickness of the coating is less than 6 mm (Figure 8). The thickness of the riser is determined simply by the time of flight for the ultrasonic signal to reach the back surface of the pipe and return to the transducer (measured using either signal T2 or T3 as is shown in Figure 9). UT digital gauges with 4- to 5-MHz, dual-element transducers are able to inspect carbon/austenitic steel riser with a wall thicker than 1 mm. The wave propagation shown in Figure 9 is actually perpendicular to the surface, but is spread out in the image to show the source of acoustic signals. Dual-element transducer focuses the sound beam at a specific depth range and enabling optimum sensitivity on corroded, eroded, or irregular internal riser surfaces (see Figure 8). These transducers are highly sensitive to small pits in their optimum thickness range. Proper calibration of the UT gauge, for different riser materials being tested, is essential for accurate results. Resolution of 0.1 mm, accuracy ±0.5 mm, can be seen in the field. For hand-held instrumentation a typical datalogger capacity is 10,000 thickness data points or 500 waveforms (A-scans). The expandable memory options save typically any combination of up to 2,000 waveforms or 40,000 thickness readings.

External inspection for internal general loss or pitting of risers without surface coatings or with coatings thinner than 6 mm and without casings typically involves marking the riser surface into a grid pattern, followed by point-by-point ultrasonic thickness measurements of individual grid sections using manually manipulated measuring instruments. This tedious task often results in limited measurement accuracy. The costs and difficulties of this process are compounded by the need for inspection personnel or divers to work in the hazards of the splash zone.

Conventional single- or dual-element transducer techniques cannot be used for inspection of external corroded surface because of poor contact between the transducer and the surface, and spurious signal caused by scattering. A focused transducer concept was introduced in early 1980s for automated UT (AUT) of corroded metal surfaces.[9] Spurious signal generated by sidelobes and shear wave mode conversion (Figure 10) were eliminated using a single focused transducer (Figure 11). An AUT system was developed and demonstrated in the field to externally inspect corroded steel tubulars on offshore structures in early 1980s.[10]

Currently, to improve the measurement accuracy corrosion mapping scans are performed using single or multiple ultrasonic immersion transducers attached to manipulators or scanners. Sub-sea manipulators and AUT submerged scanners using focused single or multi-probes are available for shallow water applications. An example of sub-sea system with a scanner is shown in Figure 12. In addition to corrosion mapping, shear wave pulse-echo (P/E), TOFD, and PA ultrasonic inspection techniques are also available with some systems. A basic for these techniques is given in section 3.1.1.2 of the report. Typical inspection range for the popular

diver-deployed system is 110 m. By redesigning of systems to be remote-operated vehicle (ROV) deployable depth in range of 400 to 2000 m can be achieved. When the AUT system is operated from a ROV, a tool skid is placed under the ROV, containing the system and power supply in an electronics bottle, cables, and the sub-sea scanner (see Figure 13). The scanner is placed on the object by the ROV.

AUT comparison results of ultrasonic scans performed across a corrosion-damaged area of a riser sample are described below. The length of the corrosion damage was approximately 50 mm and contained corrosion pits of varying depth on the outside surface of the sample. Figures 14 and 15 show the calibration sample and the pipe sample. All UT scans were performed using the immersion ultrasonic method with the UT probes located just above the outside surface of the sample. The software used was capable of performing measurements to $\pm$0.1 ms. This in turn translated into a depth measurement accuracy of $\pm$0.15 mm. Figure 16 shows the depth measurements obtained by six ultrasonic techniques and mechanical measurements. Table 3 describes the ultrasonic techniques and the average error in corrosion depth measurements between the mechanical measurement and the corresponding ultrasonic technique. In general, the single-element spherical focus probe and the PA 10-MHz probe with a water path of 47 mm and a circumferential focusing performed the best. The PA probes were consistently more accurate when focused in a direction parallel to the circumference of the pipe than when focused parallel to the longitudinal (axial) pipe axis. It was also noted that while all ultrasonic techniques tended to make the corrosion appear slightly deeper than the actual depth, smaller sound beam dimensions resulted in dimensions that are more accurate. Visualization of AUT corrosion mapping using single-element spherical focus probe and circumferential focused PA 10-MHz probe are shown in Figures 17 through 20.

A portable, hand-held camera for displaying real-time ultrasound images of external corrosion has been designed recently.[31] To generate C-scan images using “Acoustocam" camera, ultrasound is introduced into the target through a large, unfocused transducer. The pressure wave strikes the target and is scattered. This scattered energy is collected by an acoustic lens and focused onto the array, identical to the infrared (see Figure 21). The use of a lens provides a simple, inexpensive alternative to complex beam forming often employed in ultrasound imaging. The user basically focuses by adjusting a lens while looking at the image. The camera provides a means to trade off resolution and area coverage, or zoom in and out. Standard video electronics and image processing are used to format the image for presentation to the user on a hand-held LCD. Each time ultrasound is sent into the material (up to several thousand times/s), information can be collected at the array. To remain compatible with standard video equipment, the imagery is typically presented at 30 frames/s. A prototype of the

camera is shown in Figure 22. This unit features a 2.5-in. display for the local display of ultrasound images. To demonstrate capability of this technology for detection and visualization of corrosion within metal structures, samples such as shown in Figure 23 are employed. These samples contain known features (holes, slots, etc.) as well as the rough surfaces typical of corrosion-attacked steel plates. Typical images collected using a 5-MHz non-focused transducer are shown in Figure 24. While these are still images, the operator views a real-time, 30 frames/s. Display makes the detection of flaws much more apparent. No sizing capabilities were reported.

Reliable thickness measurements from the external side can be obtained also using a thin flexible strip that consists of a multi-element array of UT transducers, permanently bonded to the riser. Permanently attached UT flexible strips allow continuous corrosion monitoring of local critical area and supply the trend analysis with more accurate on-line thickness readings.

3.1.1.2 Ultrasonic Inspection of Riser Welds

UT inspection of riser girth welds investigates the total weld volume and the heat-affected zone (HAZ). Because girth weld geometry permits, the weld is inspected from two sides. This inspection includes the root, sidewall, crown, and HAZs of the weld. Recently, there is a strong trend to rely more and more on mechanized or AUT line scanning using an array of angle beam shear wave single-element multi-probes or multi-element PA probes. When using the line scanning approach, an array of probes is attached to the scanner, which is designed in a manner to inspect the weld in one external or internal circumferential pass. Multiple transducers, each dedicated for a specific inspection zone, arranged in P/E or pitch-catch mode are mounted precisely at the correct position on a multi-probe scanner head. Typically, 12 to 24 single-element multi-probes or two multi-element PA probes are utilized to inspect the HAZ and the complete weld volume in a single line scan. Once an inspection procedure has been tuned, AUT is inherently very reliable and repeatable. Current approaches for mechanized UT of pipeline girth welds are based on combinations of amplitude-based P/E methods using single-element multi-probes (focused or non-focused) or PA transducers and the time-based TOFD method. These approaches are applicable not only for inspection of riser girth welds during the fabrication but also for internal or external in-service inspection.

3.1.1.2.1 Amplitude-Based Zonal Discrimination Techniques

3.1.1.2.1.1 Focused Multi-Probes

The principle of the current zonal concept for AUT of girth welds was described in the early 1960s and was applied for field inspection of CRC welds in Canada in the late 1970s.[32,33] Typically, the weld is divided in two virtual halves during the AUT – up and downstream. In addition, the weld volume is divided into vertical inspection "zones" approximately 1 to 3 mm (0.04 to 0.12 in.) in height.[32-50] The number of vertical zones is dependant on the material thickness, bevel type, and welding procedure. An example for a weld with 14.9-mm (0.59-in.) wall thickness and a modified J bevel is shown in Figure 25 (left). In this figure LCP denotes "lack of cross penetration" zone and HP1 and HP2 denotes "hot pass" inspection zones. An individual ultrasonic inspection channel is assigned for each zone. In ideal conditions, "ultrasonic inspection zones" exactly match welding passes. Inspection zones to match weld passes may be ideal; however, it is not practical. A typical arrangement of ultrasonic channels and beam paths per vertical zone is shown in Figure 25 (right).

Typically, flat-bottom holes and internal diameter or outside diameter (ID/OD) notches are used for calibration targets. Signal amplitude and transit time are set up on these targets. Initial flaw gate settings are assumed to start at least 3 mm (0.12 in.) prior to the target and end at least 1 mm (0.04 in.) past the weld centerline, while stacked "A" scan "mapping" gates extend for 15 to 20 mm (0.59 to 0.79 in.). These targets are machined in a calibration block (reference standard) and arranged along the specific weld bevel profile. The material for the calibration block should be cut from production/project pipe material. Inspection parameters such as inspection angle, focal spot size, and focal depths are dependent on the weld characteristics and zone geometry. A summary of typical inspection parameters, typical search units, range of angles, and frequencies are shown in Table 4.

In P/E mode the refracted sound wave will bounce off a reflector (discontinuity) in the path of the sound beam, see Figure 26.[51] With proper angle beam techniques, echoes returned from the weld zone may allow the operator to determine the location, size, and type of discontinuity. The vertical extent of the flaw is sized by using a comparison between the amplitude of the calibration target in each zone and the amplitude of an unknown flaw in the same zone. In the pitch/catch configuration the transmitter and receiver are typically two separate probes transmitting or receiving at different refracted angles.

In the traditional zonal approach, if the defect is contained in only one zone, that channel will register a reflector over the 40% full-screen height (FSH) reporting level and adjacent channels will not show a reportable reflector since only a small portion of the defect is within the ultrasonic beam.[32-34,39,41,42,45] Therefore, the defect is sized to a single zone. When a defect is equally in two adjacent zones and is at least one zone in height, both zones will register reportable reflectors. The amplitude of both will be less than the 80% FSH reference level since only a portion of the defect is in each ultrasonic beam. The defect is sized to the height of two zones. When two defects are located in separate but adjacent zones, each channel registers its proper reflector. The two reflectors are considered to be combined since they are in adjacent zones. The defect is sized to the height of two zones. When two defects are separated by at least one zone, only the zones with defects register a reportable defect. The "middle" zone may see both reflectors but they will be below the reportable level. The defects are characterized as separate, each with a height of one zone. Currently, the same approach is used for both multi-probe and PA systems. If two adjacent zones exhibit mirror-like signal characteristics, the defect is assumed to sit between the two zones and is assessed as one zone high. This minimizes oversizing errors.

The traditional zonal approach is conservative with some possibilities for over sizing. All efforts to accurately size flaws in the vertical extent using amplitude comparisons are prone to errors because they are based on several assumptions:

- Flat reflectors smaller than the sound beam diameter
- Simple reflection behavior (flat-bottom hole, side-drilled hole, and notch)
- Size increases proportional with the maximum echo amplitude.

Using focal spot dimensions that very closely match the zone height can minimize these errors. For the traditional or simple zone height approach, the accuracy of defect height measurements for bevel fusion zone flaws is achieved only by optimization of the beam profile of each single crystal focused probe through variation of the radius of curvature (lenses or curved element), element size, and frequency.

A focused probe with a curved element usually incorporates the transducer and replaceable wedge. Each focused probe is designed and fabricated for a specific focal size and focal length (range). For example, bevel fusion zone flaws such as side wall lack of fusion (LOF) are inspected using transducers designed to focus on the bevel face with typical focus spots of 2 to 3 mm (0.08 to 0.12 in.) and a focal range of 10 to 15 mm (0.4 to 0.6 in.). Using focused transducers allows the flaw height to be sized with resolution better than the zone height. To

increase the probability of detection (POD) of sidewall LOF, the ultrasonic beam should intersect the bevel face at 90 degrees. To determine the exact wedge angle that allows the ultrasonic beam to intersect the bevel face close to perpendicular, velocity measurements are performed for each transducer angle during optimization procedures. Assessment of the vertical extent of sidewall LOF can be improved by observing zonal interaction of signals from zones with smaller heights using beams with similarly small spot sizes. The weld volume is inspected with focused transducers also, but arranged in a different way so that the entire weld volume can be mapped. To ensure repeatable results wedges incorporate wear strips or carbides for field inspection.

Certain modifications to the zonal approach can be used for sizing optimization. A so-called modified simple zone approach can be used to assess the indications. This approach considers not only amplitude but also the length. For example, indications with a short length and an amplitude near the reference level are considered to approximate the calibration target, while longer indications with an amplitude just over 40% are considered not to occupy a full zone, etc. Another modification for sizing optimization is the amplitude linearization approach. This approach assesses the indications by equating amplitude to vertical extent and multiplying the zone height times the signal amplitude. Optimization of sizing is achieved also through proprietary precision sizing algorithms and correct combinations of focused transducers and reference targets. Recently, it was reported that sizing accuracy was achievable within $\pm$30% of the designed zone or plane height.[35,36]

Generally speaking, the simple zonal approach is an amplitude-based sizing approach similar to the distance-gain-size (DGS) technique that relies on relationship between distance, gain, and amplitude. The Krautkramer brothers introduced the DGS technique in the late 1950s,[29,43] but they never declared this to be an accurate sizing technique. The technique links the amplitude at specific distances to the equivalent disk-shaped reflector of a certain size and then determines the resulting value of “equivalent reflector size”. Theoretically, their idea is valid for a disk-shaped reflector perpendicular to the beam spot and located in the centerline of the beam. For a typical angle beam shear wave having a probe frequency of 4 to 10 MHz the reflector’s size is between the half wavelength [0.4 to 0.8 mm (0.02 to 0.03 in.)] and the beam focal spot size, which is 2 to 4 mm (0.08 to 0.16 in.). In reality, the accuracy of sizing depends on variations in sound velocity, acoustic coupling, and attenuation. The orientation, roughness, and shape of the reflector, as well as beam profile, are also critical sizing factors. At a reflector misorientation equal to or greater than 4 degrees, the distance, gain, and amplitude relationship is lost for an ideal disk-shaped reflector. Fifty percent inaccuracy was reported for ideal misoriented disk-shaped reflectors and higher inaccuracy for realistic weld defects having

irregular shapes. It was also shown that larger misoriented flaws are more likely to be missed than small reflectors. For an ID rectangular notch the relationship between the flaw height and amplitude is not linear. The reflection from the corner formed by the weld surface and flaw is more complex because of wave mode conversion and the tip diffraction phenomena.[45]

Flaw orientation on the bevel is very well known and predictable for pipeline girth welds when the welding is completed by automatic methods like the gas metal arc welding (solid wire) process. This allows optimization of probe angles and elimination of the influence of misorientation on sizing accuracy in the case of AUT of pipeline girth welds using the zonal approach. At the same time the zonal concept establishes some uncertainties and inaccuracies for AUT of girth welds. The first uncertainty is related to the beam deflection from the target zone when the diameter of the focal spot is very small [typically less than 2 mm (0.08 in.)]. The small beam results in higher sensitivity of the beam to local differences in ultrasound velocity and surface irregularities. The second uncertainty is related to amplitude "saturation" when the flaw dimension reaches or exceeds the beam size. This situation will reduce the range where there is a linear relationship between flaw size and signal amplitude. To minimize these two uncertainties some vendors closely control the minimum spot size. A spot size equal to a typical 3-mm (0.12-in.) height of selected zones was proposed and recently widely used by the same vendors.[39-40]

3.1.1.2.1.2 Non-Focused Multi-Probes

The P/E non-focused multi-probe approach heavily relies on standard (flat crystal) probes with "natural focusing" of the beam and a beam spot larger than the expected typical flaw height. To reduce the conservatism of the traditional zonal approach, users of non-focused multi-probes re-introduced the amplitude and "signature" sizing techniques for AUT of pipeline girth welds.[37,38] By incorporating a logarithmic amplifier into the AUT system, signals over 100% FSH in amplitude can be re-processed without re-inspecting the welds. So-called amplitude signature denotes the echo-dynamics of each reflection represented in full radio-frequency (RF) waveform (A-scan). It is assumed that the ultrasonic signal from a given flaw is unique based on the full waveform. This technique is used to differentiate "stacked" from inter-zonal flaws detected by two or more transducers and to overcome the disadvantage of the traditional zonal concept to distinguish these two flaws. Stacked flaws occur in two consecutive weld passes or inspection zones in the same circumferential location. If the signatures of a flaw that is detected by two transducers are the same, this flaw is regarded as an inter-zonal flaw. If the signatures are different, the same flaw is regarded as a stacked flaw. Six steps of sizing methodology based on -12-dB amplitude drop technique and signal signature are used to evaluate the flaws.[37]

Generally, users of the P/E focused multi-probe approach break up the welding hot pass into two ultrasonic inspection zones. The vertical extent of the hot pass is in the range of 3 mm (0.12 in.) for a wall thickness of 14.9 mm (0.59 in.), but the actual surface run of this portion for J bevels and modified J bevels is about 4 to 5 mm (0.16 to 0.2 in.).[43] Recently, there is a practice by users of the P/E non-focused multi-probe approach to treat the hot pass as a single ultrasonic inspection zone. Using this approach, it is possible to miss corner entrapments or make it difficult to evaluate when an indication arises from the middle of the 45-degree bevel or near the LCP on fill passes.

3.1.1.2.2 Time-Based Diffraction Techniques

In P/E mode the signal amplitude is strongly dependent on several secondary factors. Apart from the reflector's through-thickness height, the amplitude depends on:

- The angle of incidence of the ultrasonic beam on the reflector
- The roughness of the reflector
- The shape of the reflector
- The position of the reflector with respect to the beam center.

For a certain category of automated welding defects a number of these factors are known. This is the case for LOF and lack of penetration-like defects, which are known to have positions and orientation equal to the original bevel, and are of more or less predictable shape. For such defects, the amplitude can serve as a reasonably accurate sizing tool. This is not the case for other defects such as cracks in unpredictable orientations and positions and any manual welding defects. The use of time-based techniques such as TOF or so-called tip diffraction (or back diffraction or backscatter diffraction) and TOFD as additional techniques compensates for this to a certain extent. By combining the information of the redundant techniques it is, therefore, possible to size most of the natural defects in a weld within a certain tolerance. Typically, better sizing results using time-based techniques are reported in the literature.[52]

3.1.1.2.2.1 Tip Diffraction (Back Diffraction or Backscatter Diffraction)

Principles of the diffraction technique or TOF using a single transducer (single crystal or PA probe) are shown in Figure 16.[48] This technique is also known as back diffraction or backscatter diffraction. Diffraction is the phenomenon whereby sound bends around the edge of the flaw. The tip diffraction technique, with a single transducer in P/E mode, uses the effect of sound energy striking the base (corner trap) of a crack or planar reflector, to cause the tip of

the crack to radiate sound energy, see Figure 27. This sound energy radiates at the tip of the crack as a spherical wave or a cylindrical wave along the length of the crack.

Tip diffraction uses diffracted sound energy radiating from the tip of the crack to accurately size the depth of the crack from the ID or the OD. Two sub-techniques are used. One measures the TOF or sound path of the diffracted energy as it travels back to the transducer and is sometimes called the pulse arrival time technique (PATT), or absolute arrival time technique (AATT). The other technique measures the relative time travel or Delta (A) (TOF) or sound path difference between the tip diffracted signal and the corner trap or base signal and is sometimes called satellite pulse observation time technique (SPOT) or relative arrival time technique (RATT). The technique acronyms were changed due to a new author of the technique, e.g., PATT/AATT, and SPOT/RATT are the same techniques. The tip-diffracted signal is generally a low amplitude signal. The signal-to-noise (S/N) ratios can be very low (2 to 1 S/N ratio) making it difficult to properly identify the tip signal. Typically, tip-diffracted signals precede the base or corner trap signal of surface-breaking flaws. However, tip-diffracted signals may be seen trailing the base signal. This is due to the spherical wave radiating from the tip of the inclined flaw and reflecting off the ID surface and returning at a later time beyond the corner trap signal. With low-amplitude tip signals, RF signal displays may be helpful in identifying the tip signals. There is some consideration that a phase reversal is noted between the base and the tip signal. For example, the tip signal may have a positive excursion and the base may have a negative excursion.

3.1.1.2.2.2 TOFD

The TOFD technique uses a pair of probes for refracted longitudinal waves in a transmitter-receiver arrangement with an angle of incidence range of 45 to 70 degrees. A schematic of the TOFD inspection process is shown in Figure 28.[48] For most pipeline inspection applications, transducers with center frequencies between 5 and 10 MHz and a diameter of 0.125 to 0.8 in. (3 to 20 mm) are suitable. TOFD is a time-based method and relies on the diffraction of ultrasonic energies from “corners” and “ends” of internal structures (primarily discontinuities) in a component being tested. When ultrasound is incident upon a linear discontinuity such as a crack, diffraction takes place at its extremities in addition to the normal reflected wave. This diffracted energy is emitted over a wide angular range and is assumed to originate at the extremities of the flaw. In addition to energies diffracted by flaws, the TOFD method will also detect a surface (lateral) wave traveling directly between the probes and also a backwall echo from energies that reach the back of the test piece without interference from defects.

Using this configuration, the depth and through-wall height of the crack can be calculated from the equations:

$$d = \frac{1}{2}\sqrt{C^2 t_1^{\,2} - 4S^2} \quad \text{and} \quad 2a = \frac{1}{2}\sqrt{C^2 t_2^{\,2} - 4S^2} - d \tag{1}$$

where:

2S	is the separation of the probes
C	is the L-wave velocity
d	is the position of the crack below the surface
2a	is the through-wall extent of the crack.

The study of this phenomenon has led to the use of the TOFD method for: (1) flaw detection as signals may be recorded from a range of flaws, and (2) flaw sizing since the spatial (or time) separation of the diffracted waves is directly related to the height of the flaw. The diffracted signals are received via the receiver probe and are evaluated with the ultrasonic system to clear gray scale D-scan images as shown in Figure 28. In the literature D-scan is also known as linear, non-parallel, or longitudinal scan. D-scanning is normal to the direction of the beam along a weld or flaw. B-scanning is across the weld or flaw and is also known as transverse, parallel, or lateral scan.

For flaw orientation in a direction vertical to the surface, the size and depth can be evaluated using TOFD. A typical figure for the accuracy that may be achieved is 1 mm (0.04 in.) for internal flaws with sharp edges. It is assumed that the ultrasonic energy enters and leaves the specimen at fixed points under the probes and that the probes are separated by a fixed distance. This is a simplification of the true situation but is sufficiently accurate for most purposes. The time taken for the ultrasonic energy to interact with a flaw tip at specific depth and return to the specimen is given by a simple equation, and by use of today's advanced computer techniques it is possible to calculate the depth and height of the flaw very rapidly. This makes it possible to perform scans at relatively high speed that are, in practice, limited only by the mechanics of the system. A similar inspection procedure can be used to conduct multiple-skip TOFD as shown in Figure 29.

3.1.1.2.3 PA Technology

Corrosion damages, including localized pitting, tend to taper away and start/stop points of the defect are not well defined. An accurate and reliable measurement for the length, width, and depth of taper and complex/multiple corrosion damages is still a difficult task with conventional focused UT transducers. The angle, focal distance, and focal point size of ultrasound beams generated by conventional UT transducers are fixed by the probe, probe lens, and probe wedge. To generate a different beam angle or focal size, different conventional transducers, lenses, or wedges must be used. In contrast, PA technology can generate a range of ultrasound beams from the same transducer, controlled in real-time by software.[45,48] The dynamic control of the beam properties and dynamic depth focusing offers new inspection capabilities not feasible with conventional transducers. Instead of one crystal, the PA transmitting/receiving element is split into a set of individual elements. The multiple elements in a PA housing are arranged in linear, rectangular (matrix), or circular (annular and sectored) patterns. Each element of these probes is connected to a different electronic channel, either directly or through multiplexers, depending on the electronic design. Each element can be pulsed or not for each shot. The size and location of the active aperture of the PA probe depends on the activated elements. An electronic delay can be applied to each electronic channel when emitting and receiving the signal to/from the transducer elements. The setup corresponding to all the delays of a given shot is called delay law (focal law). Each delay law defines a different acoustic beam with a particular direction, focusing distance, and lateral resolution. PA technology requires probes with very low acoustic and electric cross coupling between the elements, so that all the elements can be fired independently. Piezocomposite materials with 1-3 structure are completely adapted to this feature.

The elements in a PA probe can be pulsed simultaneously or in a programmed pattern. *Electronic scanning* is accomplished by pulsing a group of elements electronically in sequence along the length of the transducer. The resulting wave front travels along the length of the PA transducer. No third axis of mechanical movement is required for C-scan mapping. *Beam steering* is accomplished by delaying the pulsing of each element electronically at a set rate. The resulting wave front travels along at an angle dependant on the time delay between firings, see Figure 30.

Beam focusing is achieved by varying the *rate of delay* for the pulsing of each element. The resulting wave fronts propagate toward one another and focus at a programmed distance from the transducer, see Figure 31. The actual size of the focal point is determined by the number and size of the elements used. The delay law is computed so that all element contributions

interfere at a given point at the same arrival time to focus the beam at a given point for better detection and sizing.

Axial beam focusing and electronic beam steering in the array axis plane is available with linear arrays. The sectorial (azimuthal) scan shown in Figure 32 (right) is a real-time side view generated from a single inspection point, without any physical motion from the PA transducer. The sectorial-scan visualization significantly increases imaging and sizing capabilities of the PA UT technique. PA technology offers the potential for more reliable and fast detection and accurate sizing of fabrication flaws in girth welds by manipulating the ultrasound beam electronically, see Figure 32 (left).

Currently, 16/64 or 32/128 channel PA equipment is commonly used for different industrial applications. This equipment allows simultaneous pulsing (firing) of up to 32 elements in a single PA probe with a maximum of 128 individual elements in the probe that can be pulsed separately.

Limited data is available for POD and sizing accuracy of flaw height using PA technology. The results of the first PRCI project showed that PA technology is capable of reproducing typical conventional mechanized UT and accurately measure the length of UT indications. It was demonstrated that with only two PA transducers positioned on each side of the girth weld centerline, a PA system was capable of reproducing all of the channels of a multi-probe system and perform a mechanical line scan to inspect the welds circumferentially.[46,47] The expectations are that the vertical assessments of defect size will be further improved using smaller sub-zones with PA technology. The second PRCI project[48,49] revealed that in the best case only 45% of the flaw population will be sized within ±0.5-mm accuracy. The majority of the defects will be sized within ±2-mm accuracy (see Table 5). In Figure 33, A4, A5, and A6 denote PA blind trials sizing results and A6A denotes PA open trial sizing results for sizing of LOF in 14.9-mm-thick girth welds. It was recommended that additional research be conducted to analyze the latest trial results.[48-50] The additional research should include new open and blind sizing trials to bring the PA technology to a higher level of demonstrated accuracy. POD for PA technology should also be generated and provided to the public.

3.1.1.2.4 Electromagnetic Acoustic Transducers

A non-contact electromagnetic acoustic transducer (EMAT) generates acoustic waves in electrically conductive materials by the Lorentz force or by magnetostrictive effect, or by combination of these two phenomena.[53,54] Both phenomena act on the atomic lattice of the

component so the acoustic wave is generated directly in the component rather than in the transducer, as is the case for conventional ultrasonics using piezoelectric transducers.

The Lorentz force is an interaction between an electric current (J), which is induced by an eddy-current coil, and magnetic flux (B_0). The direction and magnitude of the force F_L is given by the vector product $F_L = JxB_0$. The Lorentz force, electric current, and magnetic field are, therefore, at 90 degrees to each another, see Figure 34.

Nearly all ferromagnetic materials show a mechanical deformation if they are subjected to a magnetic field. This phenomenon is called magnetostriction (in simple terms it is the magnetic equivalent of the piezoelectric effect). The deformation is generally parallel to the applied field. If an eddy-current coil is placed at the surface of a ferromagnetic material (e.g., carbon steel), dynamic fields are induced which creates dynamic magnetostrictive force F_{ms}. These forces are generally parallel to the applied magnetic flux B_0, see Figure 35.

To achieve an adequate ultrasonic beam configuration it is necessary to use large apertures, (i.e., large eddy-current coils). Two concepts for the coils exist – one large meander-shaped coil or an array of small coil segments, see Figure 36.

A transducer with a non-segmented meander coil behaves like a single transducer. A transducer with a segmented coil behaves like an ultrasonic array transducer. The coils are energized by a tone burst of alternating current (AC) for a duration related to the dimensions of the coils. Given the frequency of the tone burst and the velocity of the wave mode generated, the wavelength can be calculated. Large non-segmented coils produce small band signals, this means the axial resolution is pure. In addition, EMATs with non-segmented coils radiate the same energy in the forward and backward direction. EMATs with segmented coils working like an ultrasonic array deliver ultrasonic signals with larger bandwidths than non-segmented transducers and produce forward to backward ratios in the order of 30 to 40 dB. Typically, EMATs are used to generate shear waves with horizontal polarization or so called SH-waves. High-resolution pigging tools based on EMATs technology are available for detection of cracking gas pipelines and risers with no need for liquid batching. The minimum detectable crack depth is 1 mm and the detectable crack length is $\geq$30 mm. The EMATs pigging detectability capabilities and sizing accuracy are compatible with the pigging tools using 45-degree shear vertical inspection technique where a liquid batching is required. No EMATs field data from riser inspections are reported in the open literature. Expected minimum detectable crack depth is 1mm or higher and minimum detectable crack length in the order of 30mm for riser wall thickness in the range of 9 to 16 mm.

3.1.1.2.5 AUT Imaging and Strip Charts

Although there are some differences in current mechanized (automated) ultrasonic techniques, all of them provide similar information that can be used for flaw detection and size measurements. In addition to the typical A-scan tip diffraction presentation, a combination of B-, D-, and C-scans, angle corrected B-scans, and non-corrected/corrected sectorial (S-) scan imaging are used for better data visualization, interpretation, and depth/length measurements. A typical split screen of advanced images deployed in AUT systems for broader applications is shown in Figure 37.

All commercially available software for the current specialized systems for mechanized ultrasonic inspection of girth welds comprises a module that is capable of performing disposition of indications against a code or standard, including through-thickness sizing and application of defect interaction rules. UT data is displayed in multiple views using proprietary graphical-user interface displays almost identical for the current approaches. Each inspection zone is represented by multiple sets of vertical strips displaying amplitude, TOF, couplant and volumetric mapping data. The strips are labeled with the inspection zone symbol and form a so-called strip chart, see Figure 38. Unique features and color spectrum provide support to the operator for rapid identification of amplitude and TOF, flaw characterization, calculating the height and length, and electronic marking. A ruler is incorporated also in the screen window to indicate the circumferential location of UT indications. In addition, TOFD data is presented in gray scale on the screen and can be used for vertical sizing or to evaluate misaligned and off-axis defects.

The following information on indications found in a weld is available on the strip charts as a basis to establish the through-thickness size of reflectors using for zonal discrimination:

- The location of zones and number of zones in which the indications are detected
- The signal amplitude of indications in one zone or several different zones detected by P/E or pitch/catch channels
- TOFD image showing upper and/or lower tip of the reflector (dependent on the reflector's nature and location).

Examples of riser inspection results using several advanced techniques and systems are given below. Internal ultrasonic inspection often requires bleeding down the riser and filling it with fluid resulting in significant lost production costs. A compact umbilical riser inspection tool was developed in the early 1990s to inspect risers from the inside.[4] The system uses multiple

straight beam conventional ultrasonic transducers for corrosion mapping and TOFD technique for circumferential weld erosion corrosion inspection and corrosion-fatigue damage. Because most corrosion occurs between the 5 and 7 o'clock positions, a dense array of probes provides full coverage in that area, with less complete coverage used in the probe arrays for the remaining circumference. Recent advances in the tool allow inspection of horizontal members using a crawler and can be configured to negotiate bends, T-connections, and other odd configurations.[27] These inspections can be conducted through up to 17-km length. An example of the tool deployed internal to the riser is shown in Figure 39. The latest version of tool is motor-driven and can propel itself in a liquid-filled riser where no flow is present in vertical and horizontal sections. The bottom part of Figure 39 is an example of typical corroded area, which was detected in a splash zone of a riser using this tool. The top part of C- and B-scans shows the internal surface. No internal damage is present. The bottom part of C- and B-scans shows an area of approximately 1.5 m in length where external corrosion is visible over the entire circumference. Especially close to the circumferential weld the corrosion is severe. Locally, the wall thickness is reduced to 6.8 mm of the original 15.1 mm.

Another integrated internal drilling riser inspection tool (RADAR – riser active data-acquisition recorder) has been produced recently.[28] This system includes two TOFD channels for weld volume inspection, four shear wave transducers to inspect the root and cap regions of the weld, four longitudinal wave transducers to inspect for corrosion damage, and a video recorder to visualize the internal condition of the riser during inspection. A general view of the system is shown in Figure 40.

3.1.2 Long-Range Ultrasonics

Long-range ultrasonic techniques were introduced for initial screening for internal or external corrosion of in service plant pipe work under insulation.[11-15] These techniques were deployed successfully to detect a significant reduction in wall thickness using guided waves. Guided waves, also known as Lamb or plate waves, are similar to longitudinal waves, but are constrained by the sheet or plate surface and thus propagate along the surface of the specimen. Figure 41 shows three possible wave modes (longitudinal, torsional, and flexural) for guided waves in a pipe. Due to the nature of guided waves, they only penetrate approximately one wavelength into the specimen. Therefore, there can be some loss of sensitivity for internal corrosion or other internal defects if the specimen thickness exceeds one wavelength. Guided waves do have the distinct advantage of being able to travel long distances making these of great interest for the inspection of risers. A schematic of guided wave inspection is shown in Figure 42.

Guided, longitudinal and torsional, and SH-waves can propagate many hundreds of meters in plane pipe. The propagation of these waves in the pipe wall is similar in nature to Lamb waves in plates. However, unlike bulk waves used for conventional UT, where generally only a single mode such as either compression or shear exists, a large number of longitudinal, torsional, and flexural wave modes are possible. In addition, each of these wave modes propagates at different velocities as seen in the dispersion curve of Figure 43. This curve shows the frequency-dependant propagation velocity of various wave modes in a 6-in. (150-mm) -diameter steel pipe. In an inspection system, it is important to carefully control the wave mode in order to ease interpretation of the reflected signal.

In guided wave testing, the sensitivity is dependent on the signal to coherent noise ratio – or the noise caused by excitation of unwanted modes. One way to avoid generating unwanted flexural waves is to induce L(0,2) guided waves with a sufficient number of transducers elements in the ring to suppress flexural waves whose cut-off frequency is within the bandwidth of the excitation signal.

In order for the responses from corrosion damage in risers to be interpretable, it is necessary to use selected wave modes, which allow the signal to be simplified. Full-wave RF signal and processed simplified signals are shown in Figure 44. To achieve this it is necessary to operate in a typical frequency range 10-80 KHz in which the most attractive mode is non-dispersive in pipes (i.e., its velocity is independent of frequency). This technique uses a belt of dry-couplant ultrasonic transducers,[11-16,19-25] magnetostrictive sensors (MsS)[17,18] or EMATs that can be positioned on the outside of the riser.

Various guided wave transducer rings and belts have been developed that are able to inspect pipe lengths of over 80 ft (25 m) using dry-coupled piezoelectric transducers (Figure 45). These systems are designed to detect localized corrosion on the order of 10% of the pipe cross sectional area (Figure 46). Commercialized guided wave inspection systems use flexible clamping arrangements to hold three to four rings of transducers for use with the L(0,2) wave mode or two rings of transducers for use with the T(0,1) wave mode. These configurations have been chosen to avoid generation of unwanted wave modes. This method would be restricted to above water or the depth that could be reached by divers.

Long-range UT screening of risers in the splash zone performed by two inspection vendors using dry-couplant transducers is given in Figure 47. The figure shows the dry-coupling transducer ring set up by the technicians on the riser using rope access technique. The riser shown in the top/left part of Figure 47 is protected in the splash zone with long-lasting elastomer

Splashtron. It was reported also that transmission of ultrasound past the anchor riser flanges is possible and that the sprayed aluminum coating had no adverse effect on propagation of guided waves. The pipe ends, 63 m away, were detected and screening of the splash zone, 18-20 m from the transducer, for less than 10% metal loss damage was possible.[25,26]

MsS consist of an electrical coil and a bias magnet. A strong, pulsed current in the coil induces a time varying magnetic field at one end of a ferromagnetic pipe. By the magnetostrictive effect, a mechanical wave is generated that travels to a second receiving coil, changes the magnetic induction of the material and induces a voltage in the receiving coil (Figure 48). Defects on both surfaces of the component are detected over a range of 100 ft (30 m) or more without removing insulation. However, the method requires inspection from the outer surface using an array of sensors, restricting its use to above water or near the surface.

EMATs have also been used to generate guided waves in pipe walls. A conducting coil under a magnetic field will induce an electromagnetic wave in the material through Lorentz forces and, in the case of ferromagnetic materials, a magnetostrictive effect. Longitudinal, shear, or Lamb waves can be generated, depending on the configuration of the magnet and direction of current flow. The transducer does not need to be in contact with the inspected pipe, so coupling concerns of conventional UT is avoided. One limitation with EMAT transducers is the lower S/N ratio which requires more signal processing and conditioning to obtain a clean signal. The SH_0 or SH_1 wave modes are generally used at low frequencies for guided wave applications to avoid multiple wave mode generation.

Long-range ultrasonic inspection techniques typically function as a screening tool for inspection. The techniques can detect corrosion within several meters in both directions from the transducers. The riser needs to be cleaned on the outside (above the waterline) only in a small area where transducers are attached. Current use of this technology is accurate to plus 30 m (100 ft). In some cases with long-lasting riser protection elastomers inspection distance shorter than 10 m (30 ft) were reported.[27] Most do not have the capability to quantify the discontinuities; rather they provide the inspector with a tool for finding suspect areas for a more detailed examination. It is imperative for the owner/user to realize that long-range UT does not provide an absolute wall thickness measurement. The technique is sensitive to the combination of wall loss, extent of circumferential damage, and to some extent on the length of damage. Reportedly, long-range ultrasonic is to be equally sensitive to both internal and external discontinuities. Indications are classified according to three qualitative categories: minor, moderate, or severe. For example, an area determined by the interpreter to be severe warrants

supplemental inspection to make a final determination for FFS. The performance is influenced by several factors.

- The size of the corrosion interacting with the ultrasonic beam as the beam propagates the length of inspection. Detectability is related to amount of corroded pipe wall cross section. The limits of detectability are 3% of the original pipe wall cross sectional area.

- The depth of the corroded area affects the sensitivity of the signal response more than the circumferential area, i.e., deep short areas of corrosion tend to produce greater signal response than a wide shallow response of the same area.

- The technique is somewhat sensitive to longer defects.

- Various pipe features, such as coatings/insulation (Splashtron), disbanded coatings, biomass, and geometry changes, affect the ultrasonic signals and can impact discontinuity detection.

Long-range UT using low-frequency transducers ensure 100% inspection coverage over a testing range of ±30-180 m, depending on the corrosion level in the pipe, whether the pipe is loaded, and whether there is insulation on the pipe. Longitudinal accuracy is of the order of ±0.1 m.

3.2 Electromagnetics

3.2.1 Eddy-Current Testing

Eddy-current testing (ET) uses the principles of electromagnetic induction to identify specific material characteristics and conditions.[6] ET can be used to detect surface and near surface discontinuities. ET is extremely sensitive to very small changes in the material structure, hence is capable of finding small discontinuities of only a few thousands of an inch in highly conductive materials.

ET has several distinct advantages. First, the process does not require direct contact of the test probe to the specimen. However, the probe must be in close proximity to the test specimen in order to induce eddy currents into the specimen.

ET is sensitive to surface or near surface discontinuities only. The process requires a skilled operator to calibrate and interpret indications. Once the range of specimen conditions is known the system can be set for automated interpretation. However, a reliable set of reference standards, preferably of production conditions, needs to be developed or procured to calibrate the system. Inspection can also be performed very rapidly in production applications, as the technique is conducive to automation.

Eddy currents are generated using electromagnetic induction. When an electric current is generated in a conductor, a magnetic field is subsequently generated that surrounds the conductor. If the conductor is formed into a coil, each individual turn of the coil combines to increase magnetic flux density around the coil.

If AC is used, the magnetic flux alternates with the current flow. This alternating flux can induce a current in a second coil placed in close proximity to the first coil. However, if the coil is placed near an electrically conductive part, the alternating flux will induce currents into the specimen. These induced currents are called eddy currents. The eddy currents are fairly localized in the immediate region of the coil. The exact depth of penetration of the eddy currents is dependent on the magnetic permeability and conductivity of the specimen as well as the frequency of the AC in the test coil.

Standard depth of penetration is the distance below the surface of a flat specimen in which eddy currents are 37% of the density at the surface:

$$\delta = \frac{1}{\sqrt{\pi MTf}} \tag{2}$$

where:

M = Relative permeability
T = Electrical conductivity
f = frequency.

Once the instrument has been “nulled” over an acceptable area of the test specimen, discontinuities such as cracks, seams, laps, etc. will cause a change in the flow of eddy currents. This in turn changes the impedance in the test coil which is detected by the instrument, subsequently shown as an indication on the presentation screen.

Impedance (Z) is comprised of AC resistance (R) and the inductive reactance (X_L). ET signals are typically plotted on an impedance diagram with R as the x-axis and X_L as the y-axis. A sample ET screen is shown in Figure 49 for a calibration block with EDM notches of various depths.

ET is extremely sensitive to a change in distance between the probe and the part. This distance is known as liftoff. Changes in liftoff can be caused by a host of items, e.g., weld spatter, corrosion, wear, etc., can adversely affect liftoff, hence the quality of the ET inspection. A common technique to overcome liftoff effects is to calibrate the ET instrument so liftoff signal is different in the R- X_L plot. Figure 50 demonstrates this concept.

Material properties also affect the quality of the ET inspection. For example, ET can be used to sort materials based on electrical conductivity, permeability, and microstructural changes caused by heat-treating, welding, and forming operations.

ET probes come in two basic, readily available varieties, absolute and differential. Both types can be custom configured for specific applications as determined by each situation. Absolute and differential coil schematic diagrams are shown in Figures 51 and 52.

An absolute probe is composed of a single eddy-current coil. The probe is calibrated, i.e., balanced, over a known acceptable area. Changes in the material properties or geometry cause an impedance change in the coil displayed on the R- X_L plot. Absolute coils are well suited for conductivity and coating thickness measurements as they are sensitive to gradual changes in material characteristics when compared to differential coils.

A differential coil measures the change in impedance between two balanced coils as the means of detection. If the two coils are placed over a material having similar characteristics, both coils are balanced. However, as shown in Figure 50, once one coil passes over a change in material, in this figure the notch, an imbalance occurs which is displayed on the R- X_L plot. These coils have the advantage of detecting sudden changes in the material structure. However, gradual changes are not readily detectable by the differential coil as the coils remain in balance.

Array eddy-current test equipment combines a differential and absolute coil into a single system, thus enabling the user to take advantage of both coil arrangements. These systems are typically known as Array Eddy-Current systems.

3.2.2 Remote Field Eddy Current

Remote field eddy current (RFEC) was developed in the 1950s and is widely used for inspection of metallic pipes and tubing.[55-57] RFEC inspection is conducted by exciting a relatively large, low-frequency AC coil inside the pipe. A pick-up coil, offset by approximately two pipe diameters, can then be used to detect changes in the flux field due to the tube wall condition, thickness, permeability, and conductivity. Figure 53 shows a schematic of RFEC testing.

In operation, an electromagnetic field is transmitted into the pipe thickness. This direct path is attenuated rapidly to create circumferential eddy currents, which diffuse radially toward the outer wall. Once reaching the outer wall, the field spreads rapidly with little attenuation. This field then re-diffuses back to the inner wall, interacting with defects in the remote field region, before being detected by the pick-up coil. Because this is a through-wall technique, defects at any depth in the pipe wall can be detected with similar sensitivities instead of just surface defects which can be detected by conventional EC.

Advantages over conventional EC include: equal sensitivity to defects on either the inner or outer surface, insensitivity to probe wobble or lift-off, and not being limited by the penetration depth. However, RFEC is usually limited to the detection of wall loss. Attempts have been made to detect pits using differential receivers and multiple receiver coils, but the sensitivity is usually unacceptable due to the interference of corrosion byproducts with signals from pits.[58] Additionally, the speed of inspection using RFEC is significantly slower than with conventional EC testing.

3.2.3 MFL

MFL is the oldest and most commonly used in-line inspection method for finding metal-loss regions in gas-transmission pipelines (see Figure 54).[59,60] MFL is typically used to detect metal loss due to corrosion or gouging, but can sometimes find other metallurgical conditions such as inclusions or weld porosity. MFL is not well suited for detection of cracks or other long, narrow, or shallow defects. However, there may be some limited success finding deep circumferential cracks.

MFL uses a magnet to induce a magnetic field in adjacent metallic pieces (see Figure 55). Flux lines are used to show the strength and direction of the magnetic field. When the magnet is placed next to a metallic component most of the flux passes through the component wall, since that is the preferred path for the flux. The magnetic field must be strong enough to saturate the

pipe wall, resulting in some magnetic flux outside the wall, in order to have optimum detectability. An example of typical MFL tool is shown in Figure 56.

Corrosion causes a decrease in the thickness of the wall, leading to flux leakage at both sides of the wall. A sensor positioned inside the magnet side of the wall is typically used to measure the magnetic field adjacent to the wall. At metal loss regions, a higher flux density is recorded. The change in the magnetic field depends on the radial depth, axial length, circumferential width, and shape of the defect.

MFL can work through coatings of up to 10-mm thickness.[10] MFL is generally limited to pipe thicknesses of 12-15 mm. Above this thickness, it is difficult to obtain magnetic saturation.[14] Typical wall thickness sizing accuracy is on the order of ±10% and length accuracy of ±0.5 in. with an 80% confidence level.[60] However, sizing is impaired by noise signals produced by oxides on the tube ID. Limited MFL field data from riser inspections are reported in the open literature.

3.2.4 AC Field Measurement

Alternating current field measurement (ACFM) was developed to be used for detection and sizing of surface-breaking fatigue cracks in sub-sea offshore structures. ACFM is a non-contact electromagnetic technique, which can operate in extreme environments. A uniform electric current is used to produce a magnetic field in the pipe being inspected.[61] Two small magnetic field sensors are used to detect changes in the Bx and Bz components of the magnetic field. If defects are present, disturbances in the magnetic field can be quantified and related back to the length and depth of the defect.[62] A schematic of the magnetic and electrical fields created during ACFM are shown in Figure 57.

ACFM can be applied through nonconductive coatings up to 5-mm thick.[63] In contrast to EC testing, sizing with ACFM can be conducted without calibration.[64] Additional benefits to EC testing include inspection through much thicker coatings, less sensitivity to lift off, and a greater measurable defect depth. Little pre-inspection cleaning is required and data can be easily automated and archived for later analysis. ACFM has been used with data filtering and normalization to defect corrosion pits as small as 0.75-mm diameter $\times$ 0.75-mm deep.[65]

For application to risers, ACFM arrays have been developed to allow large areas to be inspected in a single scan.[63] However, for outer surface inspection, any insulation coating would likely have to be removed. A second scan would still be required for internal inspection.

3.2.5 Field Signature Method

The field signature method (FSM) was developed and patented by the Center of Industrial Research (CorrOcean) in 1985 for crack formation and growth in welded offshore steel jackets.[66] The principles have since been shown to be applicable to corrosion damage as well. The system consists of sensors with up to 50 metallic pins arranged in a rectangle, which are connected to the outer surface of the pipe in the region to be inspected. A small current is applied, which travels from one side of the matrix to the other. The voltage between neighboring pins gives an electrical signature of the component dependant on the geometry/thickness and electrical conductivity of the pipe (see Figure 58). Any changes in the pipe due to corrosion affect the electrical signature by lowering the voltage between the pins.

Because the FSM sensor is generally permanently attached to the component, measurements can be taken online, with daily measurements to monitor the state of the riser. Subsequent measurements are easily compared to historical data to obtain life trends. However, data is averaged over the volume of the section of pipe inspected. This may lead to less sensitivity to localized corrosion and would likely still require inspection using a second technique to more thoroughly investigate the cause of signal changes and find the precise location of the defect for sizing purposes. Even sizing of very large defects is difficult with the FSM.[67,68] The depth and length of corrosion defects are interrelated in the effect they have on the FSM. In addition, because the FSM measures over a large inspection volume, the fraction of damaged area can greatly affect the interpretation of the results. A special post-processing module can extend the analysis capabilities to include pitting-type damage. However, the quantitative capabilities of the FSM for localized corrosion, and even uneven general corrosion damage, are questionable. However, the method does seem to perform well for uniform corrosion with reported sensitivities of 0.1-5% of the wall thickness. For subsea use, temperature changes must be measured and compensated for in the measured voltage. This is generally built into the FSM system.

3.2.6 Pulsed Eddy Current

A pulsed eddy-current technique was developed in 1980s and deployed in early 1990s for detection of CUI in plant pipes.[12,16] Recently, it is used also for riser inspection.[27] A pulsed eddy-current approach allows the detection of wall-thinning areas in the riser without removing the outside protection coatings or biomass. The advantages of a pulsed eddy-current technique are its larger penetration depth, relative insensibility to lift-off, and the possibility to obtain a quantitative measurement result for wall thickness. A pulsed eddy-current technique uses a stepped or pulsed input signal for the detection of CUI. The probe coil sends a pulsed magnetic field. This penetrates through any non-magnetic material between the probe and the object

under inspection (e.g., insulation material). The varying magnetic field will induce eddy currents on the surface of the object (see Figure 59). The diffusive behavior of these eddy currents is related to the material properties and the wall thickness of the object. The detected eddy-current signal is processed and compared to a reference signal. The material properties are eliminated and a reading for the average wall thickness within magnetic field area results (see Figure 60). One reading takes a couple of seconds and is an average of wall thickness under the transducer footprint. The signal is logged and can be retrieved for later comparison in a monitoring approach. This technique can be applied for nominal riser wall thickness between 6 and 65 mm and insulation thickness less than 150 mm using transducers within 50- to 100-mm-diameter range. It performs spot measurements and measures the remaining wall thickness of the riser. Performance comparison of several pulsed eddy-current tools has been reported.[12,16] The systems can also be used under water. An example of pulsed eddy-current riser corrosion measurements is shown in Figure 61. An operator performs spot measurements and measures the remaining wall thickness of the riser. It is not necessary to clean the riser from coating or biomass.

3.3 Radiography

Radiography of pipes involves measuring penetrating X- or γ-rays after they pass through the pipe walls. Differences in the thickness and absorption/scattering characteristics will affect the level of radiation that passes through the part and is recorded on the other side. Thus, defects such as bulk metal loss, cracks aligned parallel to the inspection plane, and inclusions of different densities are easily detected with radiography.

3.3.1 Tangential Radiography

Tangential radiography, also known as profile radiography, is used for detailed inspection of small pipe sections under insulation. Figure 62 shows a setup that can be used to inspect for corrosion in the pipe walls. From the contrast in the radiograph image, the thickness of the pipe wall can be measured for both edges of the pipe. An example radiograph from a pipe and the corresponding contrast profile are shown in Figure 63. From the profile, the thickness at that location of the pipe can be extracted from the distance from the peak to the edge of the pipe, as shown by the arrow in the bottom right of the profile. In order to ensure complete inspection, successive measurements must be made while rotating the source and film around the circumference of the pipe. Among the drawbacks to tangential radiography is the difficulty of inspecting pipes with diameters greater than about 10 in., [69] radiation concerns which require care to ensure nearby workers are not exposed to unhealthy levels of radiation, and the expense of film. In addition, film-based tangential radiography is a slow process, requiring

images to be acquired from many angles since only a small quadrant of the pipe can be inspected at one time.

3.3.2 Digital Radiography

Recently, film-less, real-time, and digital radiography has been used to find internal and external corrosion defects in an insulated splash zone while the riser remains in service.[12,16] One example is the real-time inspection system, ThruVU™, that addresses some of the time expense concerns of film radiography. A typical scanning digital radiography system uses Iridium 192 source and a linear array of radiation detectors.[69,70] The system is placed on the riser using rope access personnel. The vertical and tangential track system is used to scan the riser. A typical industrial scanning digital radiography system, which consists of a radiation source and a linear array of radiation detectors, is designed to examine insulated riser ranging from 100 to 600 mm (200 to 900 mm with insulation) in diameter. During the detection process, a narrow beam of radiation is projected through the riser wall and onto the detector array, which is positioned on the opposite side of the riser. As the scanner moves along the pipe, data are acquired, and a color-coded image that shows the relative thickness of the pipe wall is generated and displayed on the monitor in real time scanning can only be performed down to the splash zone. Figure 64 reveals typical real-time, color-coded digital radiography images of corrosion damage in pipes. In this figure, the black areas represent severe corrosion, while the yellow areas indicate no corrosion. The graph indicates the severity of the corrosion in cross section. The digital radiography system detects corrosion defects as small as 6 mm in diameter and 1.2-mm deep. Inspection speeds using any radiographic system are currently limited to around 5 ft per minute.[70]

3.4 Infrared Thermography

Thermography is an emerging inspection technique that monitors the changes in the thermal patterns of an object as they are heated, cooled, or kept in a steady-state ambient condition. Thermography is becoming a more popular NDE tool as equipment costs become more reasonable and computer technologies are able to handle the large quantities of data generated by the thermographic equipment.

Commercial thermographic equipment is available that can detect a 0.2°C temperature difference in materials up to 500°C. Beyond that temperature, a 2°C difference is detectable for temperatures up to 3500°C. Thus, thermography is becoming a very well established NDE method. The technique offers the added benefit of being somewhat intuitive, due to the vivid color images produced, leading itself to easier operator training, qualification and certification.

Figure 65 is an example of a thermographic image of a laser weld. Note that in this figure, you can clearly distinguish the focal area of the laser beam, the “white hot spot”, the backing bar of the weld joint, and overall heating pattern of the weld joint, which in this instance was of critical importance for the assembly integrity.

Recently, a process has been developed for infrared imaging of subsurface defects by ultrasonically stimulating the component. In this technique an ultrasonic transducer is coupled to the part and then the ultrasonic energy from the transducer causes the defect areas to heat up. Consequently, these heated areas are detectable by the thermal imaging system.[71] There is a timeframe inherent to the thermographic methods used by this method. Essentially, the timeframe is due to the need to observe a thermal transfer, which can be substantial depending on part geometry. Testing procedures developed for thermography will need to incorporate specific time frames to ensure sufficient time elapses before drawing conclusions about the part integrity, else defects could be missed and the part incorrectly evaluated or examination time could be protracted. Due to the comparative nature of this process, it would likely be beneficial to image the part during new construction, archive this thermal image, and compare future inspection thermal profiles with the original fabrication thermal profiles.

The distinct advantage of thermography is the intuitive nature of the process and its ability to image a wide variety of materials. The key to using thermography is whether it can detect discontinuities of relevant size in the composite. Calibration standards, reference samples, and components with known defects will need to be developed to properly ascertain the capabilities of this NDE method. This NDE method is gaining in popularity as more research demonstrates the vast amount of information to be ascertained from the thermal profiles of materials. It will be difficult to implement for riser inspection.

3.5 Acoustic Emission

Acoustic emission (AE) is a form of monitoring components for stress waves that are generated in the material due to events such as hydrogen evolution, stress corrosion cracking, plastic deformation, or crack propagation. These events generate stress waves with the sudden release of strain energy. AE is often used during proof testing to test for the presence of defects in the material. Often, the acoustic signal is generated by propagation of a small crack under loading, as shown schematically in Figure 66.

Advantages are that AE is rather insensitive to part geometry, non-intrusive on the process, requires access only at sensors, and tests large areas at one time. However, there are a

couple of severe drawbacks to the method. AE is very sensitive to the material. In addition, external sources of noise, such as ocean waves hitting the structure, complicate AE analysis.

In-service testing using AE must overcome the noisy environment. The environmental noise has potentially prohibitive effects on AE. However, by applying suitable frequency filtering, signal recognition techniques and spatial filtering, monitoring is possible in otherwise prohibitive conditions.[72]

For application to risers, permanent sensors would need to be installed to continuously monitor for corrosion, deformation, and crack initiation or propagation events. However, due to the large size of riser structures, a large number of sensors would be required, placed at intervals of 1 to 6 m. This could make AE prohibitively expensive.

3.6 Conventional/Enhanced Visual Inspection

Visual inspection includes a wide array of techniques, ranging from an experienced welder looking for undercut on the weld to the use of boroscopes to inside narrow tubes to newer "enhancement" techniques such as D Sight™ or Edge of Light™.[73] All of these methods can only be related to surface damage and are beneficial primarily for initial detection of defects since surface-related measurements can be misleading, depending on the damage morphology.

Conventional visual inspection is the most basic of NDE methods and is practiced regularly with most every application, generally referring to direct observation of the surface, either without aid, with a tool such as a boroscopes to gain visual access inside tight locations, or with some magnifying system. For many defect types, such as surface cracks, general corrosion, and geometric weld defects (undercut, drop through, distortion, etc.), visual inspection can act as a first line of defense by providing fast, inexpensive guidance for areas which should be more closely examined.

Enhanced visual inspection builds on any of the conventional inspection tools by using some strategic lighting conditions, image processing, fusion of images from various angles, or other enhancements. D Sight™[74] uses double pass retroreflection to visualize the surface topography of a piece (see Figure 67). Edge of Light™[75] uses diffraction effects as light passes through a narrow slit to highlight slope changes on the test surface (see Figure 68). Both of these methods are methods to enhance the contrast due to surface topography.

For application to risers, visual inspection is not likely to be a major part of the inspection methodology, due to the difficulties in gaining visual access to the affected areas.

3.7 Magnetic Particle Inspection

Magnetic particle inspection enables detection of surface or near-surface discontinuities in ferromagnetic materials. To inspect, the component is magnetized and fine ferromagnetic particles are applied over the surface. Surface defects in the component will cause a flux leakage field around the defect. The magnetic particles placed on the surface near the defect will then align themselves with the field while particles not near a defect will slide off the test article (see Figure 69). The result is an outline of the defect indicating its location, size, shape, and extent.

Magnetic particle inspection is a sensitive method of locating small, shallow surface cracks in parts of all shapes and sizes without elaborate pre-cleaning. Larger sub-surface cracks may also be detectable. However, there are many limitations to the method. Magnetic particle inspection:

- Can only be used with ferromagnetic particles
- Will not work with wide cracks
- May require magnetization from different directions to perform a complete inspection
- Post-cleaning may be necessary to remove remnant particles
- Large currents are needed to magnetize large structures
- Inspection is not easily quantified as with some other methods.

4.0 Survey of Riser Inspection Experience

A survey of NDE manufacturing companies, NDE inspection companies, and operating companies was completed to collect information about current instrumentation and inspection/operators' experience for riser inspection.

Per the vintage of the platform, API RP 2A dictates what level of inspection is required for the structure and risers. It usually falls in a 3- to 5-year period for conventional risers. Typically, a visual inspection for above the water dynamic riser components is performed once a year and for below water components in a 3- to 5-yr interval. During visual inspection, depth measurements are performed using depth gauges. NDE for all components is conducted as needed. UT is the traditional method for riser corrosion damage assessment. Ideally, the industry would like to see full UT mapping that would give sufficient information to run FFS assessments. A simple magnetic particle testing has been applied if external cracks are

suspected in bare risers and more complicated ACFM techniques has been used for detection and accurate sizing of external or internal cracks. NDE techniques such as short-range UT, ACFM, and MFL are mature and commercially available on a broad base. The inspection cost varies and is defined on case-by-case basis. Other techniques such as long-range UT, pulsed eddy current, and digital radiography are still under development and for that reason equipment and services are available only from limited number of vendors. Several techniques such as short-range UT and ACFM are already deployed on ROVs for shallow and deepwater inspection applications using a specialized instrumentation.

Current piping pigs adapted for riser inspection can miss defects (false positives) and indicate the presence of defects that are not present (false negatives). The speed control of older generation pigs, are also a concern, although currently only 6% of the approximately 35,000 miles of offshore pipelines in GOM including risers are piggable.[2,5] Thus far, this search has found that assessing the remaining service life of aging risers will be largely dependent on the accuracy of analyzing corrosion damage to the riser surface in the atmospheric, splash and submerged environmental zones using several primary NDE technologies. Significant uncertainties for wall piping thickness measurements based on the MFL pig's recordings have been reported.[1] Pigging of flexible risers has been reported for geometric verification. Flexible risers are difficult to inspect from the outside due to their complex structure and the lack of developed nondestructive techniques. A feasibility study has been performed to investigate the best possible NDE techniques and their limitations to be incorporated in a dedicated flexible riser inspection system. Results of radiographic (standard film radiography, imaging plates, linear detector, and image intensifier) and electromagnetic (eddy current and MFL) have been published.[6]

The following discussions related to MFL and deep water riser issues are adopted from the summary of a white paper issued by Pipeline Inspection and Leak Detection Working Group at 2003 International Offshore Pipeline Workshop.[5]

The inline inspection industry is highly dependent on the electronics and computer industries. The miniaturization of electronic components has allowed for the development of highly advanced electronic packages which make up the "intelligence" of intelligent pigs. This has a particular influence in the areas of configuration of the intelligent pigs, sensor technology, data storage and onboard data processing. Storage media such as hard disk drives, digital audio tape, and flash memory enabling the storage of hundreds of gigabytes up to terabytes of data.

Tools are becoming more compact as the result of electronic miniaturization. Pipelines of ≥ 3 in. are being inspected currently.

The use of “Hall” effect sensors as a standard, as opposed to induction coils, for intelligent pigs utilized for MFL metal loss inspection (smaller sensors means an increased circumferential resolution and more data). Shear-wave ultrasonic sensors utilized for “crack” inspection and EMAT sensors utilized for crack inspection.

The last decade has also seen the development of new techniques or technologies being used for intelligent pigging. In particular:

- High-resolution metal loss inspection
- XYZ mapping of pipelines (GPS coordinates)
- Ultrasonic intelligent pigs for crack inspection
- Wheel coupled, shear wave ultrasonic, intelligent pigs for crack detection
- Circumferential MFL intelligent pigs long axially oriented defects
- ILI tools equipped with speed control (i.e., for use in high flow speed natural gas pipelines).

Another important advance within the inline inspection industry in the last 10 years is the use of service providers’ software packages that give the customers quick access to the inspection results and associated signal data recorded.

With the use of new rare earth magnets and yoke designs, the ability to inspect >1-in. wall thickness is now possible in some diameters. Also, advances in battery packs used make for increased inspection lengths. The capability of imaging thicker wall pipe is significant in deepwater pipelines and in Arctic areas, where historically thicker wall pipes may pose a problem to sufficiently magnetize the pipe.

Pipeline ILI can potentially be improved by:

- More educational opportunities, similar to the SGA Pigging School or the OPS-TSI Pigging School
- Bi-directional pigging
- Unpiggable pipelines, e.g., robotic applications
- Real-time computational analysis of pig run data.

Pipe-in-pipe applications do present a challenge for inspection with intelligent pigging. The inner pipe can be fully inspected. The outer pipe is extremely limited. The transition/weld areas are also quite complicated for pipe-in-pipe applications. A risk analysis may show that a pipe-in-pipe design is “safer” by design, however this would not automatically prove that it is safer to operate and maintain over it’s lifetime in comparison to a single pipe application. With ILI, the integrity of the outer pipe cannot be fully monitored over time.

The term “un-piggable” is not well understood in the industry. There are no numbers available, however, there has been quite some experience and knowledge gained that shows, for example, because a pipeline segment is not equipped with a launcher and/or receiver, it is deemed un-piggable. The fact of the matter is that the ILI service providers have been able to negotiate a great number of what used to be thought of as restrictions. It is a matter of sitting down and understanding the pipeline physical parameters that make a line un-piggable and determining which modifications are necessary and how much money they would cost. Pigging through varying pipe diameters is an example of this challenge.

The subject of piggability should be considered during the design of a new pipeline or modification to an existing pipeline. Intelligent pigs do detect installations along the pipeline for which they can be characterized. This allows the pipeline operator a way to verify against the original design drawing.

After the installation of a new pipeline, the pipeline operator might consider inline inspection to provide information regarding any construction faults that should be addressed. A “baseline” inspection might also be performed in order to establish the condition of the pipeline at startup which would also assist in future inline inspection work to aide in determining any change in condition.

Inline inspection can provide very valuable information regarding where a pipeline needs to be repaired to ensure safe operation and integrity. Again, the future piggability of a pipeline should be considered when making the necessary repairs.

If it is determined that a pipeline segment is to be inspected by intelligent pigging, a maintenance pigging program should be considered to ensure throughput and piggability with respect to inspection. An inline inspection survey provides information on repairs as well as areas that may be in need of maintenance.

Most offshore export systems are gathering systems with multiple receipts and deliveries. They are typically built in a tree-like design employing subsea connections. Even new export lines tie into existing gathering systems and more often than not tie in subsea. So any move toward smart piggable pipelines typically requires:

1. A topside connection at the junction to the connecting system with appropriately sized traps, valves and other components.
2. A riser design where wall changes and the choice of the subsea connector does not preclude the ability to smart pig.

Assuming the line is built to be smart pigged, the key question to answer is: *Can we locate the anomaly identified by the inspection?* Assume for this discussion that an anomaly of 6% is to be found. Current tracking systems mapped against construction records give us our best estimate of which pipe joint contains the anomaly, but the real issue is whether the diver or ROV can confirm that the anomaly has been found. Physical confirmation of a known anomaly has been found to be difficult, even in a land based environment. Hence, the technology improvements for offshore systems must also include instrumentation and methods that enable divers or ROVs to quickly confirm the anomaly, even when working in adverse conditions.

In particular for deepwater, some of the most important of the before-mentioned issues include piggability and the limited access to the pipeline. The design needs of pipelines in the deepwater environment could hinder the ability of the current inline inspection tools in safe negotiation and successful inspection. If something were to happen during an inspection of such a pipeline, such as “sticking” a pig, accessibility to alleviate the issue is quite restricted. If an anomaly were predetermined to be critical based on an inline inspection, it could very costly or even prohibitive to verify this or to even take necessary action.

With increases in static head pressures on the pipe, some ovalization might limit inspection coverage around the full circumference of the pipe. This could also lead to tool hang-ups. The formation of hydrates may also limit inspection coverage around the full circumference over the length of the pipeline and increase the risk of sticking a pig. In addition, increased wall thickness, J-lay collars and buckle arrestors may pose a problem.

In deepwater, steel catenary risers are used to connect subsea flowlines or pipelines to floating. Riser inspection systems as noted above are not available for deepwater at this moment, but it should prove possible to upgrade the systems to greater depths. Diver accessible areas should be able to employ the same methods used in conventional risers, provided sea currents do not

interfere. Deeper water will likely rely on UT using ROVs or pigs. Since UT has an effective range of only a few hundred feet, long catenaries will pose a problem.

In deepwater pipelines, inspection of a wall thickness >1 in. is achievable for pipeline diameters >18 in.

Current UT approaches techniques probably are not capable to meet the recent very aggressive requirements for detection and accurately sizing of shallow flaws in deep-water risers (pipelines and flow lines also). In some new heavy-walled riser and tendon projects very aggressive requirements for AUT system capabilities have been proposed. It is still a challenge for current AUT practice in the field to achieve requirements for ±0.3-mm sizing accuracy for height of surface breaking defects, ±0.8-mm for buried defects, and to define the length of all defects within 2 mm of actual. Recent experimental studies demonstrated that the majority of the defects will be sized within ±2-mm accuracy for height and ±10-mm for flaw length.[48-50]

Typically, ranking of the inspection technologies is based on inspection effectiveness for detecting, locating, and sizing the damage.[76] This approach identifies three classes of inspection effectiveness:

- Fairly effective
- Usually effective
- Highly effective.

For the mature ultrasonic thickness gauging techniques the proposed highly effective inspection effectiveness to measure the corrosion rate may be where 50 to 100% of both internal and external riser surfaces are examined and measured in detail using AUT mapping. Usually, effective inspection possibly will engage mapping of 5 to 50% of both surfaces and extensive point-by-point thickness measurements. Fairly effective inspection could simply involve spot checks over less than 5% of the external surface. These classes not cover screening techniques such as long-range UT or pulsed eddy current. Because of the high uncertainties related to the accuracy of thickness measurements using these techniques and still unknown POD they would fall below fairly effective level. Screening techniques should be used only to detect a significant ricer wall loss but not for corrosion rate determination. Table 2 in this paper can be used only as a very preliminary and simple step for developing of ranking criteria.

At this moment, a scientific ranking cannot be presented because of the limited knowledge of POD and accuracy of sizing for each of the existing and probable techniques for riser corrosion

and fatigue inspection. POD and accuracy of sizing data from riser AUT qualification trials are not available for the public. Long-range UT performance demonstration is on-going effort for many years and POD database for piping inspection, including risers, is under development but still uncompleted (see Figures 70 and 71). Two research projects, the RACH and CRIS projects, have been initiated to fill this gap.[77-79] RACH project objectives have been established to generate detection and sizing reliability data only for localized corrosion realistic defects on a set of 50 test pipes and develop a philosophy for implementing these data. Seven NDE techniques have been assessed: ultrasonics A-scan manual, computerized UT thickness mapping, low-frequency long-range ultrasonics, creeping head wave ultrasonics, pulsed eddy current, MFL, and ACFM. In the CRIS project other techniques such as x-ray has been investigated. RACH addressed several problems with producing and using POD curves. For the RACH project, corroded area dimensions have been sized at minimum tolerance and depth measurements associated to nominal thickness. The response of different NDE systems has been addressed also. It has been described that negative results for POD against depth measurements can be obtained by comparison pulsed eddy current (large footprints) with ET or MFL (small footprints) results or long- with short-range UT results. The CRIS project is still ongoing.

To increase the reliability of the current/new NDE techniques a formalized inspector training and approval is needed. Programs for qualification/validation of capabilities of the equipment/procedure are needed also. There is still a need for initiation of research projects, and for additional funding for NDE R&D organizations/industry. Additional research is required to boost the development of new riser inspection NDE techniques with better detection and sizing capabilities for deepwater, robotics developments and improvements/applications of long-range UT (resolution, accuracy, coatings etc), pulsed eddy current (probe footprint reduction, better accuracy, and higher penetration), and digital radiography (better detectors).

5.0 Recommended Practice

A complete solution to riser inspection must utilize multiple, complementary NDE techniques in order to overcome the limitations of each method. For example, some methods are exceptional at testing over a long distance of piping but have limited abilities to determine the exact location of the damage and accurately quantify the damage state. Other methods are capable of excellent damage quantification but are too expensive or slow to apply over large sections of the riser. The advanced technique chosen for a specific riser inspection depends on diameter and length to be inspected, material, damage phenomena, accessibility, accuracy of results, and cost. So, the recommended inspection process will be a multi-step approach, first utilizing a

less expensive, fast method to screen for damaged locations, followed by closer inspection at damaged locations.

External riser inspection:

1. Long-range UT (drycouplant or MsS) for initial localization of the damage area without removing Splashtron

2. Local PEC or digital radiography for a relatively accurate damage assessment without removing Splashtron

3. Local AUT (focused single or PA) corrosion mapping and the most accurate assessment.

Internal riser inspection:

1. MFL for piggable riser for corrosion mapping and relative accurate assessment

2. AUT tools (focused single or PA) for corrosion mapping and crack detection and the most accurate assessment.

The recent trends of combining several UT techniques with visual inspection are positive and will continue. Combining more than two methods such as visual, radiographic, ultrasonic, electromagnetic in one system is not feasible in the near future because of the complexity of riser inspection.

6.0 Conclusions

Operators should develop a methodology for determining which inspection technique, tool (or combination of both) is appropriate for their risers based on a prior knowledge for the corrosion damage mechanisms. Understanding the capabilities of these tools and technologies along with the design and service history of the riser, should also aid in determining the frequency and intensity of the inspection program needed. Finally, keeping in mind GOM failure statistics and the potential fatigue damage in deep water risers, more attention is warranted in ascertaining the integrity of risers and monitoring corrosion and fatigue.

7.0 Acknowledgments

This study was funded by the U.S. Department of the Interior, Minerals Management Service, under Contract Number 1435-01-02-CT-85094. ABB Vetco Gray, Canspec, GUL, Imperium, PI Ltd, SwRI, IHI Southwest Technologies, RTD, and Rosen contribution to this project and their permission to use some images is greatly appreciated.

8.0 References

1. Bea, R. G., "A Risk Assessment & Management Based Process for the Re-qualification of Marine Pipelines, Proceedings of Alaskan Arctic Offshore Pipeline Workshop", U.S. Minerals Management Service, Anchorage, AK (Nov. 1999).

2. U.S. Department of the Interior, Minerals Management Service Data Base for Pipeline Failure Statistics in the Gulf of Mexico (Nov. 2002).

3. Lozev, M. G., Smith, R. W., and Grimmett, B. B., "Evaluation of Methods for Detecting and Monitoring of Corrosion Damage in Risers", OMAE 03, Cancun (June 2003).

4. van Agthoven, R., "Ultrasonic Inspection of Risers a New and Simple Approach", Proceedings 7th European Conference of Non-Destructive Testing, Copenhagen (1998).

5. 2003 International Offshore Pipeline Workshop, New Orleans (Feb. 2003).

6. Veith, E., Bucherie, C., Lechien, J. L., Jarrousse, J. L., and Rattoni, B., "Inspection of Offshore Flexible Risers with Electromagnetic and Radiographic Techniques", *Insight*, Vol. 43, pp. 404-408 (June 2001).

7. Newton, K. and Saunderson D. H., "NDT Research for the Oil and Gas Industry", *British Journal of NDT*, Vol. 34, pp. 123-128 (Mar. 1992).

8. Still, J. R. and Nelson, P., "Development of Corrosion Monitoring in the Offshore Production Industry", *British Journal of NDT*, Vol. 34, pp. 336-340 (July 1992).

9. Singh, A. and McClintock, R., "Computer-Controlled System for Nondestructive Thickness Measurement of Corroded Steel Structures", *Journal of Energy Resources Technology*, Vol. 105, pp. 499-502 (Dec. 1983).

10. Birring, A. S., "Overview of Factors Affecting Ultrasonic Inspection of Tension Leg Platforms", Proceedings of the Sixth ASME Symposium on Offshore Mechanics and Arctic Engineering, Houston, TX, pp. 513-616 (Feb. 1987).

11. Alleyne, D. N. and Cawley, P., "Optimization of Lamb Wave Inspection Techniques", *NDT & International*, Vol. 25, pp. 11-22 (1992).

12. de Raad, J. A., “Novel Techniques for Outside Inspection of Plant Pipework”, *Insight*, Vol. 37, pp. 409-412 (June 1995).

13. Alleyne, D. N. and Cawley, P., “The Exitation of Lamb Waves in Pipes Using Dry Coupled Piezoelectric Transducers”, *Journal of NDE*, Vol. 15, pp. 11-20 (1996).

14. Alleyne, D. N. and Cawley, P., “Long Range Propagation of Lamb Waves in Chemical Plant Pipework”, *Materials Evaluation*, Vol. 55, pp. 504-508 (1997).

15. Alleyne, D. N., Cawley, P., Lank, A. M., and Mudge, P. J., “The Lamb Wave Inspection of Chemical Plant Pipework, Review of Progress in Quantitative Nondestructive Evaluation”, Vol. 16B, D. O. Thompson and D. E. Chimenti, eds., New York, Plenum Press, pp. 1269-1276 (1997).

16. Rudlin, J. R., “Review of Existing and Possible Techniques for Corrosion under Insulation and Wall Thickness Measurement in Steel Pressure Containments”, *Insight*, Vol. 39, pp. 413-417 (June 1997).

17. Kwun, H. and Dynes, C., “Long-Range Guided Wave Inspection of Pipe Using the Magnetostrictive Sensor Technology – Feasibility of Defect Characterization, Nondestructive Evaluation of Utilities and Pipelines II”, *SPIE*, Vol. 3400, pp. 326-337 (1998).

18. Kwun, H. and Bartels, K., “Magnetostrictive Sensor Technology and Its Applications”, *Ultrasonics*, Vol. 36, pp. 171-178 (1998).

19. Wassink, C.H.P., Roberts, M. A., de Raad, J. A., and Bouma, T., “Condition Monitoring of Inaccessible Piping”, 15th WCNDT, Rome (Oct. 2000).

20. Mudge, P.J., “Field Application of the Teletest® long range ultrasonic testing technique”, Insight, Vol. 43, pp. 74-77 (Jan. 2001).

21. Sheard, M., and McNulty A., “Field Experience Using Long-Range Ultrasonic Testing”, Insight, Vol. 43, pp. 74-77 (Jan. 2001).

22. Alleyne, D. N., Paclakovic, B., Lowe, M.J.S., and Cawley, P., “Rapid Long Range Inspection of Chemical Plant Pipework Using Guided Waves”, *Insight*, Vol. 43, pp. 93-96 (Jan. 2001).

23. Mudge, P.J., “Properties of Wave Modes Used for Long-Range Ultrasonic Testing”, Insight, Vol. 44, pp. 101-102 (Feb. 2002).

24. Barshinger, J., Rose, J. L., and Avioli, M. J., “Guided Wave Resonance Tuning for Pipe Inspection, Transaction of the ASME”, *Journal of Pressure Vessel Technology*, Vol. 124, pp. 303-310 (2002).

25. http://www.twi.co.uk/j32k/protected/band_13/oilgas_caseup24.html

26. Teletest ® News, Issue 4 (November 2001).

27. van Agthoven, R., de Raad J. A., “How to Inspect Platforms and Risers: an Effective Approach and New Challenges”, The Pipeline Pigging, Integrity Assessment, and Repair Conference, Houston, TX (Feb. 2003).

28. Disher, C., and Harthorn L., “Mobile Marine Riser Inspection and Management Program”, OMAE 03, Cancun (June 2003).

29. Krautramer, J. and Krautramer, H., ”Ultrasonic Testing of Materials”, Springer-Verlag (1990).

30. Matthies, K., “Thickness Measurements with Ultrasound”, DGZfP/DVS-Verlag (1999).

31. http://www.ndt.net/article/v04n01/lasser2/lasser2.htm.

32. van der Ent, J. and Dijkstra, F. H., “Evaluation of Ultrasonic Inspection Techniques for the Root Region of Girth Welds”, PRCI Final Report PR-220-9123 (1996).

33. Dijkstra, F. H. and Blinde, M. R., “Evaluation of Ultrasonic Technology for Volumetric Weld Inspection of Pipeline Girth Welds”, PRCI Final Report PR-220-9437 (1997).

34. de Raad, J. A., “High Speed Ultrasonic Inspection of Field Girth Welds During Pipeline Construction”, Pipeline Technology Conference, Ostende, Belgium (1990).

35. Kopp, F., Perkins, G. G., Laing, B. S., Prentice, G., Springmann, S. P., and Stevens, D. M., “Automatic Welding and Ultrasonic Inspection for J-Lay of the MARS Tension Leg Platform Export Pipelines”, Offshore Technology Conference (1997).

36. Kopp, F., Perkins, G., Stevens, D., and Prentice, G., “High-Resolution Sizing Capabilities Required for Automated Ultrasonic Inspection of Offshore Pipeline and Catenary Riser Welds”, *Pipes & Pipelines International* (May-June 2001).

37. Gross, B., Connelly, T., van Dijk, H., and G-Scott, A., “Providing Complete Ultrasonic Inspection on Pipeline Girth Welds”, *Proceedings of 3rd International Pipeline Technology,* Vol. III, Brugge, Belgium Elsevier Science (May, 2000).

38. Gross, B., Connelly, T., van Dijk, H., and G-Scott, A., “Flaw Sizing Using Mechanised Ultrasonic Inspection on Pipeline Girth Welds”, NDT.net, Vol. 6, No. 7 (July 2001).

39. Dijkstra, F. H., v.d. Ent, J., and Bouma, T., “Defect Sizing and ECA Criteria: State of the Art in AUT”, *Proceedings of 3rd International Pipeline Technology,* Vol. III, Brugge, Belgium Elsevier Science (May, 2000).

40. Denys, R. M., “Girth-Weld Defect Qualification Methods Need to Rationalized”, *Pipe Line & Gas Industry*, Vol. 8, No. 9 (Sept. 1999).

41. ASTM “Standard Practice for Mechanised Ultrasonic Examination of Girth welds Using Zonal Discrimination with Focused Search Units”, E-1961-98.

42. Ginzel, E., Ginzel, R., Gross, B., Hoff, M., and Manuel, P., “Developments in Ultrasonic Inspection for Total Inspection of Pipeline Girth Welds”, 8th Symposium on Pipeline Research, Houston, TX (Aug. 1993).

43. Ginzel, E. and Hoff, M., “Further Developments in Ultrasonic Inspection of Pipeline Girth Welds”, NDT.net, Vol. 1, No. 06 (June 1996).

44. Glover, A. and Hodgkinson, D., “Application and Validation of Mechanized Ultrasonic Inspection for Manual Metal Arc Pipeline Welds”, Ed. R. Denys, *Pipeline Technology*, Vol. II (2000).

45. Lozev, M., “Phased-Array Technology Promises Increased Ultrasonic Inspection Productivity, Accuracy and Flexibility”, *EWI Insights*, 14(1), pp. 1-3 (2001).

46. Moles, M., Piché, P., and Dubé, N., “Application of Phased Array Ultrasonics for Girth Welds”, PRCI Final Report PR-270-9813 (1999).

47. Zirnhelt J., Sjerve E., and Bryant G., “The Application of Ultrasonic Phased Array Technology to Pipeline Girth Weld Inspection”, WTA, Australia (Mar. 2002).

48. Lozev, M., “Validation of Current Approaches for Girth Weld Defect Sizing Accuracy by Pulse-Echo, Time-of-Flight Diffraction, and Phased-Array Mechanized Ultrasonic Testing Methods”, Final Report, PRCI Contract No. GRI-8369 and EWI Contract No. 45800-IRD (July 2002).

49. Morgan, L., “The Performance of Automated Ultrasonic Testing (AUT) of Mechanized Pipeline Girth Welds”, 8th ECNDT, Spain (June 2002).

50. Lozev, M., Hodgkinson, D., Spencer, R., and Grimmett, B., “Validation of Current Approaches for Girth Weld Defect Sizing Accuracy by Pulse-Echo, Time-of-Flight Diffraction, and Phased-Array Mechanized Ultrasonic Testing Methods”, ERPG-PRCI-APIA 14th Joint Technical Meeting (May 2003).

51. http://www.ndt.net/article/wsho0597/schleng2/frame_b.htm#5

52. Stelwagen, U., NIL Project on NDT of Thin Plate, Final Report, Amsterdam, NIL (1996).

53. Frost, H. M., “Electromagnetic-Ultrasound Transducers: Principles, Practice, and Applications”, Physical Acoustics, Vol. XIV (1979).

54. Thompson, R. B., “Physical Principles of Measurements with EMAT Transducers”, Physical Acoustics, Vol. XIX (1988).

55. Sun, Y. S. and Udpa, S., Lord, W., and Cooley, D., “A Remote Field Eddy Current NDT Probe for the Inspection of Metallic Plates”, *Materials Evaluation*, Vol. 54, pp. 510-512 (1996).

56. Atherton, D.L. and Sullivan, S., “The Remote-Field Through-Wall Electromagnetic Inspection Technique for Pressure Tubes", *Materials Evaluation*, Vol. 44, pp. 1544-1550 (1986).

57. Sullivan, S., Atherton, D. L., and Schmidt, T. R., “Comparison of Conventional, Through-Wall and Remote Field Eddy Current Techniques", *NDT International*, Vol. 22, pp. 203-206 (1989).

58. http://www.ndeassociates.com/rfec.htm

59. Bubenik, T. A., et al., “Magnetic Flux Leakage (MFL) Technology for Natural Gas Pipeline Inspection”, Battelle, Report Number GRI-91/0367 to the Gas Research Institute (Nov. 1992).

60. Nestleroth J. B. and Bubenik, T. A., “Magnetic Flux Leakage (MFL) Technology for Natural Gas Pipeline Inspection”, Battelle, Report to the Gas Research Institute (Feb. 1999).

61. Topp, D., “The ACFM Technique and its Application to the Inspection of Oil and Gas Installations”, *Insight*, Vol. 36 (1994)

62. Raine, A., “The Use of the Alternating Current Field Measurement Technique for Mechanised and Semi-Automated Inspection”, *Insight*, Vol. 39, pp. 271-275 (1997)

63. Marques, C. R., Martins, M.V.M, and Topp, D. A., “Experiences in the use of ACFM for offshore platform inspection in Brazil,” 15th WCNDT, Rome (Oct. 2000).

64. Lugg, M. C., Lewis, A. M., Michael, D. H., and Collins, R., “The Non-Contacting ACFM Technique”, Electromagnetic Inspection, IOP Short Meetings 12, Institute of Physics Publ., Bristol, pp. 41-48 (1988).

65. Raine, A. and Lugg, M., “A Review of the Alternating Current Field Measurement Inspection Technique”, *Sensor Review*, Vol. 19, pp. 207-213 (1999).

66. Daaland, A., “The FSM Method for Monitoring Process Pipelines Offshore”, *Insight*, Vol. 38, pp. 434-439 (1996).

67. Twomey, M. and Rothbart, J., "Setting Up a Condition Management Program", Maintenance Technology (1997).

68. Walker, S. M., “New NDE Developments Support Rapid, Economical Screening for Flow-Accelerated Corrosion,” First International Conference on NDE in Relation to Structural Integrity for Nuclear and Pressurised Components, Amsterdam (Oct. 1998).

69. Hecht, A., Bauer, R., and Lindemeier, F., “On-Line Radiographic Wall Thickness – Measurement of Insulated Piping in the Chemical and Petrochemical Industry”, *ECNDT ’98*, Copenhagen (1998).

70. Gupta, N. K., Goyal, V. K., and Gupta, K. K., "In-Service Inspection of Insulated Pipelines," American Nuclear Society's Seventh Topical Meeting on Robotic and Remote Systems, Augusta, GA (Apr. 1997).

71. Thomas, R. L., Favro, L. D., Han, X., Ouyang, Z., Sui, H., and Sung, G., “Infrared Imaging of Ultrasonically Excited Subsurface Defects In Materials,” U.S. Patent No. 6,236,049 (May 2001).

72. Yuyama A, “Fundamental Aspects of Acoustic Emission Applications to the Problems Caused by Corrosion,” Corrosion Monitoring in Industrial Plants Using Nondestructive Testing and Electrochemical Methods, ASTM STP 908, G.C. Moran and P. Labine, Eds., American Society for Testing and Materials, Philadelphia, pp. 43-74 (1986).

73. Forsyth, D. S., Komorowski, J. P., Gould, R. W., and Marincak, A., “Automation of Enhanced Visual NDT Techniques,” 1st Pan American Conference for Nondestructive Testing, PACNDT ’98, Toronto (1998).

74. Heida, J. H. and Bruinsma, A.J.A., “D-Sight Technique for Rapid Impact Damage Detection on Composite Aircraft Structures,” 7th European Conference on Non-destructive Testing, ECNDT ’98, Copenhagen (1998).

75. National Research Council Canada http://iar-ira.nrc-cnrc.gc.ca/smpl_5d2.html.

76. Wintle, J. B., Sanderson, R. M., and Schneider C.R.A., “An Appraisal of Statistical Inspection Strategies and Inspection Updating, TWI (2002).

77. Rudlin, J. R. and Kenzie B. W., “Probability of Detection for Corrosion Defects”, 3rd European-American Workshop on Reliability of NDE and Demining, Berlin (Sept. 2002).

78. Wall, M. and Lilley, J., “Use of POD Data in Inspection Planning and Prediction of Residual Flaw Distributions in the Offshore Industry – Do I need 90% POD”, Probability of Detection for Corrosion Defects, 3rd European-American Workshop on Reliability of NDE and Demining, Berlin (Sept. 2002)

79. Plant Integrity LTD performance demonstration and POD data (2002).

Table 1. Summary of Methods and Techniques (Technologies) for Detecting and Monitoring of Corrosion Damage in Risers

Method and Technology	Advantages	Disadvantages	Primarily Corrosion Damage
Visual conventional	Large area of exposure and inexpensive	Limited to external damage, measurements not accurate, subjective and labor intensive	External general corrosion or pitting
Visual enhanced	Large area of exposure and very fast inspection	Requires preparation, still difficult quantification and subjective	External general corrosion or pitting through magnification or accessibility
Short-range ultrasonics (manual point-by-point measurements, single echo, or echo-to-echo)	Need access only to one side, sensitive and accurate, no coating removal	Requires couplant and clean and smooth surface for single echo and coating removal if it is thicker than 6 mm for echo-to-echo	Corrosion loss and pitting
Short-range ultrasonics (bonded array, single echo, or echo-to-echo)	Continuous local corrosion condition monitoring	Requires bonding of an array of flexible transducers strip, coating removal, clean and smooth surface	Corrosion loss and pitting
Short-range ultrasonics (semi-AUT – TOFD)	Fast inspection with good resolution	Requires couplant and clean and smooth surface and coating removal	Erosion corrosion
Short-range ultrasonics (AUT mapping with single/multiple focused probes or PA)	Fast inspection with good resolution and sensitivity	Requires couplant and clean and smooth surface and rust/coating removal	External/internal corrosion loss and pitting if internal/external surface is regular
Short-range ultrasonics (AUT pigging with single/multiple L- or SV-waves probes or PA)	Fast inspection with good resolution and sensitivity	Requires couplant and clean and smooth surface, riser opening	Pitting, corrosion loss, and SSC
Long-range ultrasonics (guided waves and dry-couplant transducers)	Global screening technique, fast inspection, requires non couplant	Sensitive to both internal and external damage, no absolute measurements	General corrosion loss
Long-range ultrasonics (guided waves and MsS)	Global screening technique, fast inspection, requires non couplant	Sensitive to both internal and external damage, no absolute measurements	General corrosion loss
Long-range ultrasonics (guided/SH-waves and electromagnertic acoustic transducers)	Global screening technique, fast inspection, requires non couplant	Sensitive to both internal and external damage, no absolute measurements	General corrosion loss, SSC
ET conventional	Good resolution, multiple layer capability	Low throughput, operator training	Surface and subsurface flaws
RFEC	Portability	Sensitive to both internal and external damage	Surface and subsurface flaws
Pulsed eddy current	Deep penetration	Large footprint	General corrosion loss
MFL	Through coatings penetration	Thickness limitations	General thinning, pitting
ACFM	Through coatings penetration	Low throughput, operator training	Surface and subsurface flaws
FSM	Continuous local corrosion monitoring	Small area, expensive	Surface flaws
Digital radiography	Good resolution and image interpretation	Radiation safety	Pitting and general corrosion
Tangentional radiography	Portable	Radiation safety	General loss
AE	Global monitoring technique	Prone to false indication from wave motions	SSC
Infrared thermography	Large area scan	Complex equipment, layered	Surface corrosion
Magnetic particles	Easy, portable	Clean surface	Surface cracks

Table 2. Summary of Methods and Techniques (Technologies) Limitations

Technology	Can use on Steel?	Can use on Titanium?	Can use on Composites?	Can see through Coatings?	Can see through Insulation?	Pipe wall thickness Range?	Max length of Inspection?
Visual conventional	Yes	Yes	Yes	No	No	N/A	N/A
Visual enhanced	Yes	Yes	Yes	No	No	N/A	N/A
Short-range ultrasonics (manual point-to-point measurements, single echo, or echo-to-echo)	Yes	Yes	No	Yes, <6 mm	No	1-40 mm	N/A
Short-range ultrasonics (bonded array, single echo, or echo-to-echo)	Yes	Yes	No	No	No	1-40 mm	N/A
Short-range ultrasonics (semi-AUT – TOFD)	Yes	Yes	No	No	No	6 mm+	N/A
Short-range ultrasonics (AUT mapping with single/multiple focused probes or PA)	Yes	Yes	No	No	No	1 mm+	N/A
Short-range ultrasonics (AUT pigging with single/multiple L- or SV-waves probes or PA)	Yes	Yes	No	No	No	6 mm+	N/A
Long-range ultrasonics (guided waves and dry-couplant transducers)	Yes	Yes	No	Yes	Yes	1 mm+	<30 m
Long-range ultrasonics (guided waves and MsS)	Yes	Yes	No	Yes	Yes	1 mm+	<30 m
Long range ultrasonics (guided/SH-waves and EMATs)	Yes	Yes	No	Yes	Yes	1 mm+	<10 m
ET conventional	Yes	Yes	Yes-R	Yes	No	1 mm+	N/A
RFEC	Yes	Yes	No	Yes	No	1 mm+	N/A
Pulsed eddy current	Yes	Yes	No	Yes	Yes	6 mm+	N/A
MFL	Yes	No	Yes-R	Yes	No	12 mm	N/A
ACFM	Yes	Yes	No	Yes	No	1 mm+	N/A
FSM	Yes	Yes	No	No	No	1 mm+	N/A
Digital radiography	Yes	Yes	Yes-R	Yes	Yes	1 mm+	N/A
Tangentional radiography	Yes	Yes	No	Yes	Yes	1 mm+	N/A
AE	Yes	Yes	Yes-R	Yes	Yes	1 mm+	N/A
Infrared thermography	Yes	Yes	No	Yes	No	1 mm+	N/A
Magnetic particles	Yes	No	No	No	No	1 mm+	N/A

Table 3. Average Depth Error per Ultrasonic Technique

Probe	Water Path (mm)	Focus Direction	Focal Type	6-dB Spread		Avg. Error[(a)] (mm)
				Focal Plan	Lateral	
12.7-mm dia., 5-MHz lens	50	N/A	Spheric	1.2	N/A	0.16
PA 16 elements, 5 MHz, 1 mm	44	Axial	Linear	0.8	7.2	0.35
PA 32 elements, 10 MHz, 0.31 mm	117	Axial	Linear	1.7	1.9	0.36
PA 32 elements, 10 MHz, 0.31 mm	117	Curcumf.	Linear	1.7	1.9	0.28
PA 32 elements, 10 MHz, 0.31 mm	47	Axial	Linear	0.7	4.8	0.26
PA 32 elements, 10 MHz, 0.31 mm	47	Circumf.	Linear	0.7	4.8	0.16

Note:
(a) Average of 19

Table 4. Typical Inspection Parameters and Search Units

Zone Name	Assumed Height mm (in.)	Target mm (in.)	Technique	Angle (Degrees)	Frequency (MHz)
Root	1.3 (0.05)	0.5-1.0 (0.02-0.039) notch	P/E	50-70	4.5-7.5
LCP	1.3 (0.05)	2 (0.008) FBH	P/E	55-70	5-7.5
Hot Pass 1	1.65 (0.065)	2-3 (0.079-0.118) FBH	P/E	45-55	4.5-7.5
Hot Pass 2	1.65 (0.065)	2 (0.079) FBH	P/E	45-55	4.5-7.5
Fill 1	3 (0.118)	2-3 (0.079-0.118) FBH	Pitch/catch	40/50-45/55	4.5-7.5
Fill 2	3 (0.118)	2-3 (0.079-0.118) FBH	Pitch/catch	40/50-45/55	4.5-7.5
Fill 3	3 (0.118)	2 (0.079) FBH 0.8-1.0 (0.032-0.039) notch	P/E	55-65	4.5-7.5

Table 5. Achieved Height Sizing Accuracy

Acronym	Approach Description	Height Sizing Accuracy, Avg. Error "a" in mm and % of Detected Flaws		
		$a < \pm 0.5$	**$\pm 0.5 > a < \pm 2$**	**$\pm 2 > a < \pm 4$**
A1	Focused multiprobe, amplitude linearization	35	35	30
A2	Focused multiprobe, proprietary sizing algorithm	45	45	10
A3	Non-focused multiprobe, zone and amplitude interaction rules	30	45	25
A4	Focused PA, 48 el., amplitude linearization	40	20	40
A5	Focused PA, 64 el., amplitude linearization	15	35	50
A6	Focused PA, 64 el., sectorial scanning	25	25	50
A6-open	Focused PA, 32 el., raster and sectorial scanning	75	25	n/a

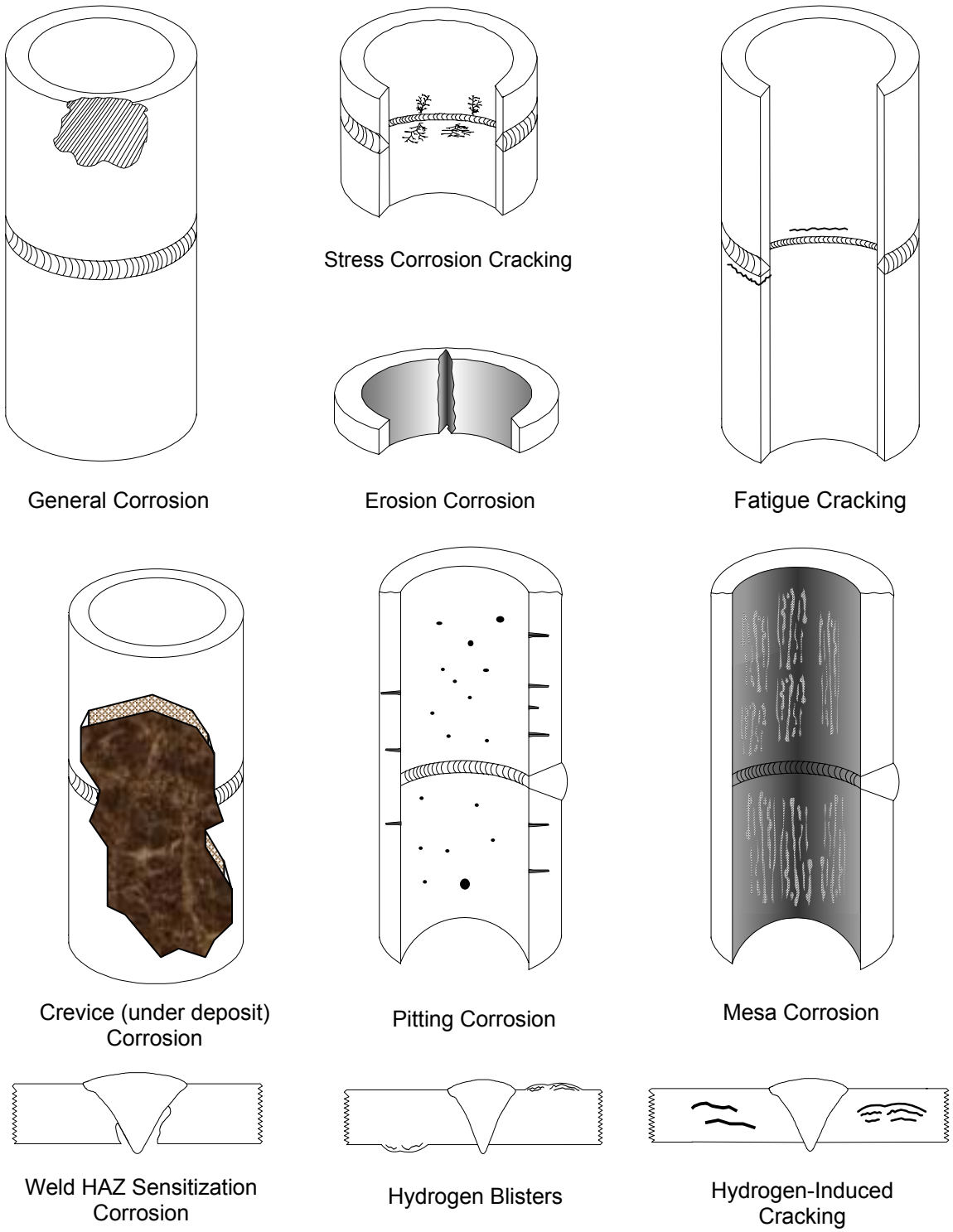

Figure 1. Anticipated Riser Corrosion and Non-Corrosion Phenomena

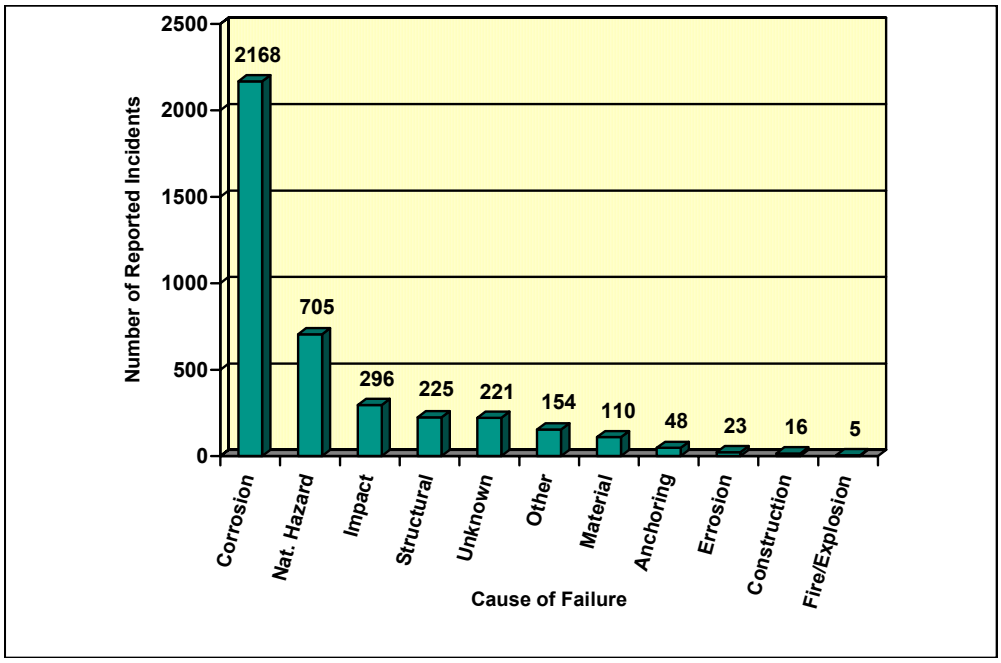

Figure 2. General Pipeline Failure Statistics for GOM (Source: DOI/MMS)

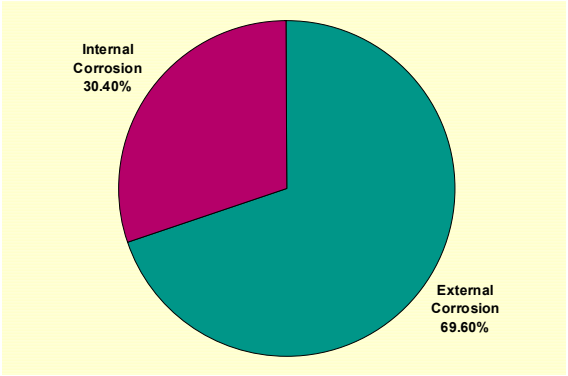

Figure 3. Location of the Damage (Source: DOI/MMS)

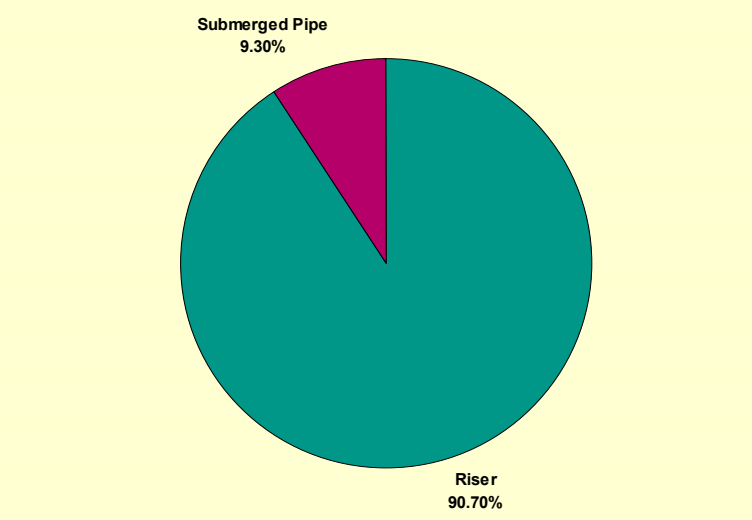

Figure 4. Location of Damage Due to External Corrosion (Source: DOI/MMS)

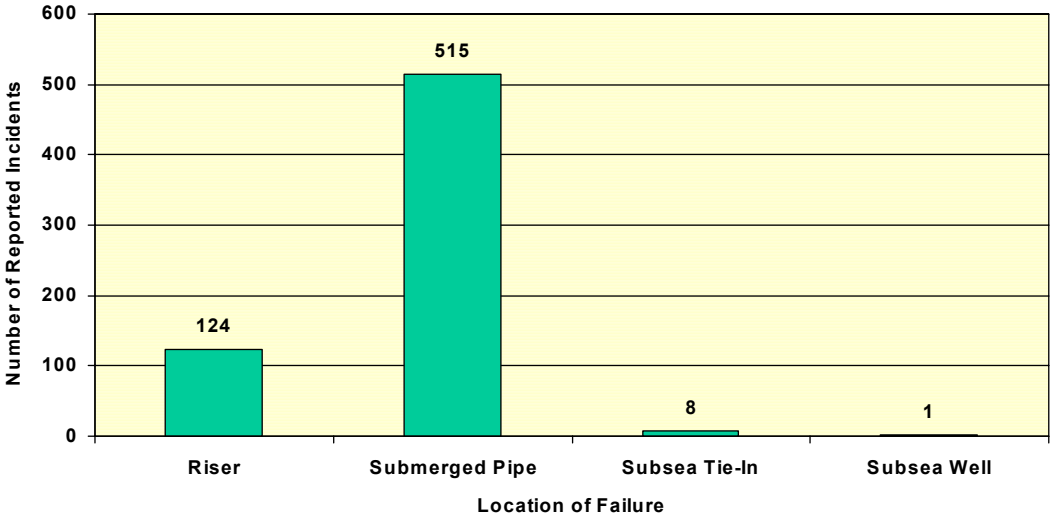

Figure 5. Location of Damage Due to Internal Corrosion (Source: DOI/MMS)

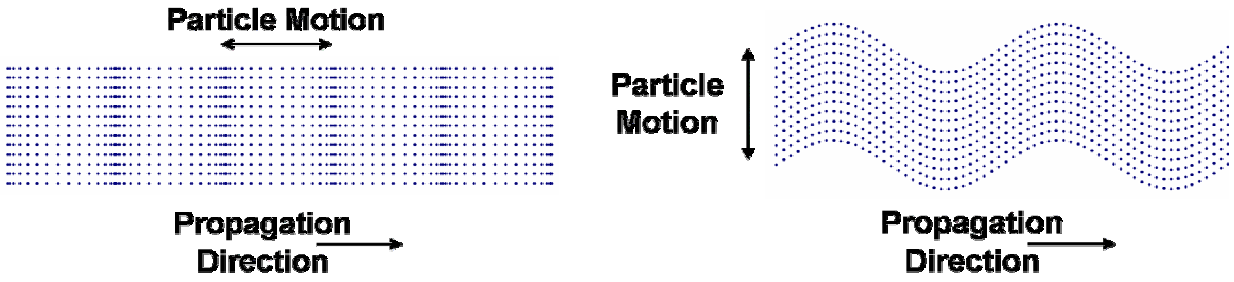

Figure 6. Particle Motion in L-Waves (Left) and T-Waves (Right)

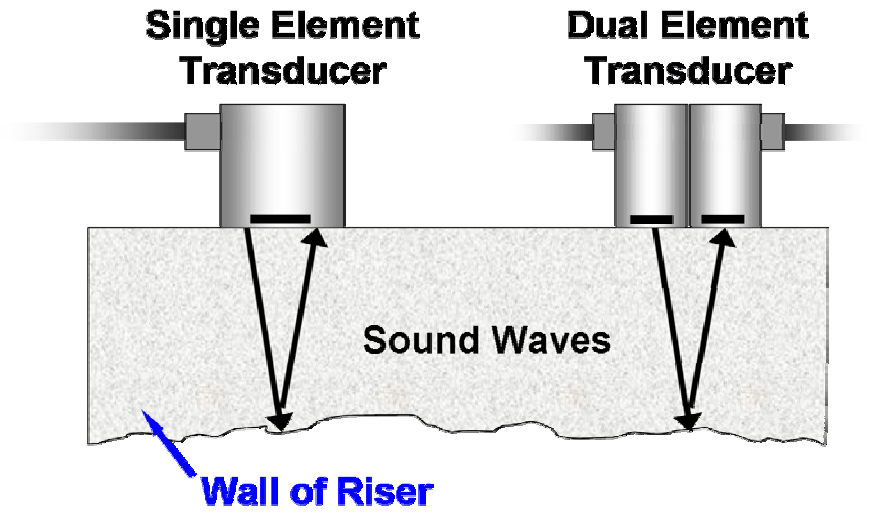

Figure 7. Thickness Measurements Taken using Two Types of UT Probes

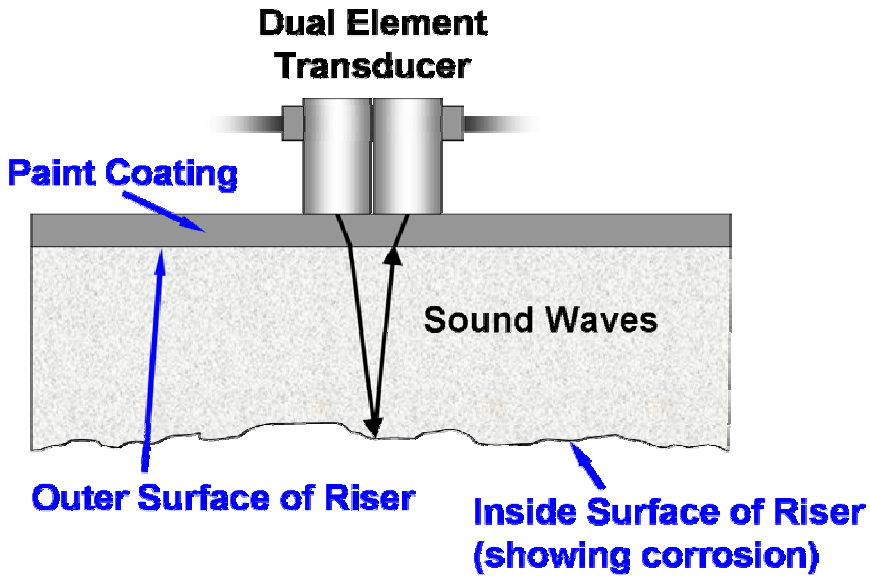

Figure 8. **Thickness Measurements Obtained Through a Paint Coating using a Dual UT Probe**

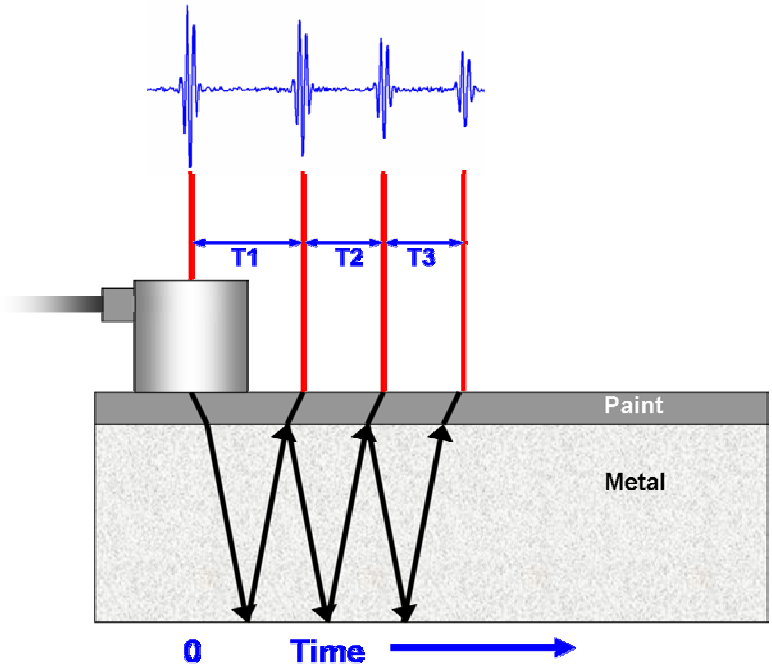

Figure 9. **Thickness Testing using Longitudinal Waves** (Wave propagation is actually perpendicular to the surface, but is spread out in the image to show the source of acoustic signals.)

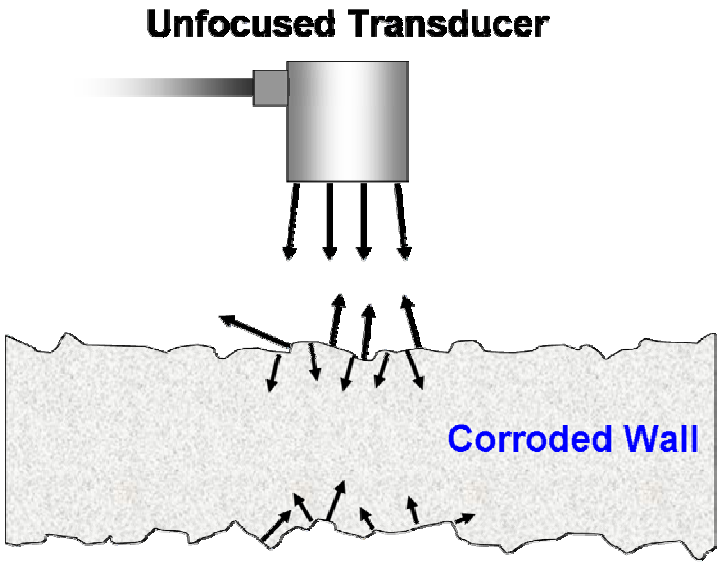

Figure 10. Effect of a Corrosion-Roughened Surface on the UT Beam

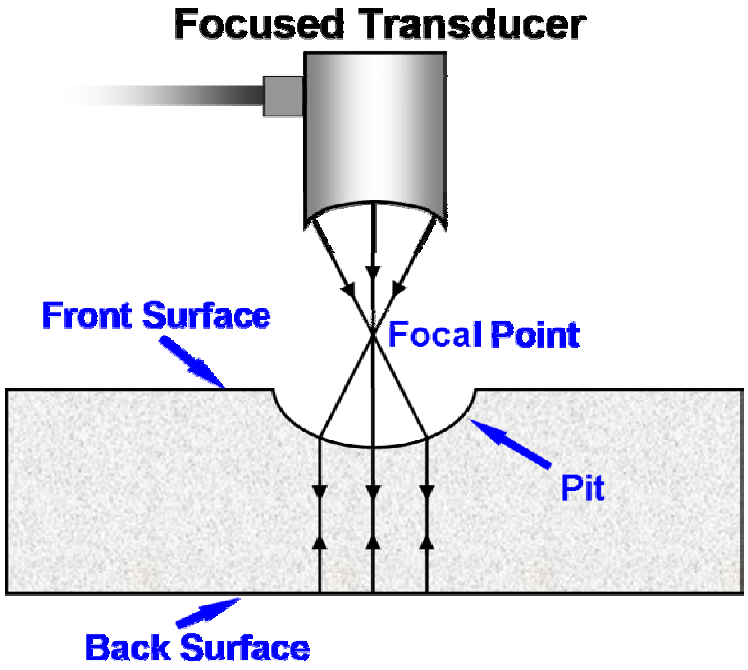

Figure 11. Advantage of a Focused Transducer in Transmitting Signals Through a Pitted Region

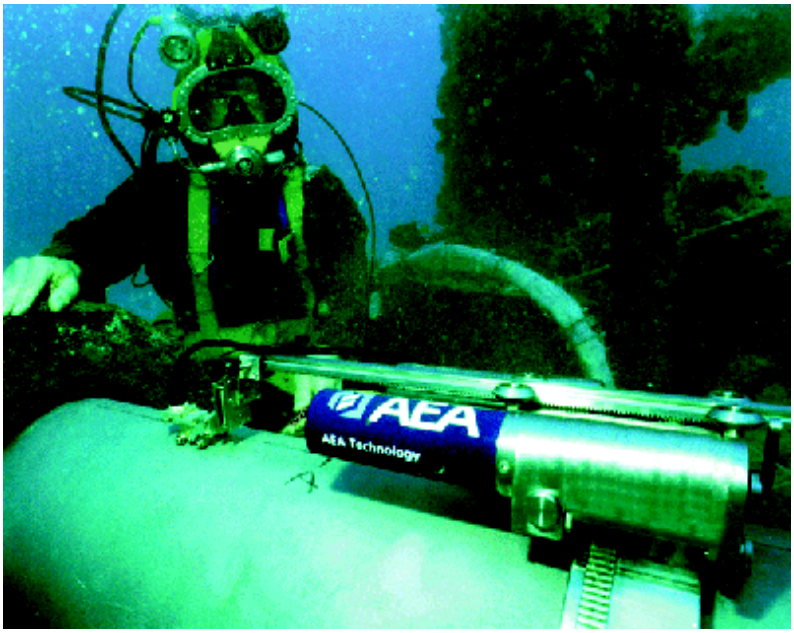

Figure 12. **Ultrasonic Shallow Water Sub-Sea Inspection System** (Courtesy: AEA Technology, U.K.)

Figure 13. **ROV with AUT System and Sub-Sea Scanner Mounted on Tool Skid** (Courtesy: Force Technology, Denmark)

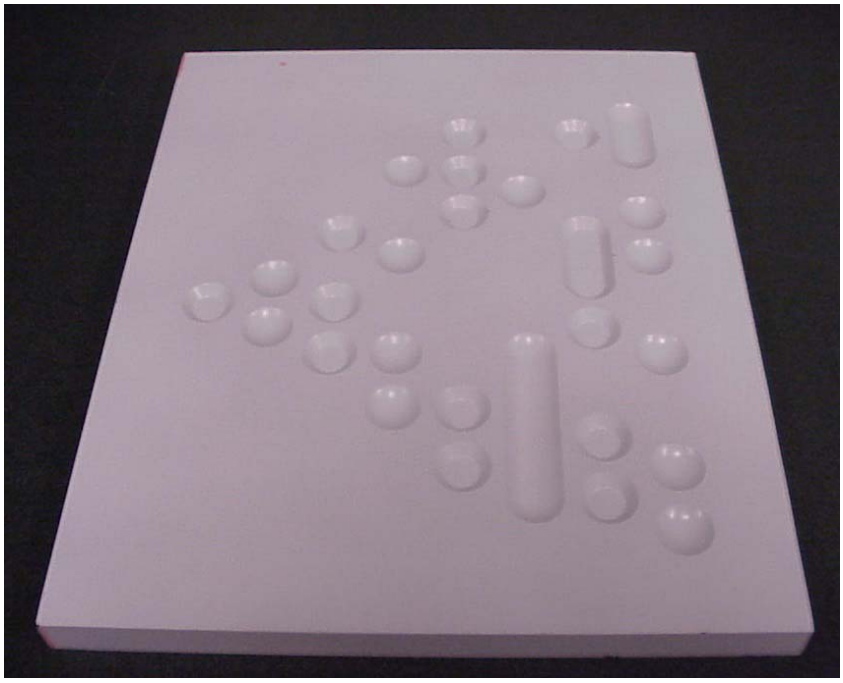

Figure 14. Calibration Block used for UT Depth Measurement Comparisons

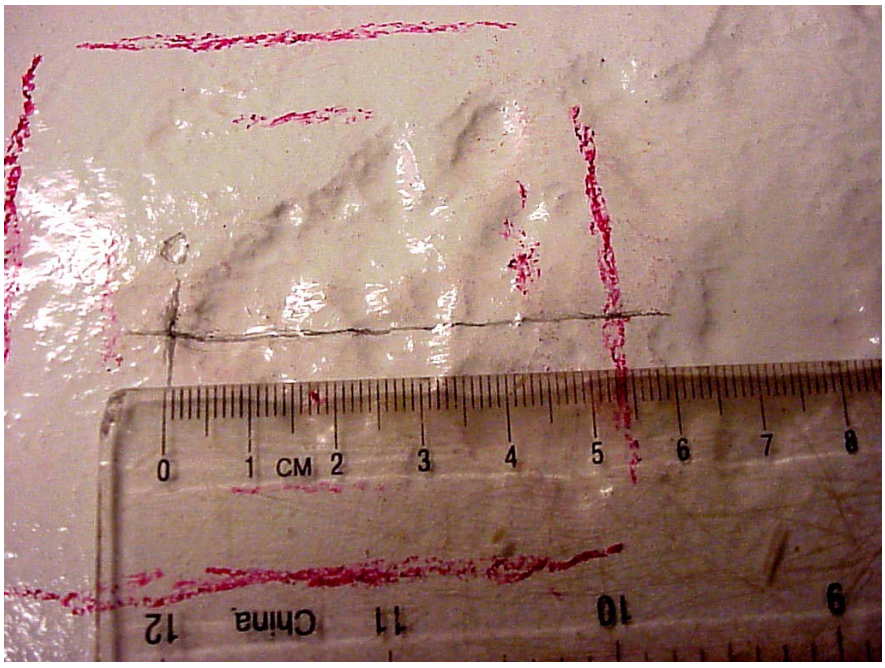

Figure 15. Corrosion Damaged Area used for UT Depth Measurement Comparisons

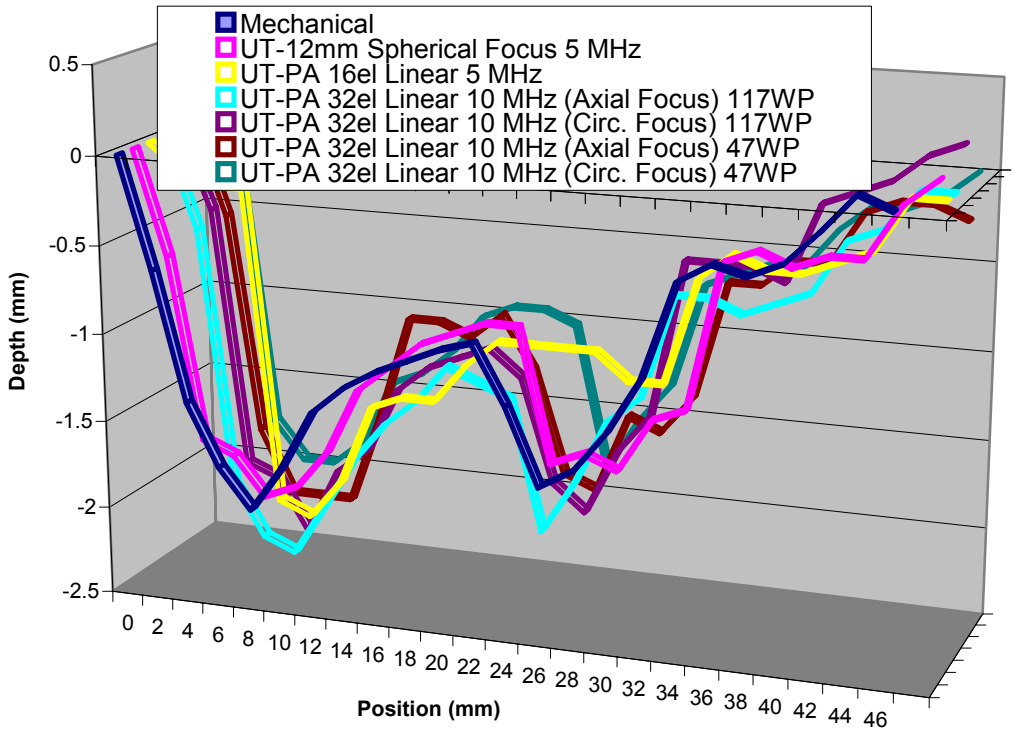

Figure 16. Comparisons of Mechanical (Destructive) Results and Automated Ultrasonic Corrosion Mapping Results using Single Focused and PA Transducers

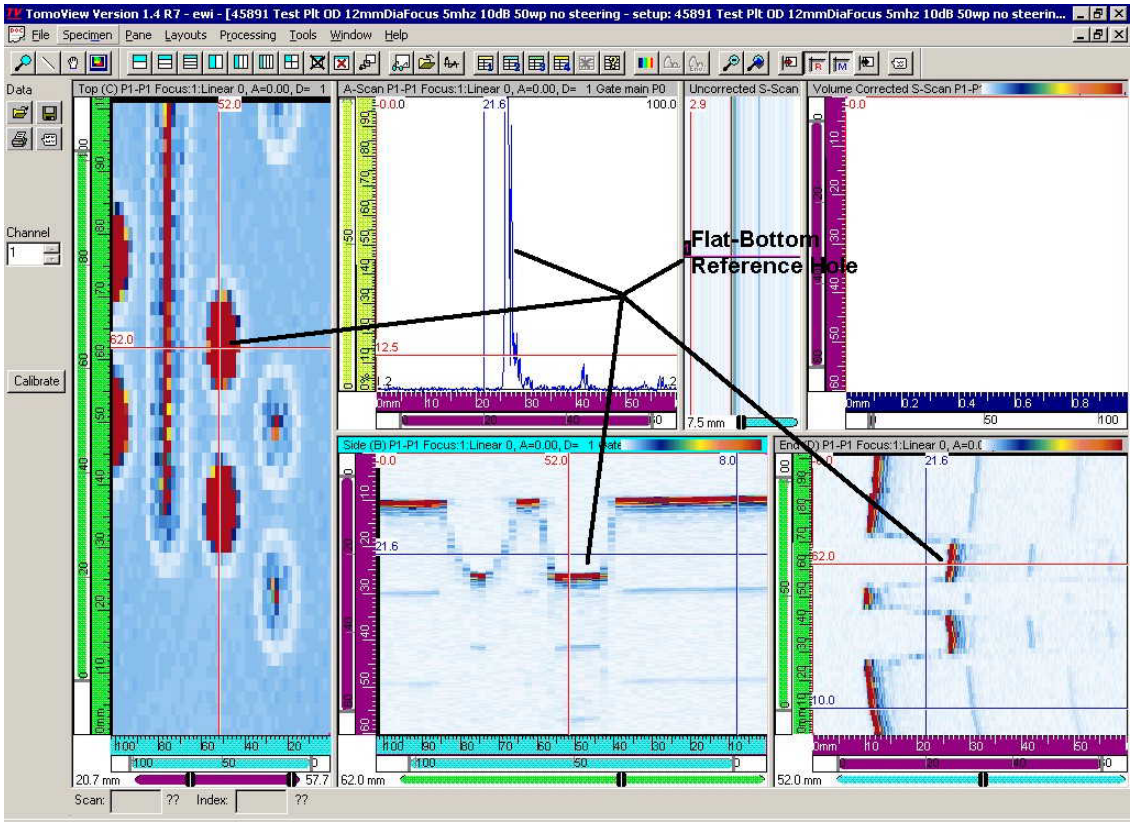

Figure 17. Visualization of Automated Ultrasonic Corrosion Mapping and Imaging of the Calibration Block using 12-mm-Diameter, 5-MHz Single-Focused Transducer

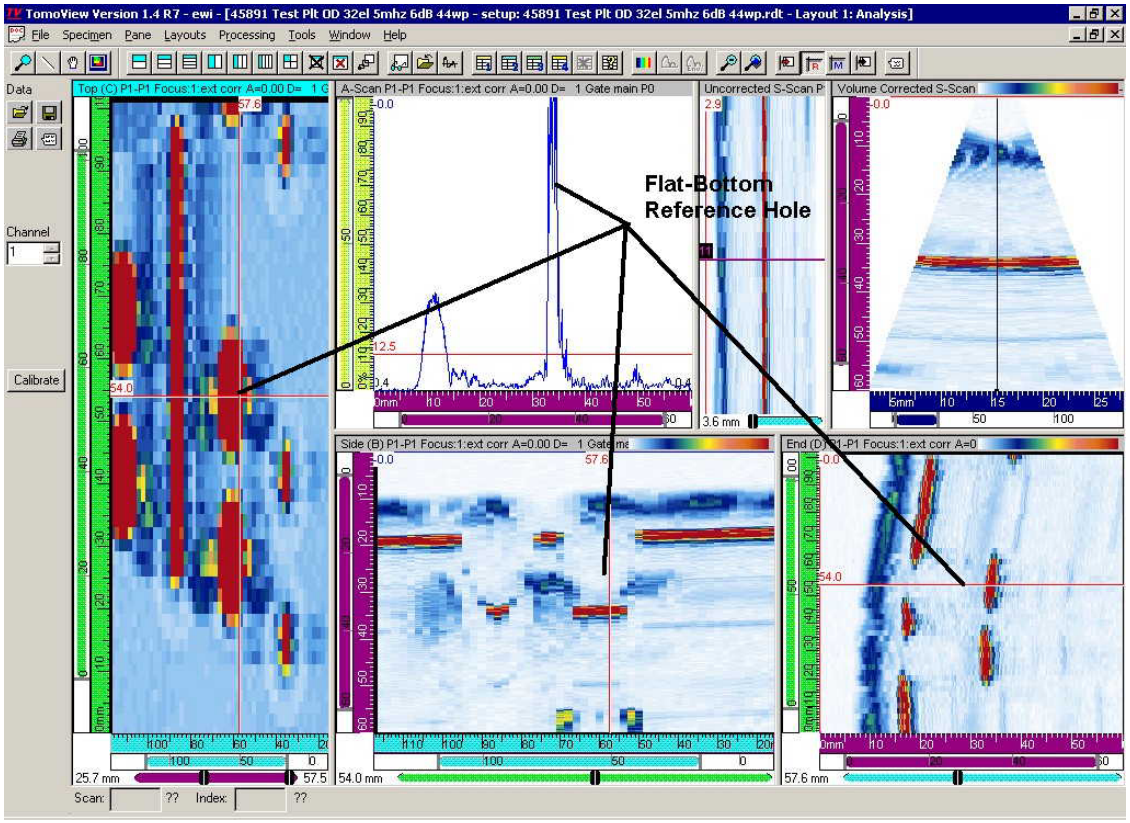

Figure 18. Visualization of Automated Ultrasonic Corrosion Mapping and Imaging of the Calibration Block using 32-Element, 5-MHz PA Transducer

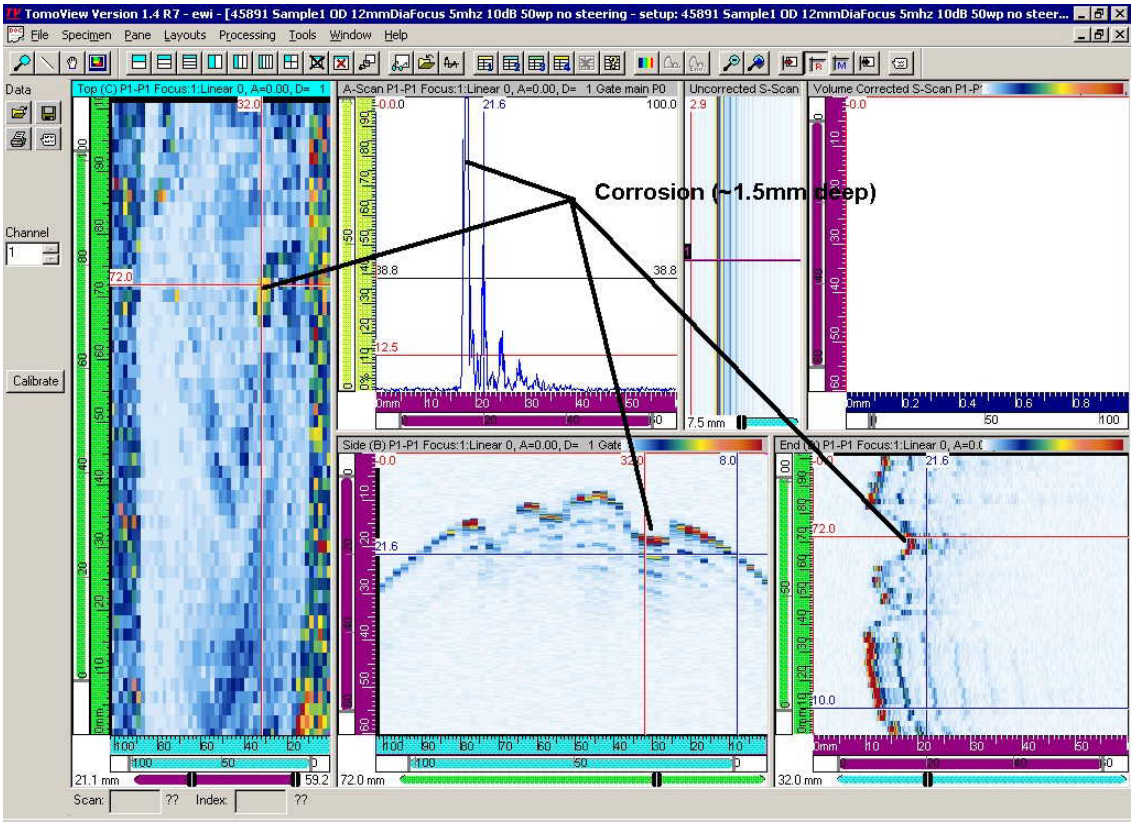

Figure 19. Visualization of Automated Ultrasonic Corrosion Mapping and Imaging of the Damaged Sample using 12-mm-Diameter, 5-MHz Single-Focused Transducer

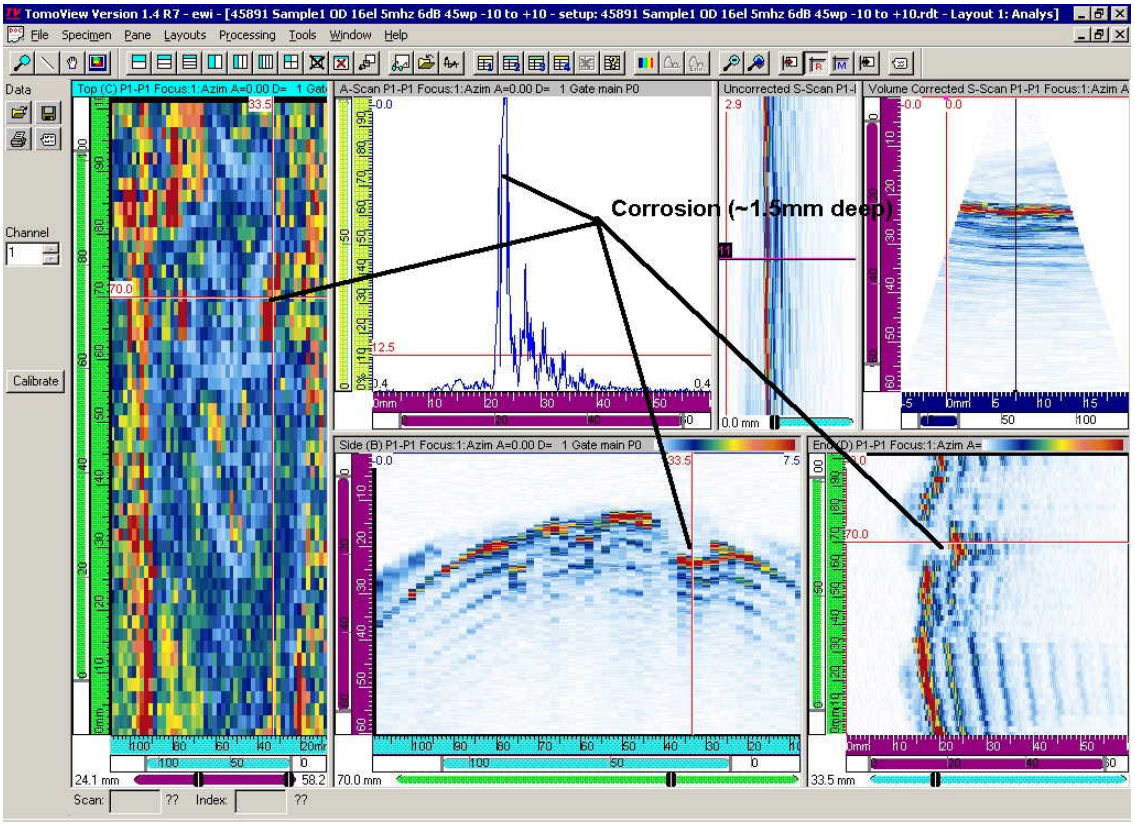

Figure 20. Visualization of Automated Ultrasonic Corrosion Mapping and Imaging of the Damaged Sample using 32-Element, 5-MHz PA Transducer

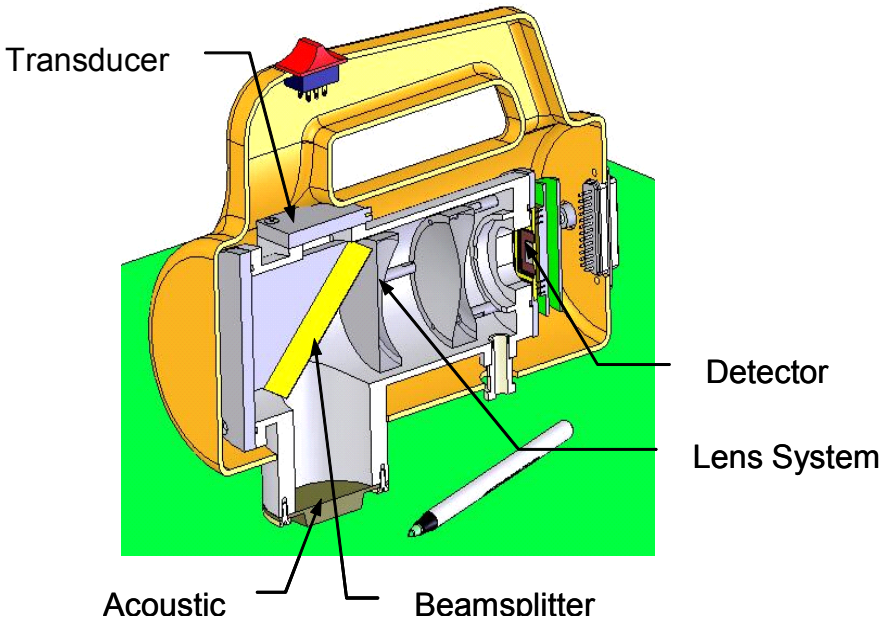

Figure 21. Principles of "Acoustocam" Camera (Courtesy: Imperium, U.S.)

Figure 22. Prototype Camera with Housing (Left) and Without Housing (Right) (Courtesy: Imperium, U.S.)

Figure 23. Steel Samples with Controlled Defects (Left) and Corrosion Defects (Right)
(Courtesy: Imperium, U.S.)

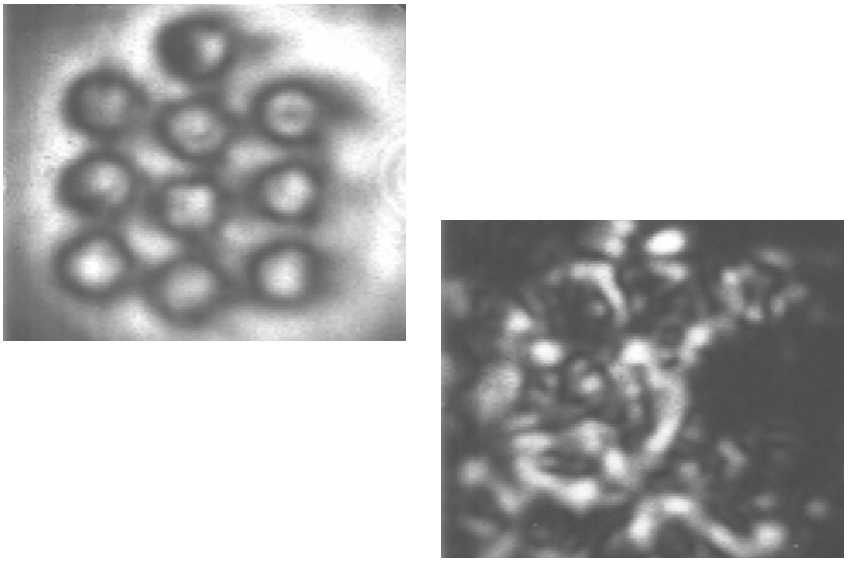

Figure 24. Ultrasound Images of Holes Pattern in the Sample with Controlled Defects (Left) and Corroded Ares in the Sample with Corrosion Defects (Right)
(Courtesy: Imperium, U.S.)

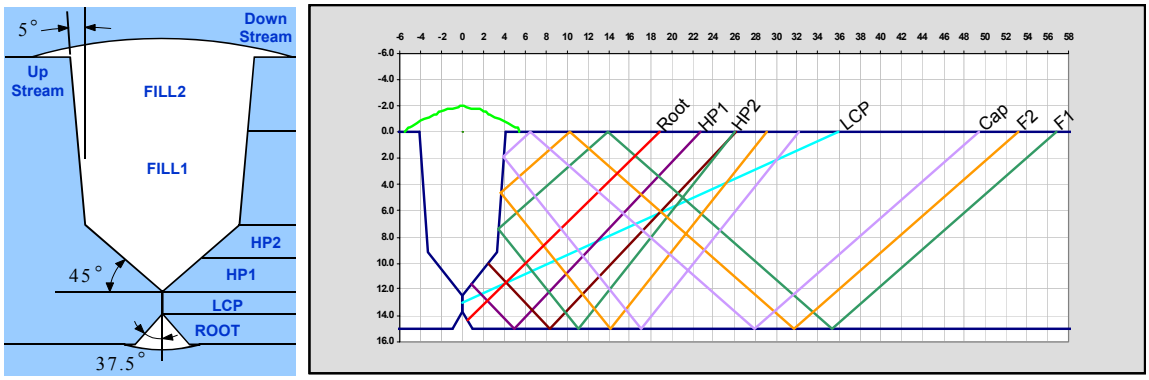

Figure 25. Mechanized Weld Inspection – Zone Discrimination (Left) and Ultrasonic Channels and Beam Paths per Vertical Zone (Right)

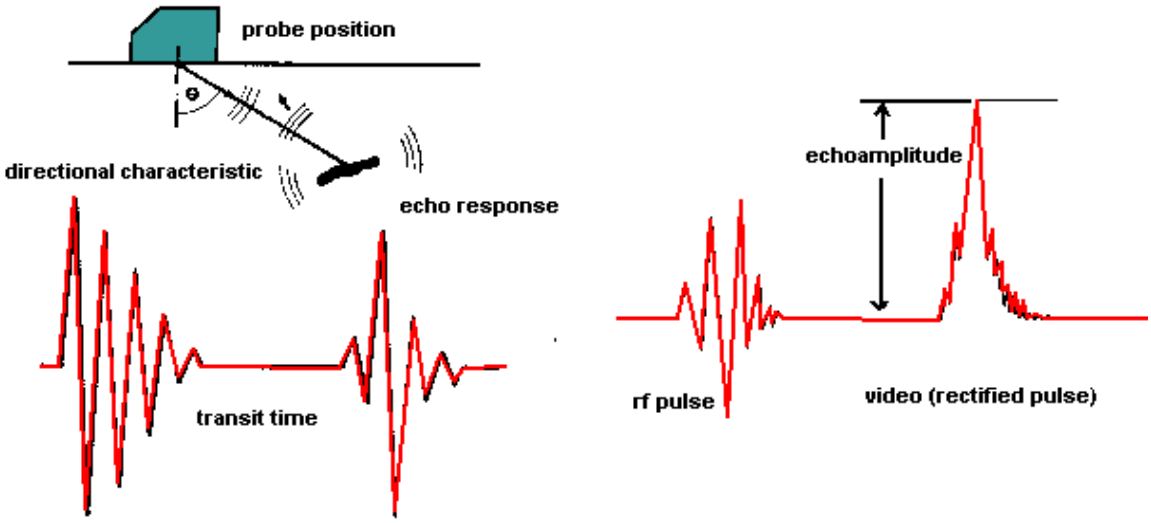

Figure 26. P/E Detection, Location, and Amplitude-Based Sizing[51]

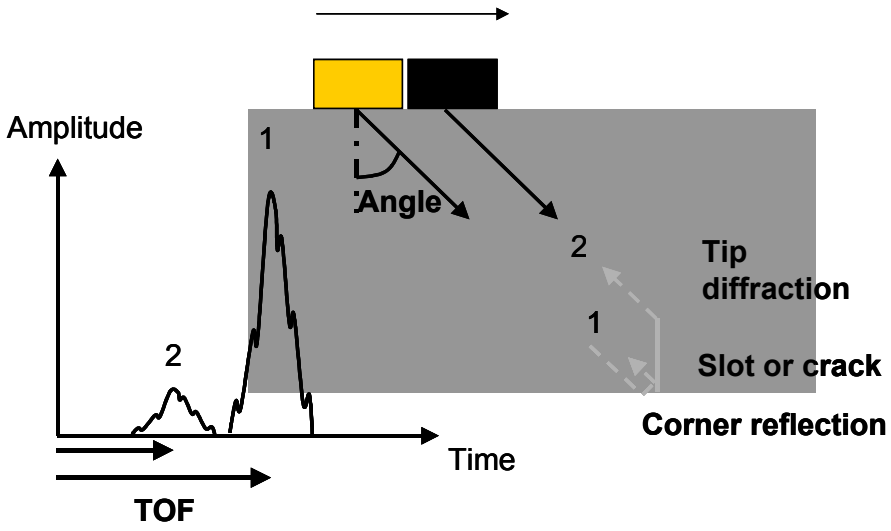

Figure 27. TOF or Tip Diffraction Principles

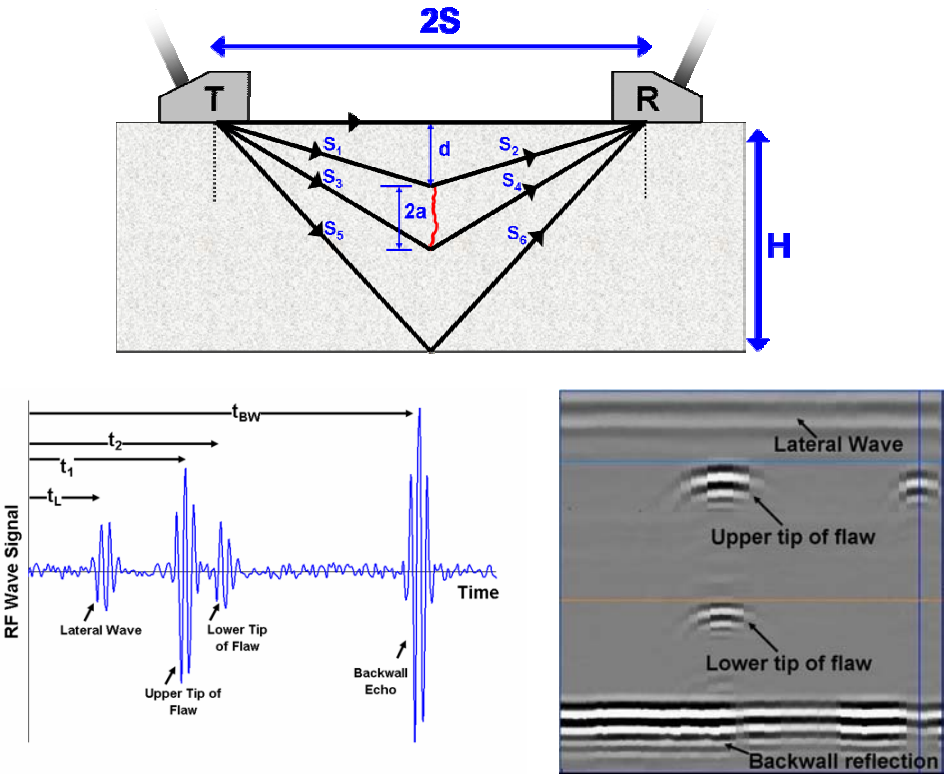

Figure 28. TOFD Inspection (Top), Resulting Waveform (Bottom Left), and an Example D-Scan (Bottom Right)

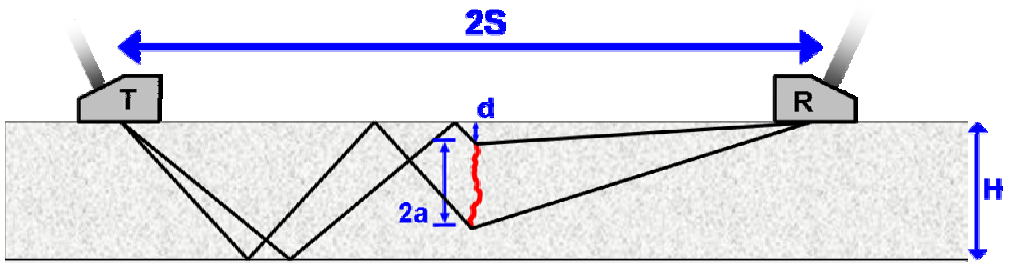

Figure 29. Multiple-Skip TOFD Inspection Schematic

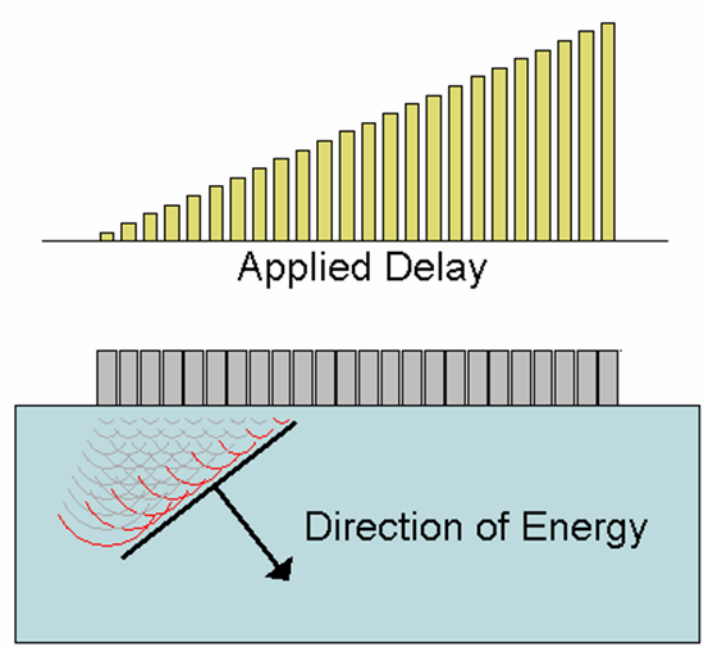

Figure 30. Electronic Beam Steering using PA Ultrasonics

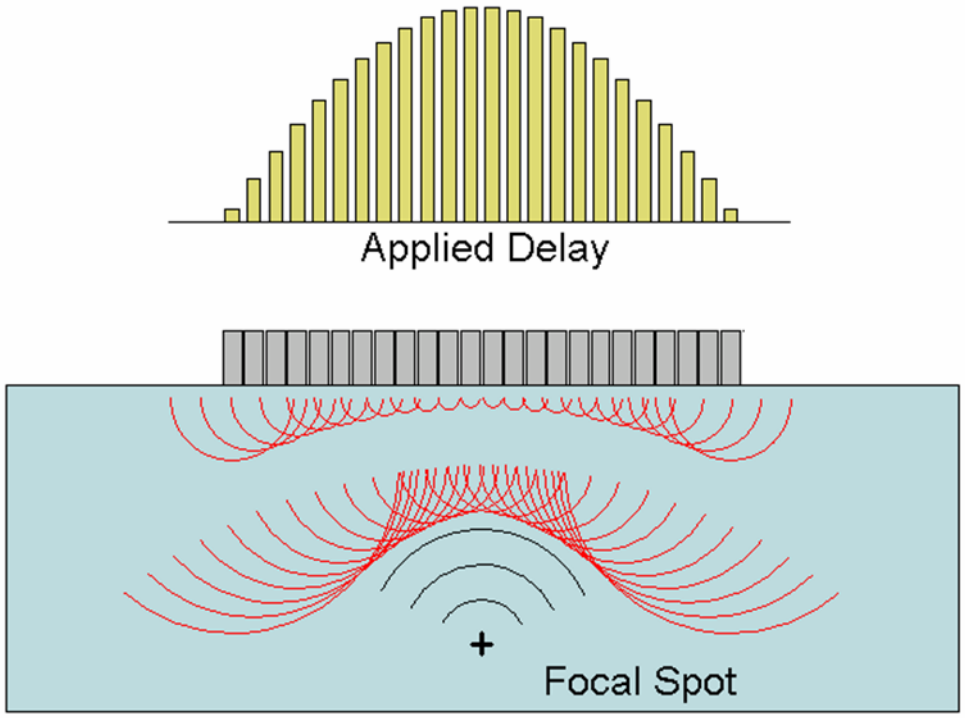

Figure 31. Electronic Beam Focusing using PA Ultrasonics

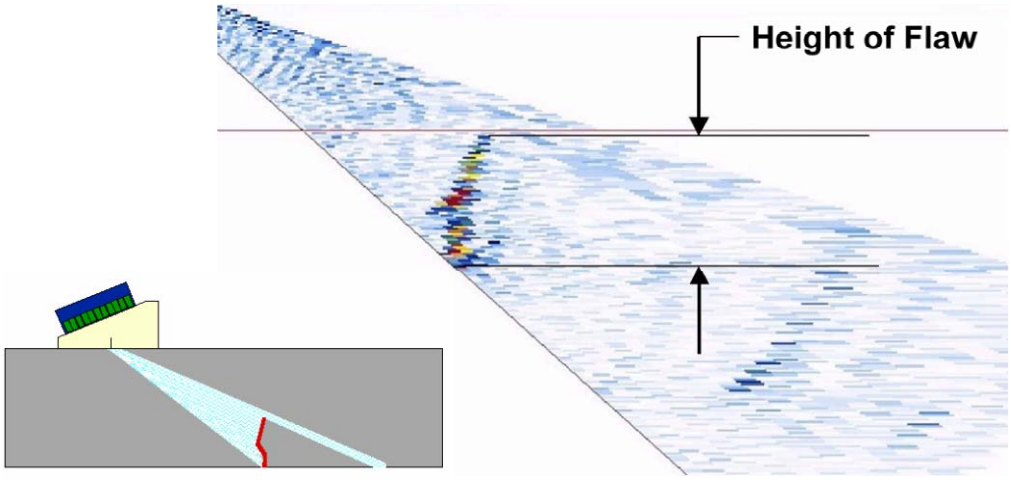

Figure 32. Sectorial Scan (Right) Measuring a Vertical Crack with a Stationary PA Probe (Left)

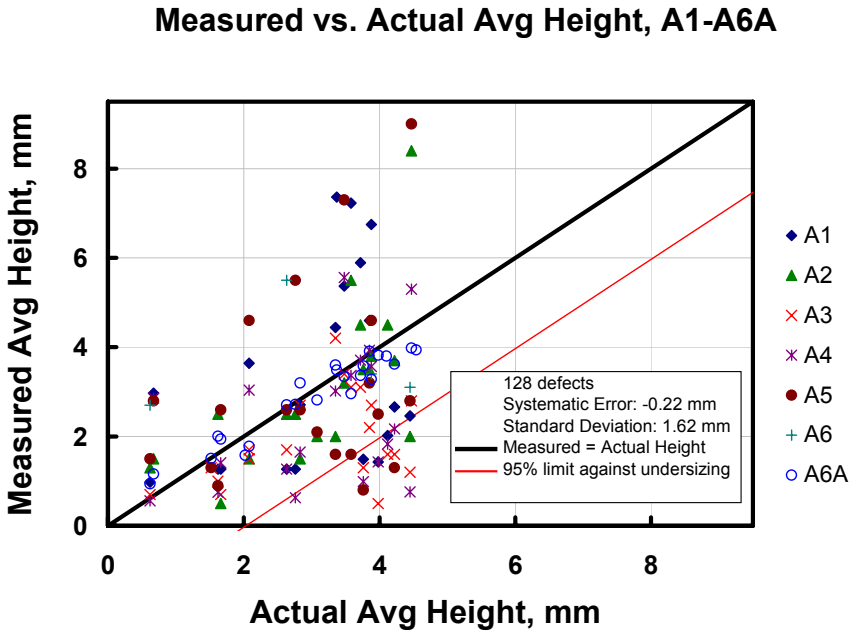

Figure 33. Measured vs. Actual Average Height – Approaches A1-A6, A6A

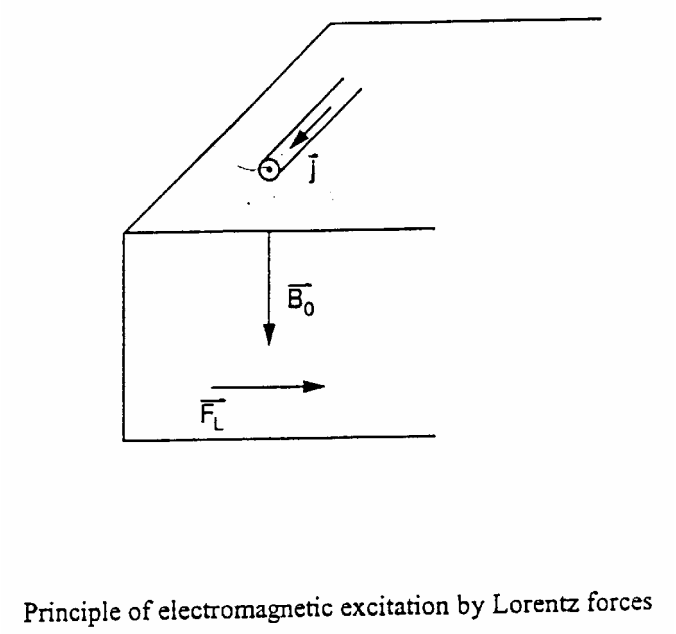

Figure 34. Principle of Electromagnetic Excitation by Lorentz Forces

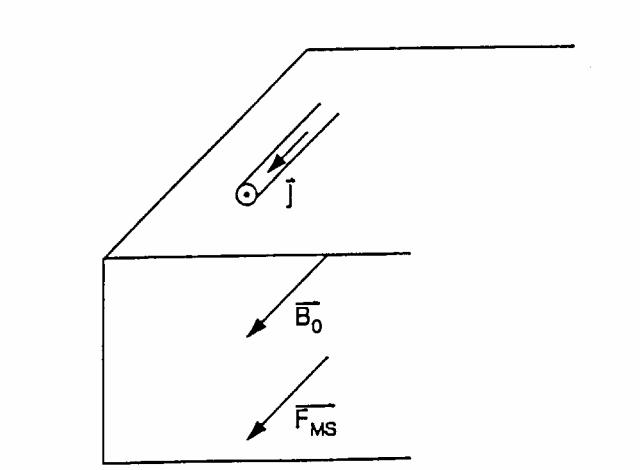

Principle of electromagnetic excitation by magnetostriction

Figure 35. Principle of Electromagnetic Excitation by Magnetostriction

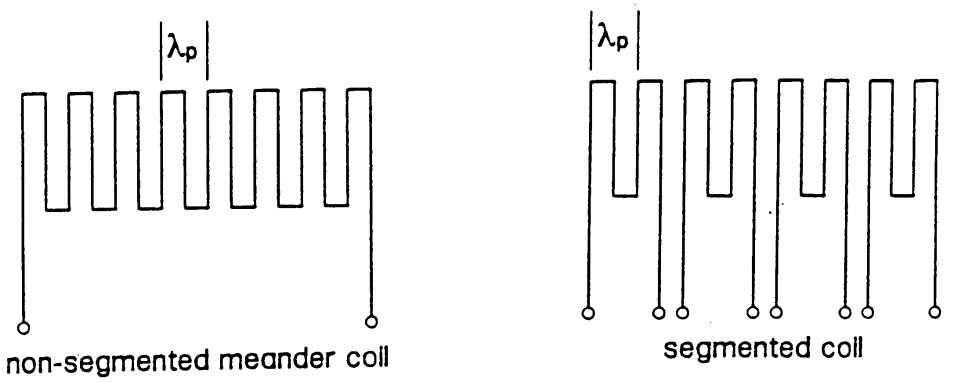

Figure 36. Shapes of Rf-Coils

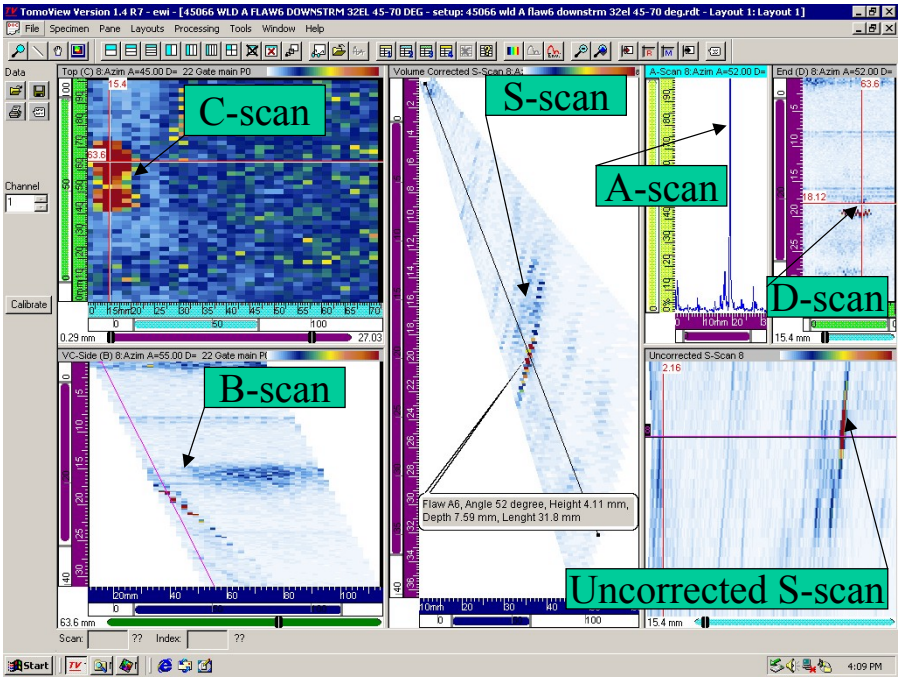

Figure 37. Advanced AUT Imaging

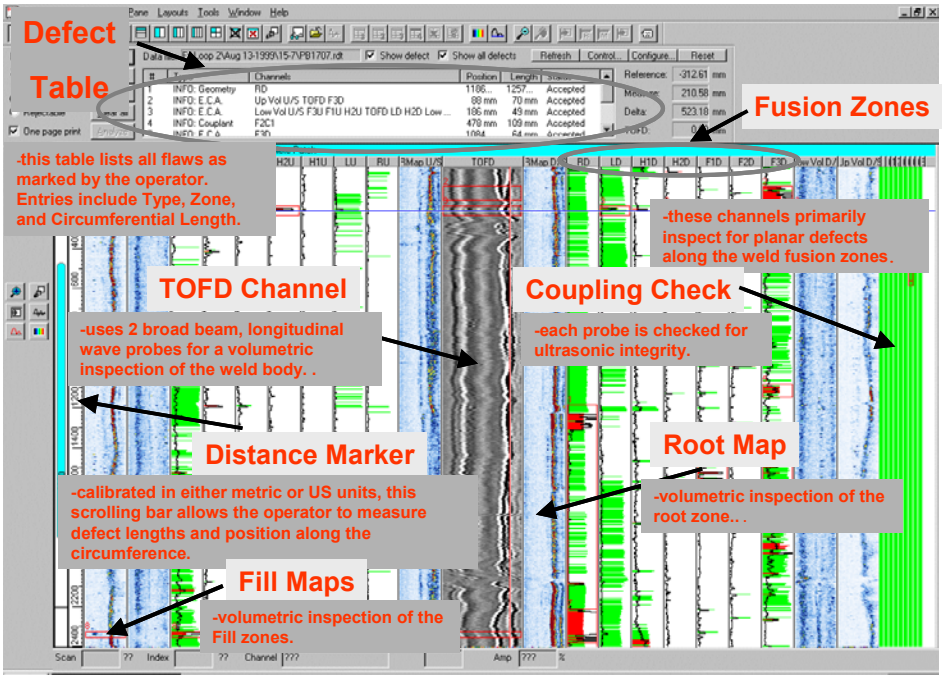

Figure 38. Strip Chart Layout (Courtesy: Canspec, Canada)

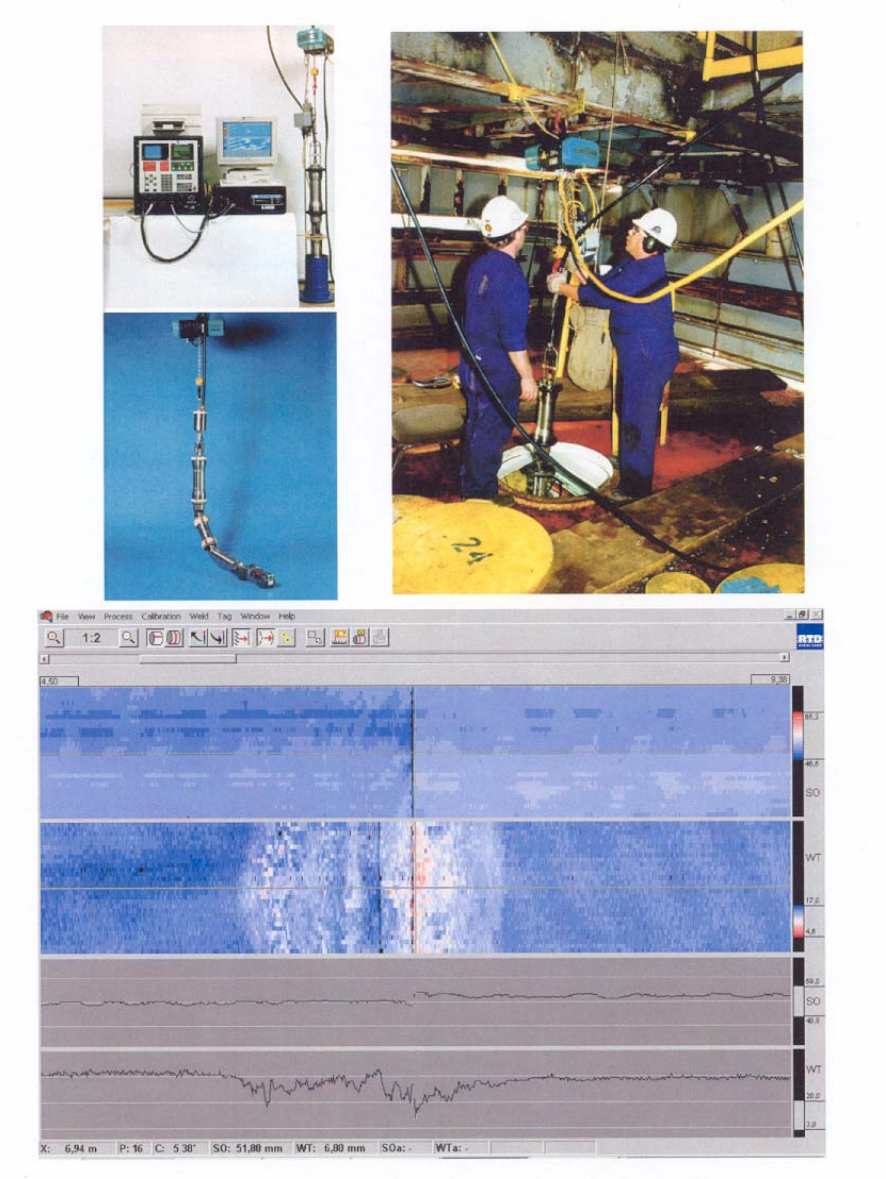

Figure 39. **Short-Range UT Instrumentation – Riser Inspection Tool and Automated Ultrasonic Corrosion Mapping using Riser Inspection Tool Non-Damaged Area (Top C- and B-Scans) and External Corrosion (Bottom C- and B-Scans)** (Courtesy: RTD, The Netherlands)

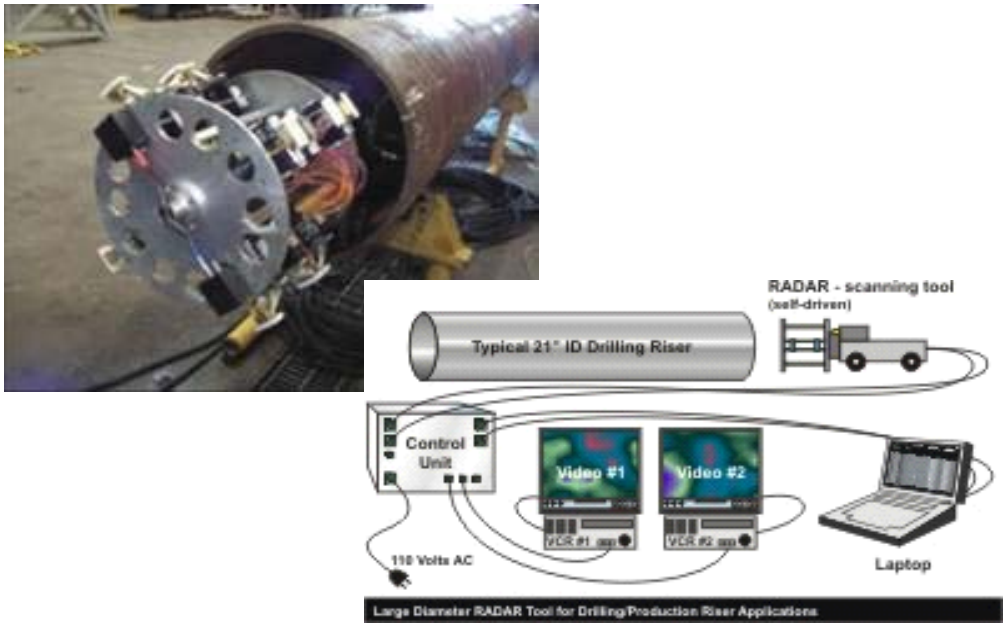

Figure 40. RADAR – Drilling Riser Inspection System (Courtesy: ABB Vetco Gray & Global Automated Systems)

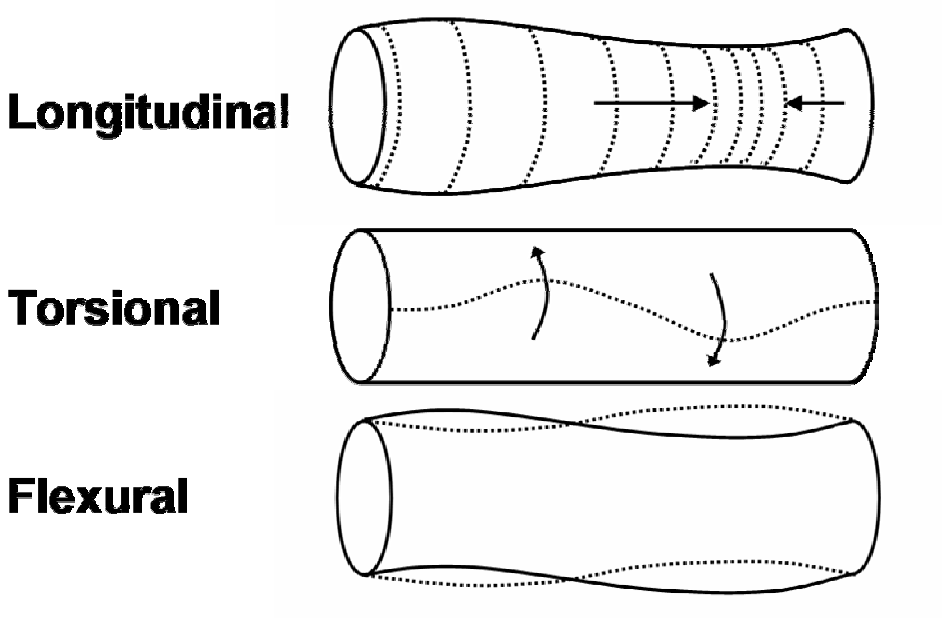

Figure 41. Guided Wave Modes in Pipes

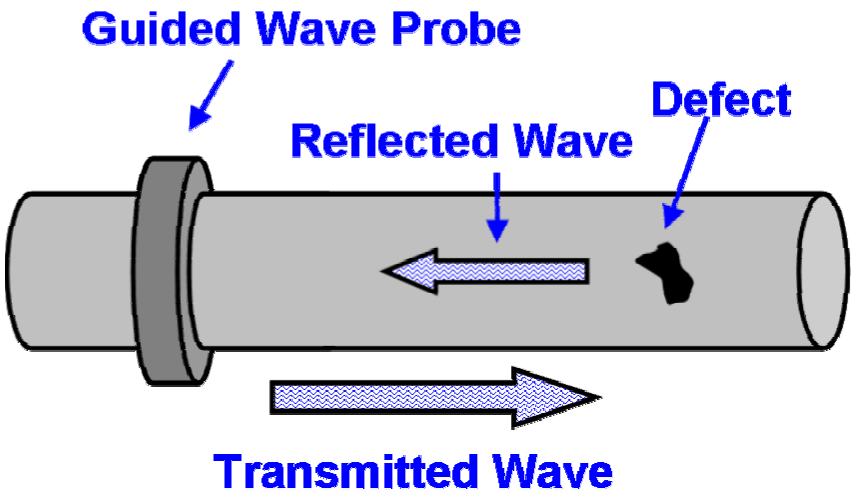

Figure 42. Schematic of Riser Inspection using Long-Range Guided Ultrasonics

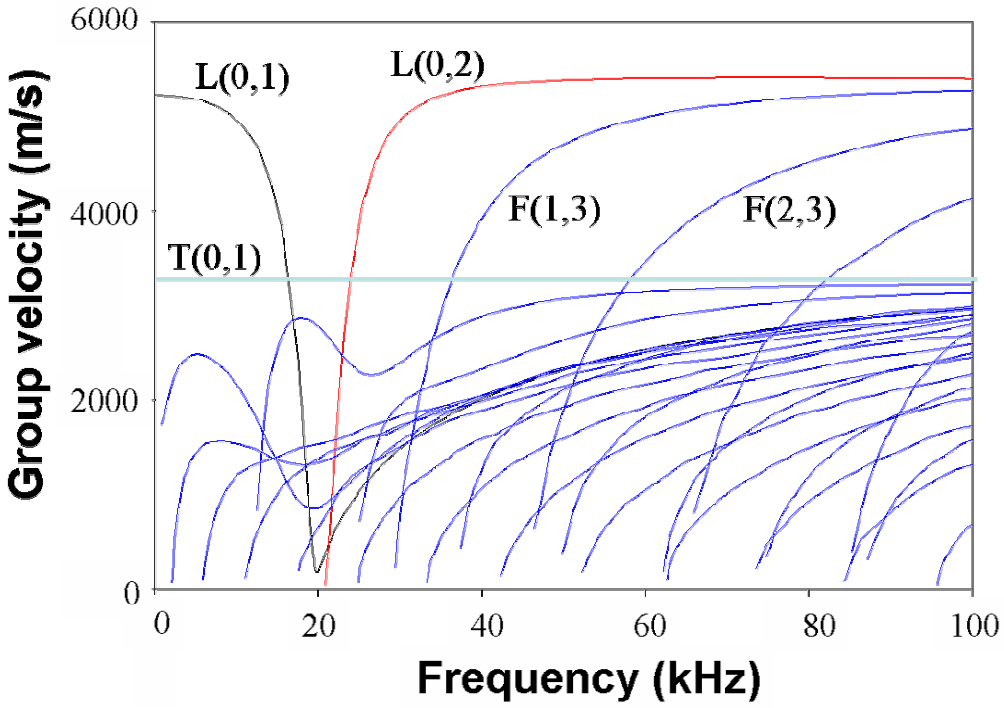

Figure 43. Group Velocities in 6-in. Steel Pipe[18]

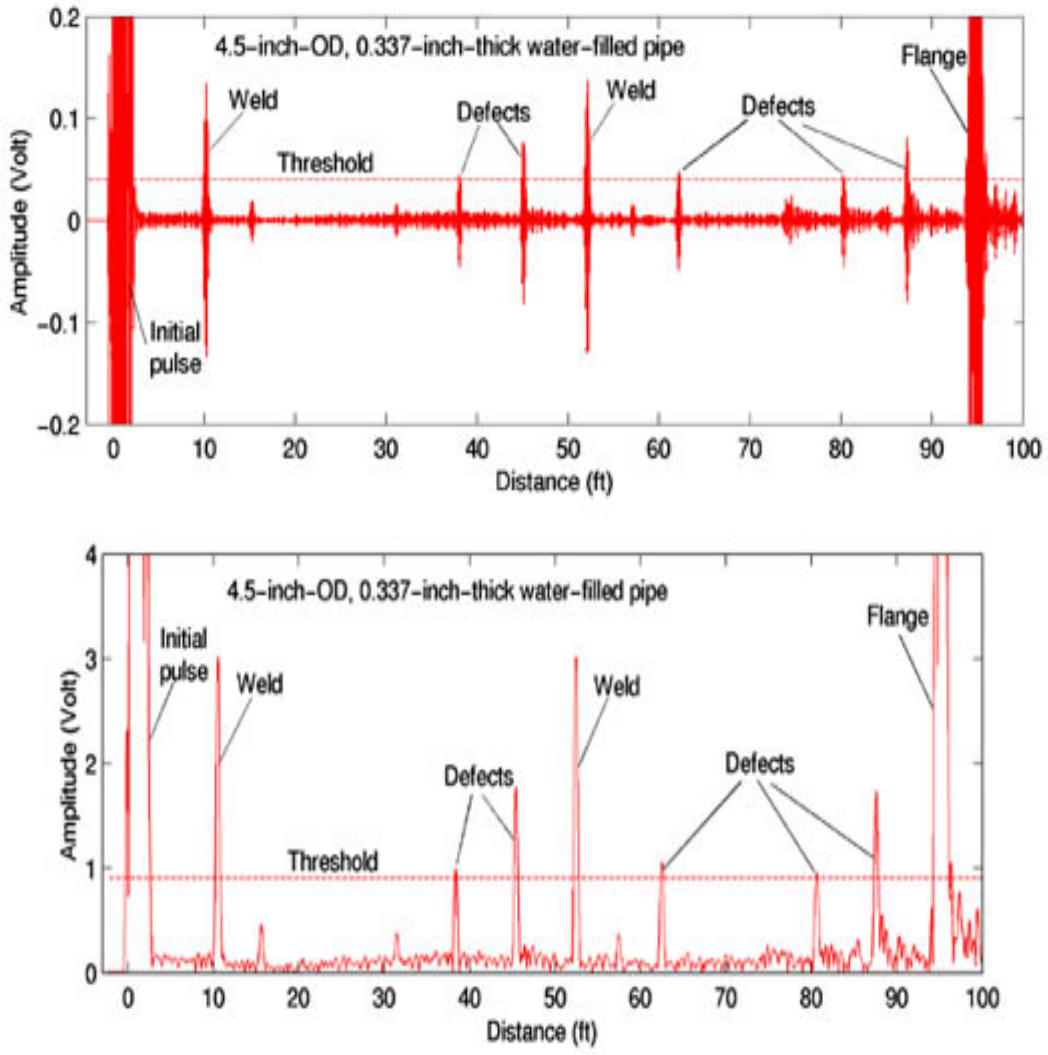

Figure 44. Guided Wave Responses – RF Signal (Top) and Processed Signal (Bottom) (Courtesy: SwRI, U.S.)

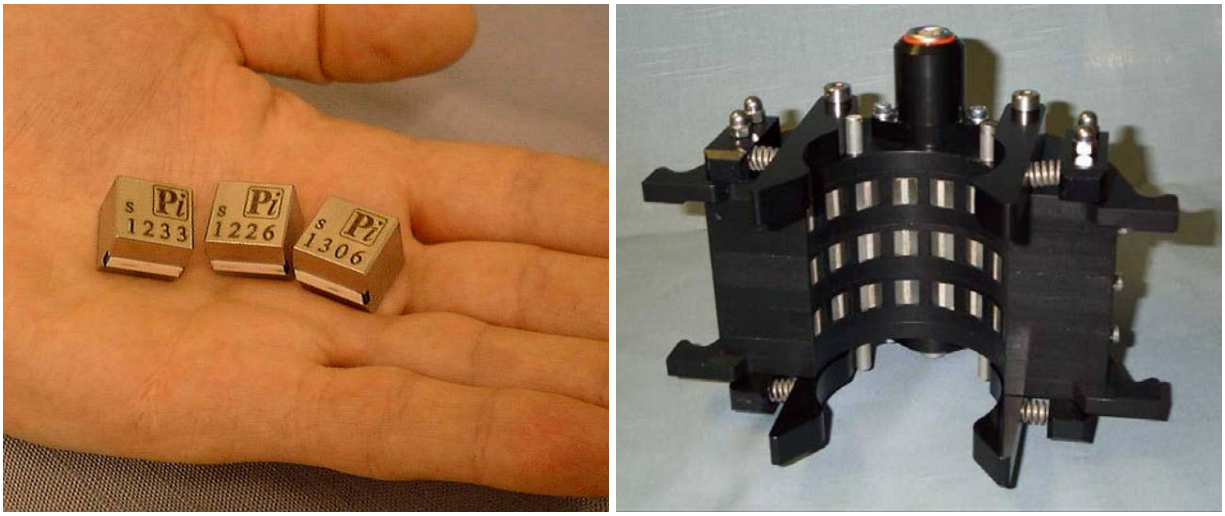

Figure 45. Transducers (Left) used in the Modular Teletest® Guided Wave Inspection Ring (Right) (Courtesy: Plant Integrity Ltd)

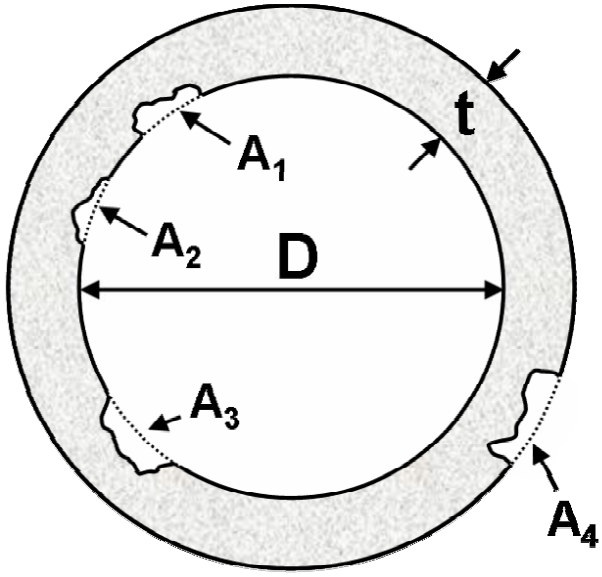

$$\text{Loss of Area (\%)} = \frac{100(A_1 + A_2 + A_3 + A_4)}{\pi D t}$$

Figure 46. Cumulative Cross Sectional Area Loss in a Corroded Riser

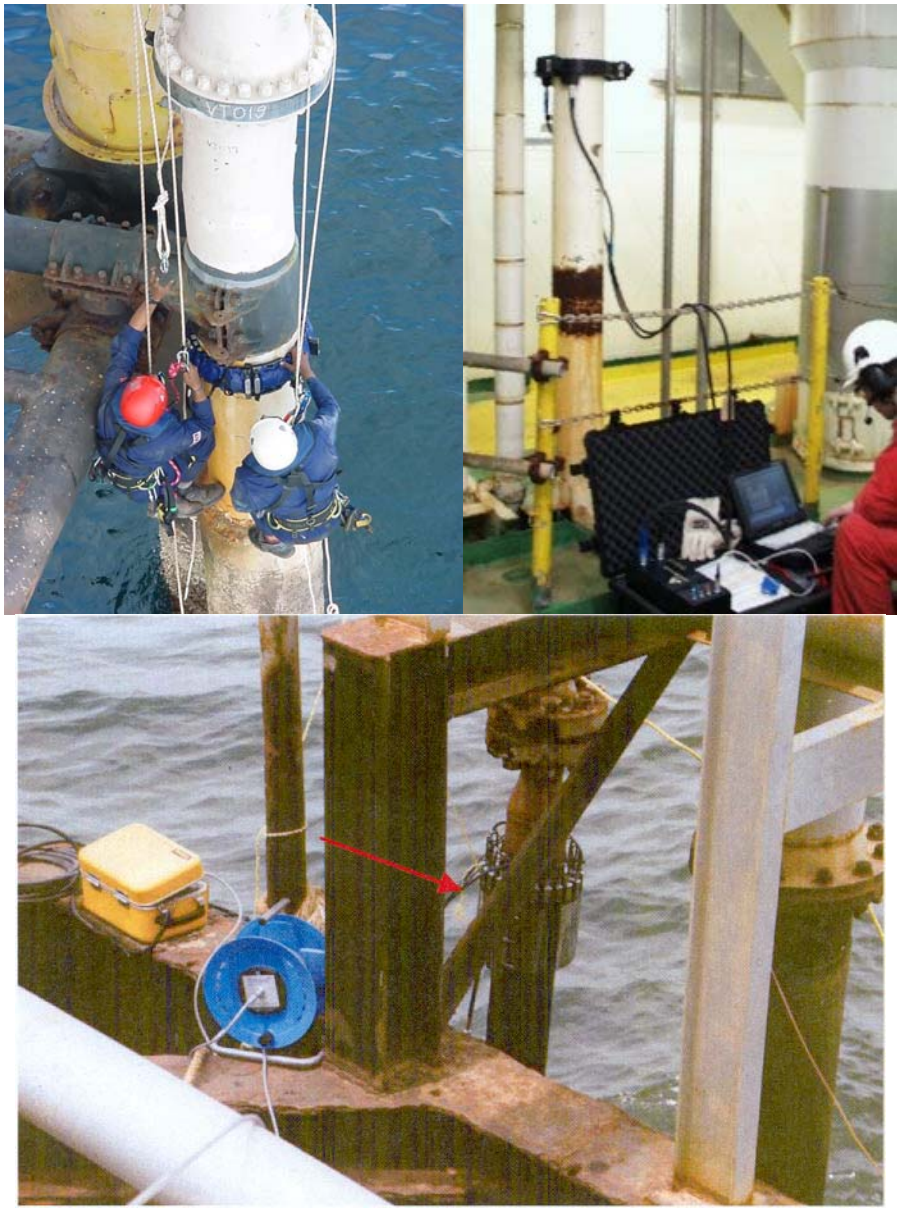

Figure 47. Riser Inspection using Long-Range Guided Ultrasonics Equipment (Top Pictures Courtesy: Guided Ultrasonics Ltd., U.K.; Bottom Picture Courtesy: PI Ltd., U.K.)

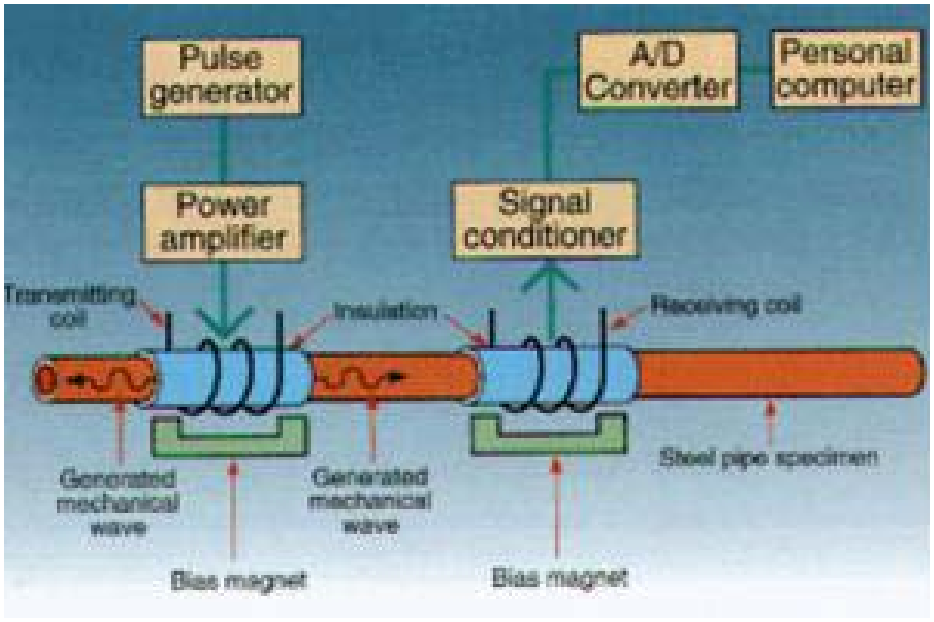

Figure 48. Inspection of an Insulated Pipe using MsS (Courtesy: SwRI)

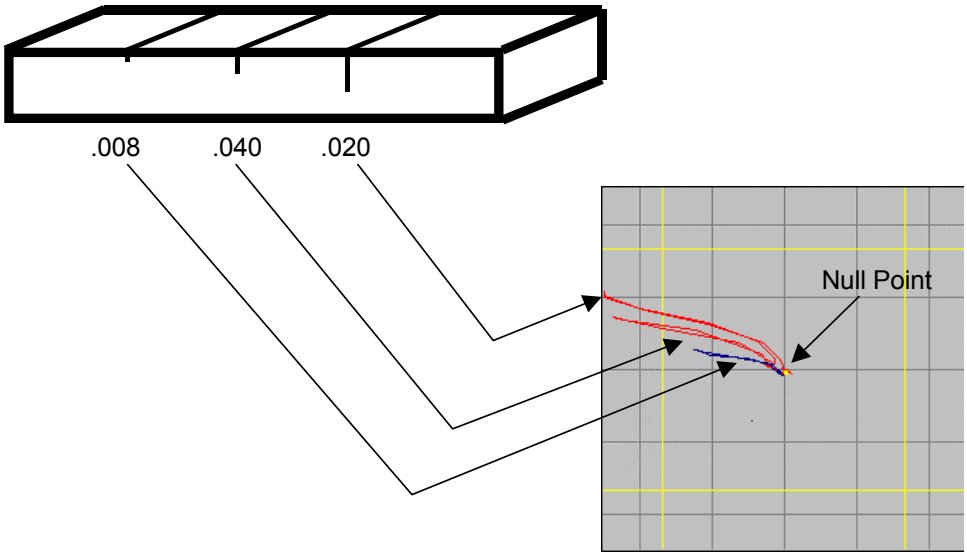

Figure 49. Sample Eddy-Current Impedance Display of Three EDM Notches in Calibration Sample

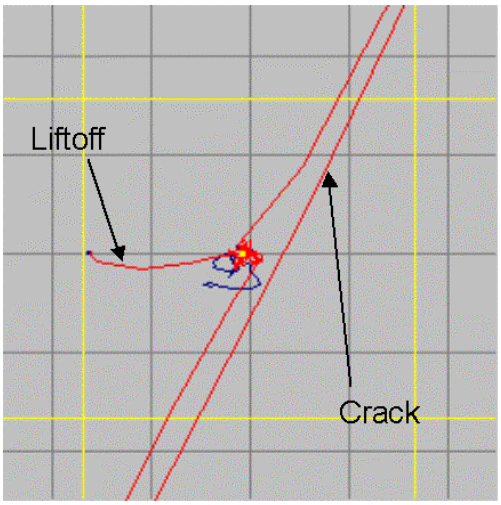

Figure 50. ET Screen Calibrated to Minimize Liftoff Interpretation

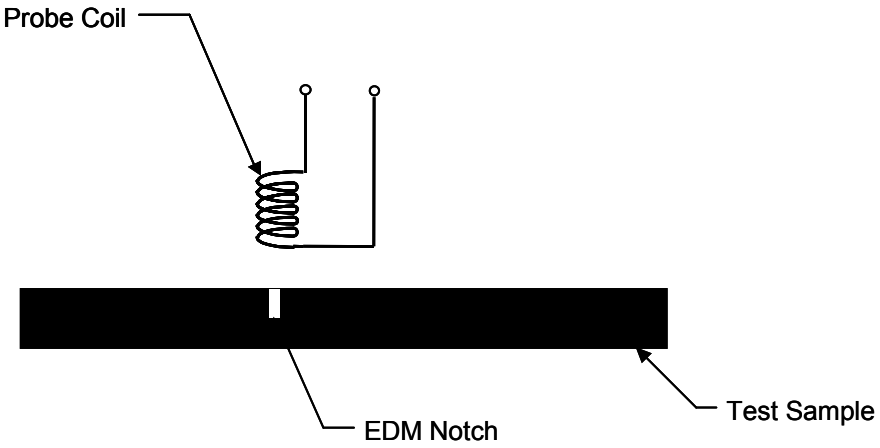

Figure 51. Schematic of Absolute ET Probe

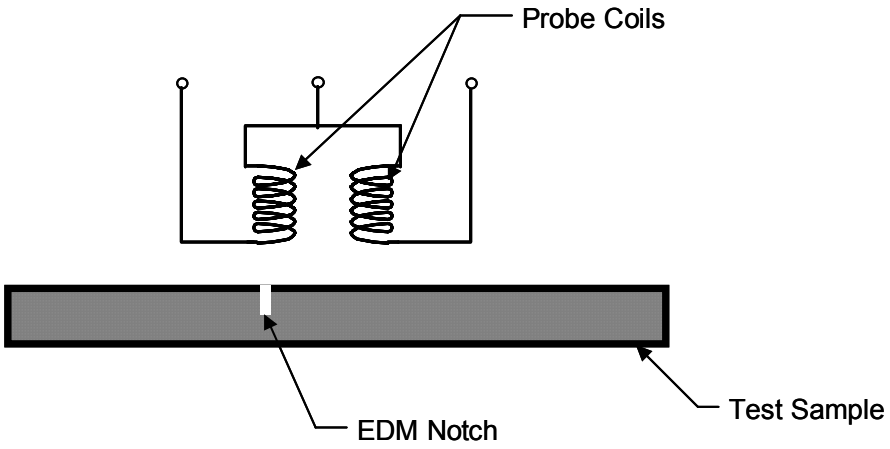

Figure 52. Schematic of Differential Probe

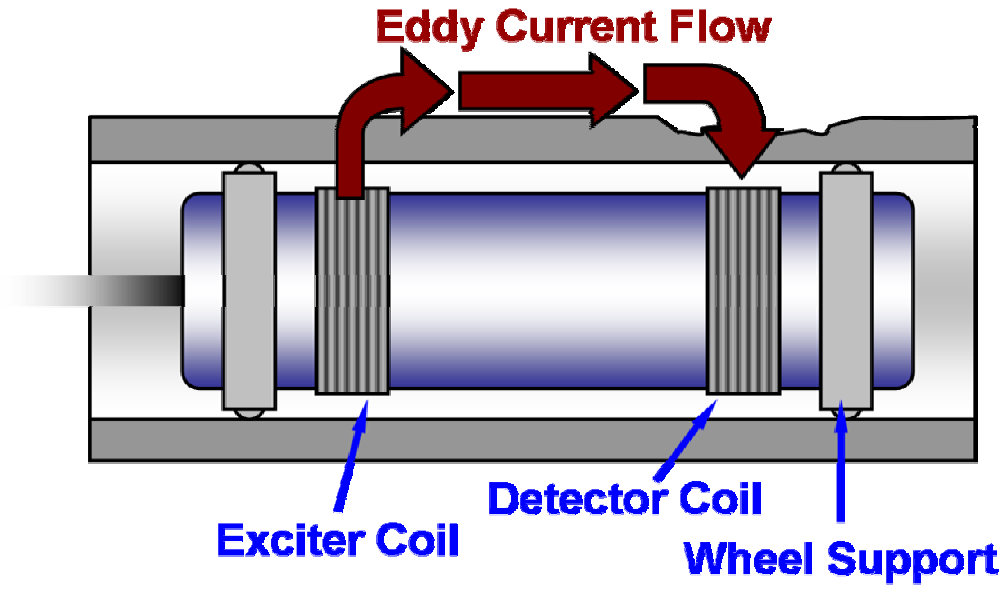

Figure 53. Remote Field ET of a Pipe

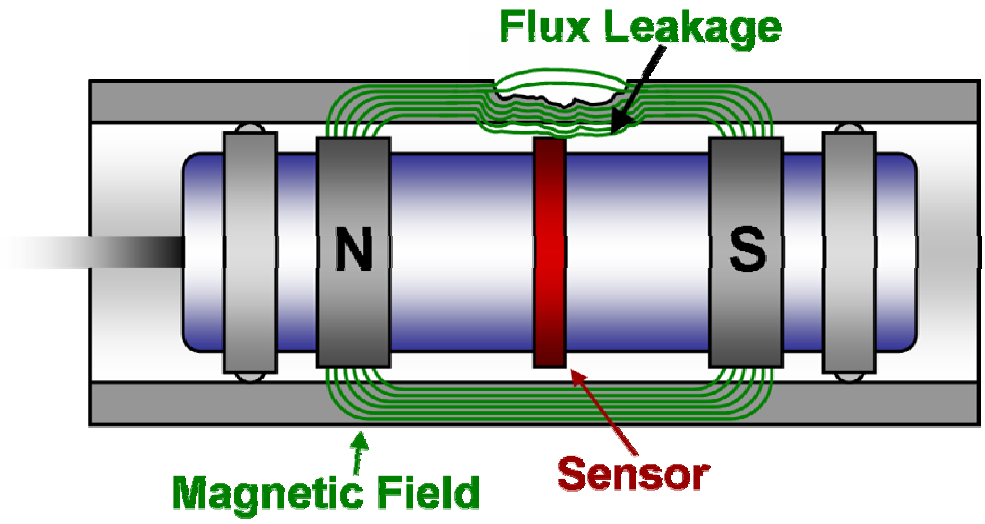

Figure 54. Pipe Inspection using MFL

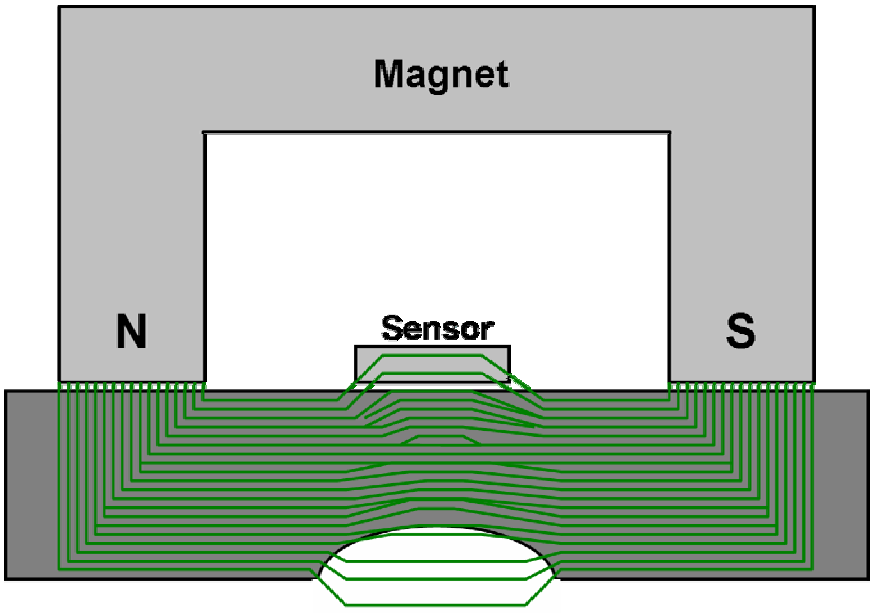

Figure 55. Flux Leakage in a Corroded Component due to Thickness Loss

Figure 56. Typical MFL Tool (Courtesy: Rosen, Germany)

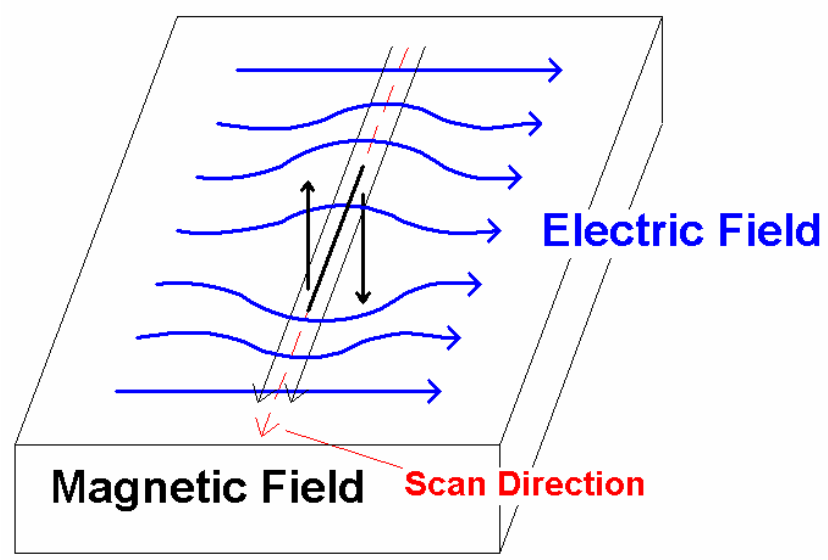

Figure 57. ACFM Perturbations in Electric and Magnetic Fields Produced by a Defect

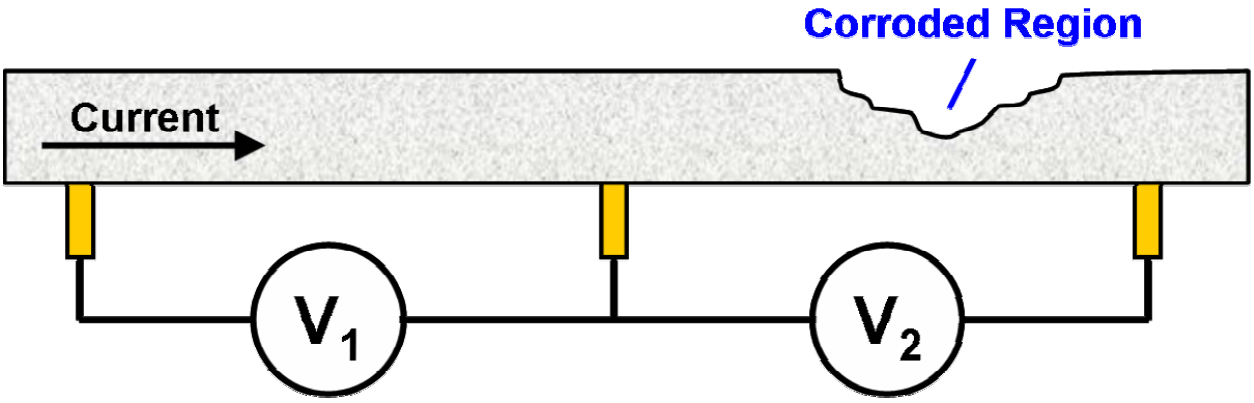

Figure 58. FSM Schematic Showing Increase in Voltage

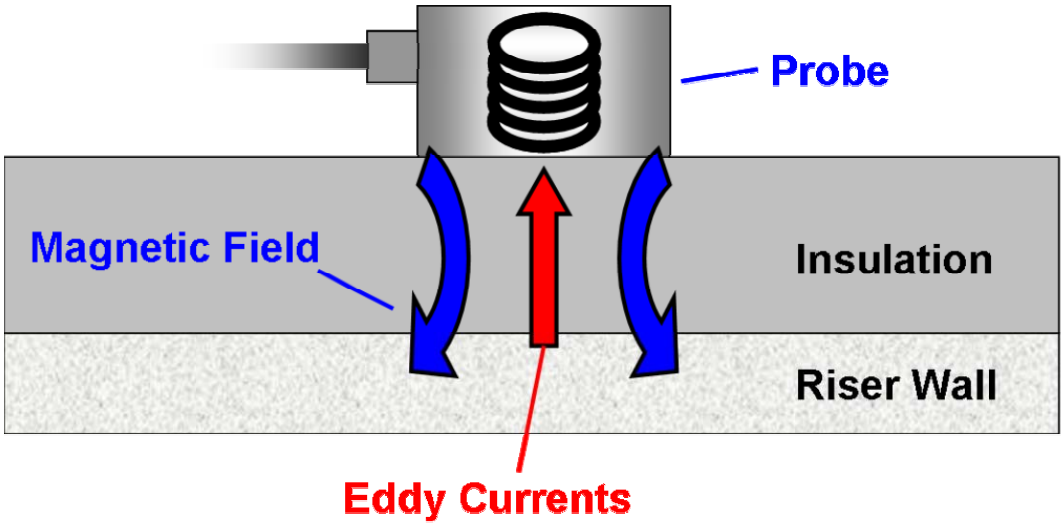

Figure 59. Pulsed Eddy-Current Inspection Through Insulation and/or Biomass

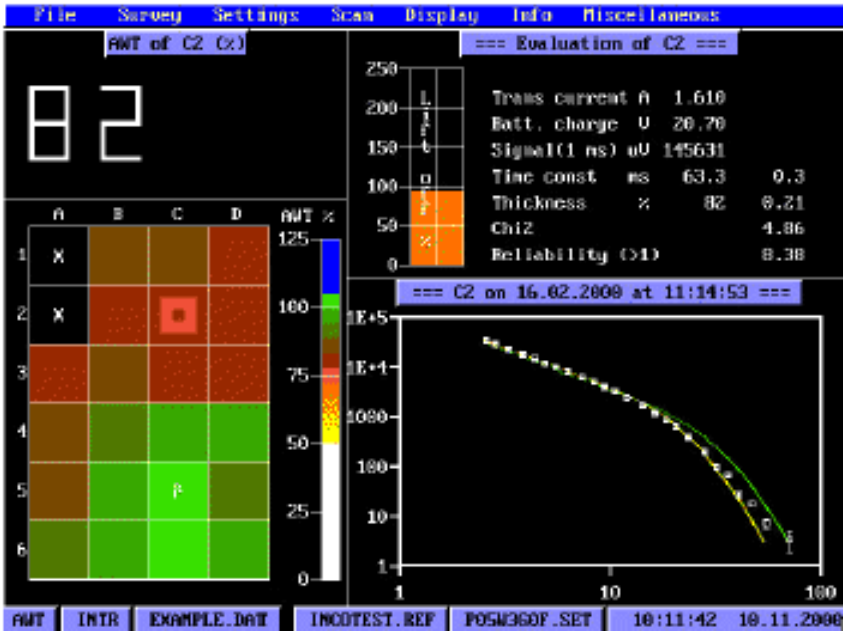

Figure 60. Pulsed Eddy-Current Thickness Measurements (Courtesy: RTD, The Netherlands)

Figure 61. Riser Inspection using Pulsed Eddy-Current Equipment (Courtesy: RTD, The Netherlands)

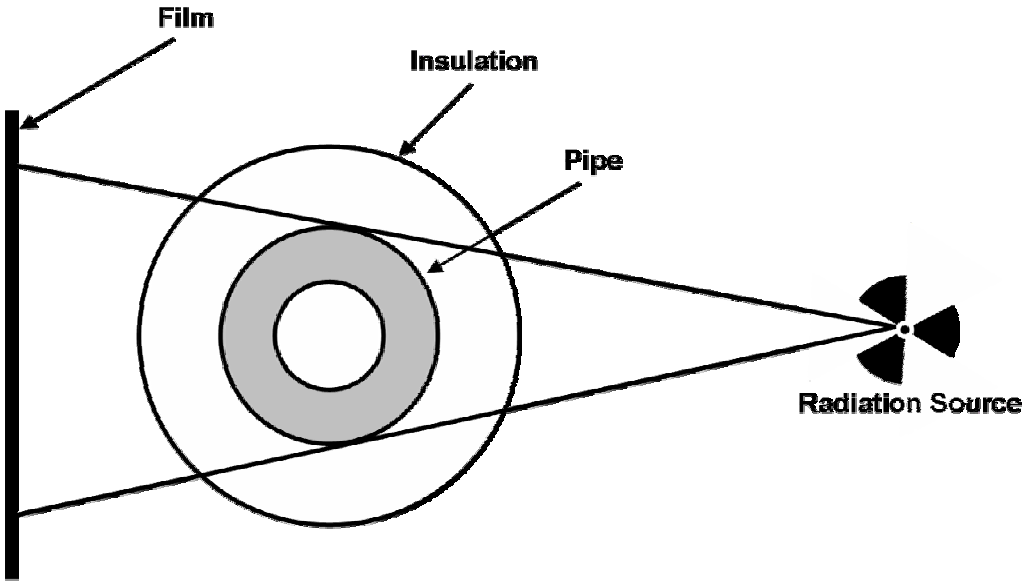

Figure 62. Tangential Radiography Setup to Measure Wall Thickness

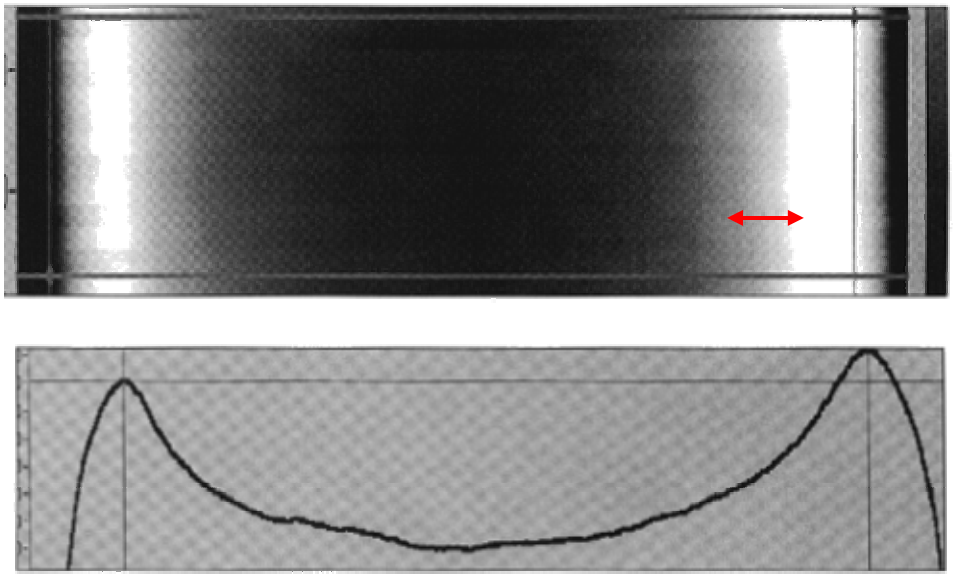

Figure 63. Tangential Radiography Image (Top) and the Corresponding Contrast Profile (Bottom)

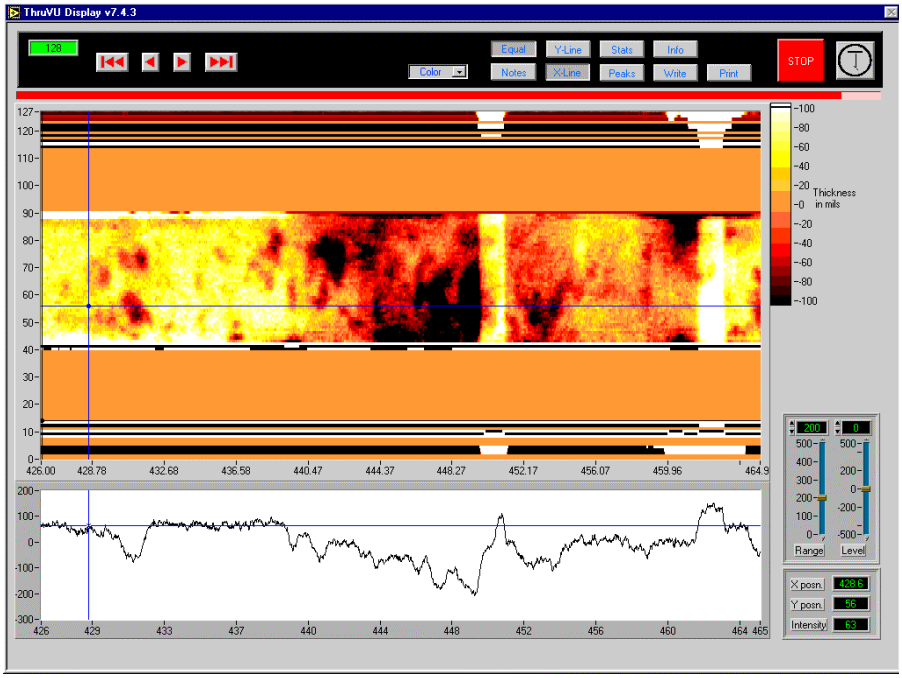

Figure 64. Digital Radiography Results (Courtesy: SwRI and IHI, U.S.)

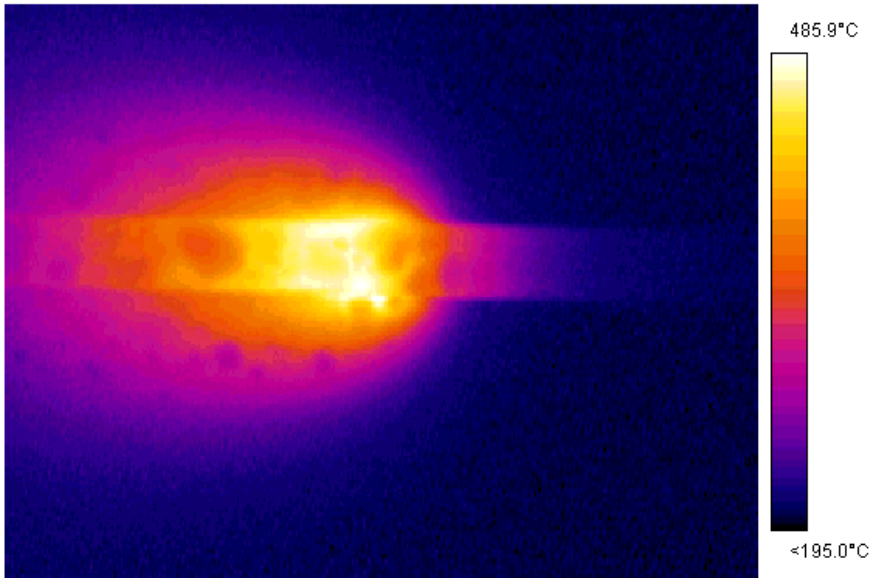

Figure 65. Infrared Thermography Image of a Laser Weld

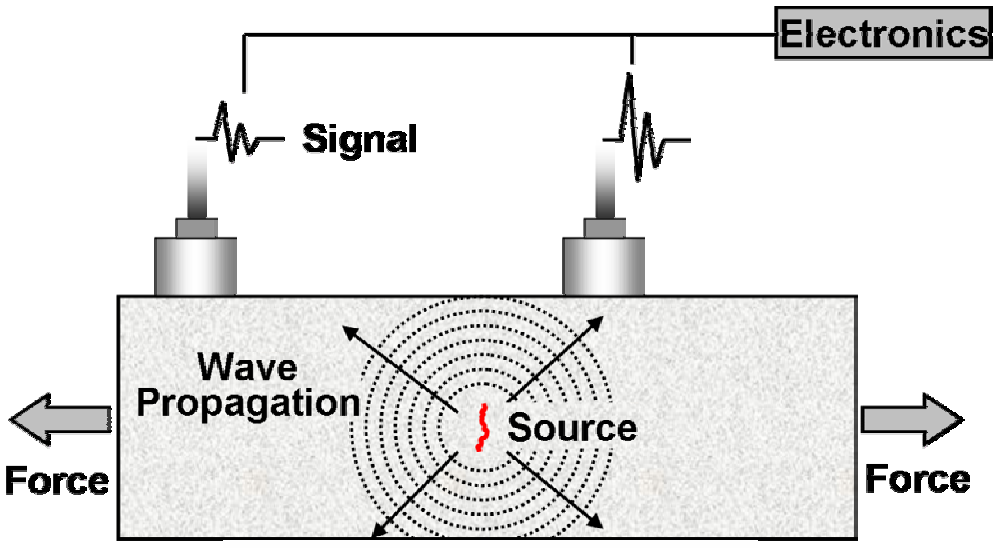

Figure 66. AE Monitoring of an Internal Flaw

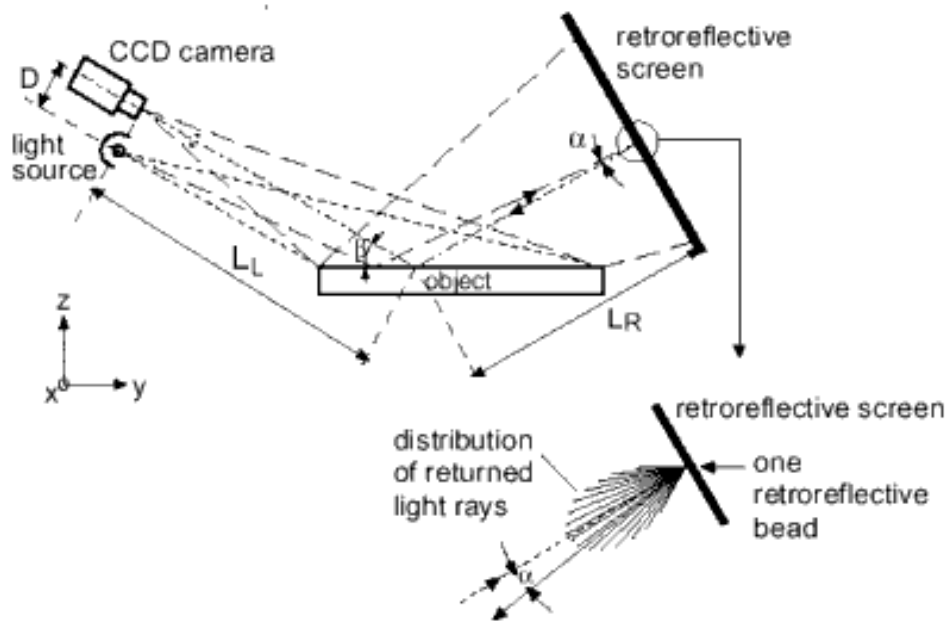

Figure 67. D Sight™ System Setup for Visual Inspection of a Test Surface[63]

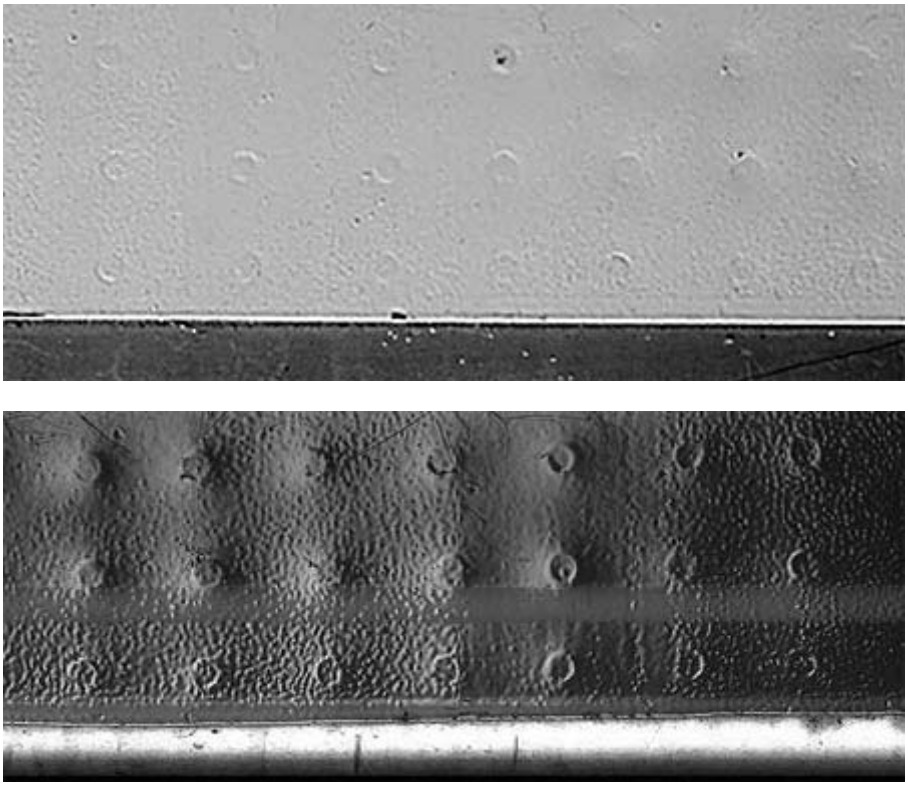

Figure 68. Optical (Top) and Edge of Light™ (Bottom) Image of a Lap Splice Joint Showing High Topographic Contrast[64]

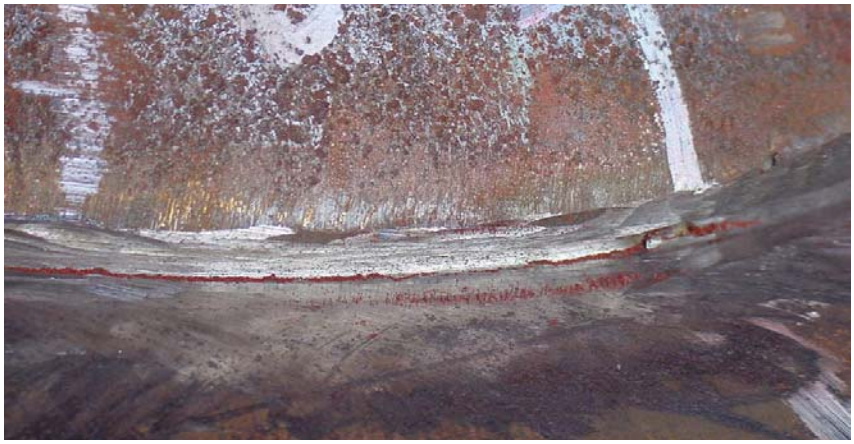

Figure 69. Indications of a Crack using Magnetic Particle Inspection

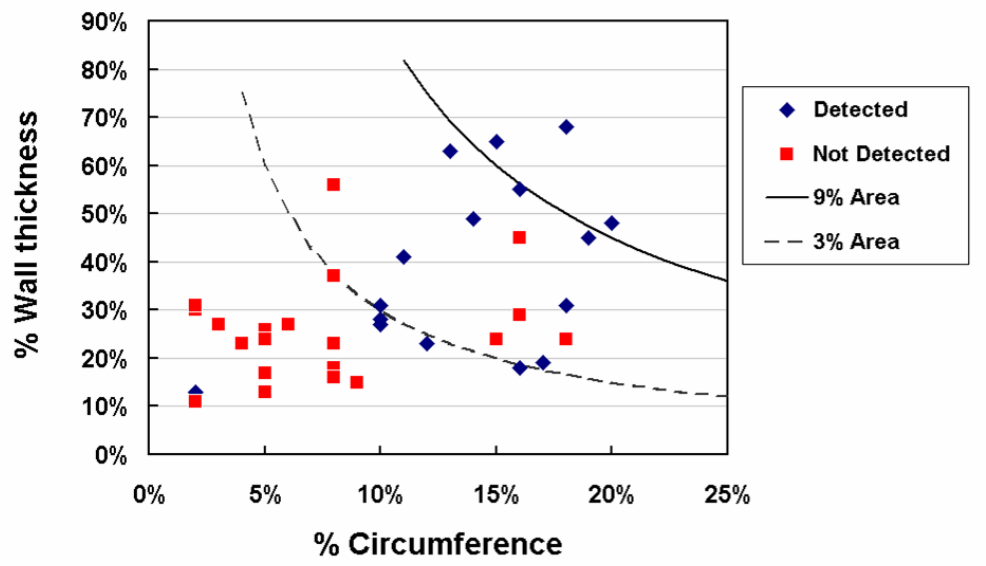

Figure 70. Performance of the Teletest® System in the RACH Program (Courtesy: PI Ltd., U.K.)

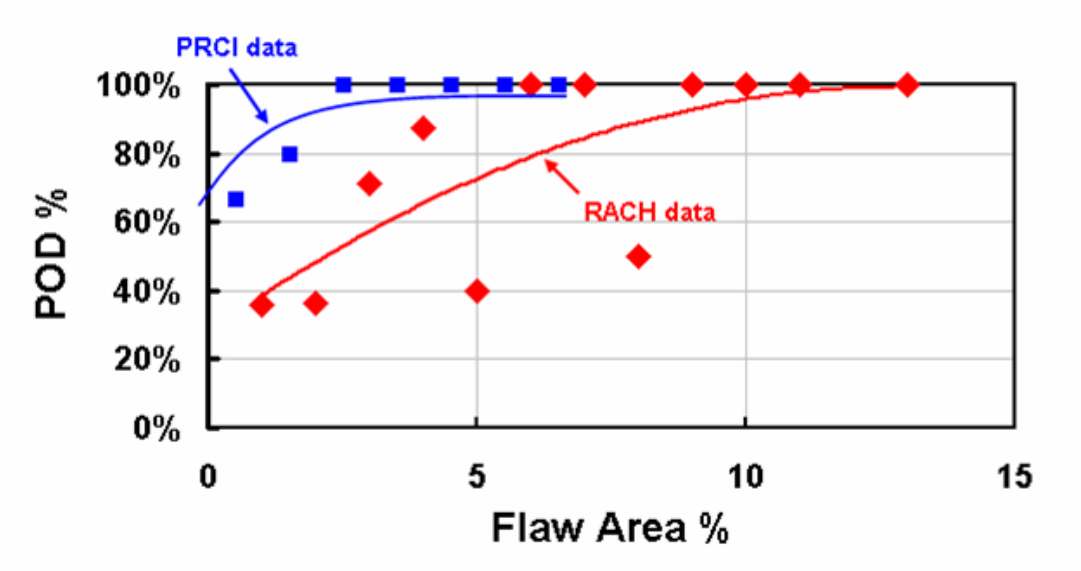

Figure 71. Comparison of POD Data in the RACH and PRCI Programs (Courtesy: PI Ltd., U.K.)